PECAM-1-DEPENDENT VASCULAR MIMICRY IN MELANOMA: CONTRIBUTIONS TO ANTI-ANGIOGENIC RESISTANCE

James M. Dunleavey

A dissertation submitted to the faculty at the University of North Carolina at Chapel Hill in a partial fulfillment of the requirements for the degree of Doctorate of Philosophy in the Department of Cell Biology and Physiology in the School of Medicine.

Chapel Hill
2016

Approved by:

Andrew C. Dudley

James E. Faber

Victoria L. Bautch

Nancy E. Thomas

Eleni Tzima

ABSTRACT

James M. Dunleavey: PECAM-1-dependent vascular mimicry in melanoma: contributions to anti-angiogenic resistance
(Under the direction of Andrew C. Dudley)

The development of a perfused blood vasculature is a requirement both in development and for many human pathologies. Critically, the formation of new blood vessels through angiogenesis has been identified as a hallmark of cancer progression. A major effort has been undertaken to target the blood vessels of nascent and metastatic tumors to inhibit tumor growth. Therapies targeting the blood vasculature have shown limited efficacy, and multiple modes or resistance have been proposed. While attempting to characterize endothelial cells from mouse models of melanoma, we discovered a novel subpopulation of tumor cells expressing the endothelial cell marker PECAM-1. PECAM-1^+ melanoma participate in a tumor cell derived vasculature in a form of vasculogenic mimicry (VM). PECAM-1^+ tumor cells form PECAM-1-dependent vascular-like networks *in vitro* and generate perfused vascular networks *in vivo* in a VEGF-independent fashion. Transcriptional activator AP-2a is diminished in PECAM-1^+ melanoma and represses PECAM-1 expression. Re-expression of AP-2a in PECAM-1^+ tumor cells blocks PECAM-1 expression and inhibits tube-forming ability, and knockdown of AP-2a upregulates PECAM-1 in PECAM-1^- tumor cells. We identified PECAM-1^+ tumor cells in both murine and human melanoma, and propose that PECAM-1^+ melanoma cells may instigate VM, collaborate with host endothelial cells, and form PECAM-1-dependent vascular channels which are refractory to VEGF inhibition.

To my parents who have supported me throughout this journey, and taught me to always ask questions; and Jess, for putting up with late nights, weekends, and holidays lost to mice.

ACKNOWLEDGEMENTS

The work described within this tome has been an intensely collaborative and fruitful process which has been a true pleasure to undertake. Through my graduate career I have been lucky enough to meet and work with a great deal of people without whom my scientific projects might not have succeeded.

I first would like to acknowledge and deeply thank my advisor, Dr. Andrew Dudley, for taking a chance on me when his lab was literally being unpacked from boxes. The project we developed rapidly after joining his lab has been an absolute joy to work on. Loving what you do is a necessity to work nights, weekends, and holidays, and Drew encouraged me to work on a project that I loved. For the last four years you have been both a mentor and friend, and it has been an honor to help you build your lab and work with you on all of the projects we have tackled. You have shaped the way I ask questions, including "why do we care about this", which is a question I have come to ask first and foremost with any experiment, paper, or talk. I hope to continue working together as I continue my career in tumor angiogenesis, and wish you the best of luck as you continue growing the lab and your research program!

Kathleen Caron has been an inspiration and great source of advice even before I was accepted to UNC's Graduate Program. My interview with her was one of the main reasons I came to UNC, and as a first-year mentor, and later as a friendly listener her advice was crucial to many of the milestones I was able to achieve in the Department of Cell Biology and Physiology. Despite the incredible demands placed on her schedule as an administrator and research director, she always had time to chat or email about career goals even if she was on vacation!

I would like to thank the members of my thesis committee, who have always been willing to provide critical advice on science and career questions, and whose feedback in multiple venues greatly helped shape and advance my work.

Lin Xiao has been a good friend and labmate since we were lucky enough to recruit her in 2011. Her help was instrumental to bringing my work to fruition and interacting with her essentially every day for four years has taught me both new ways to do science as well as provided me with an outlet to laugh with while we worked. It was been a pleasure coming to work with you every day, and I will miss your help both professionally and personally.

The rest of the Dudley lab, for all of their help with experiments, editing, applications, and all the other things that are required for the work we do. You have been an incredible group to work with, and I have enjoyed getting to know all of you through the years. This group has grown too large to thank individually, but I would like to particularly thank Josh Thompson, Mi Mi Kim, James McCann, Clay Davis and Sean Hicks for their help both on this project and in keeping the lab running smoothly.

Rocky Riviella, Dean Riddick, and Tracy Riley in the McAllister Heart Institute have been irreplaceable for their help navigating the nightmare of UNC's administrative and financial policies. Between your help with my fellowships, keeping the numbers straight for our lab, and always willing to have a good chat I cannot thank you enough.

Robert Bagnell, Vicky Madden, and Kristen White in the UNC Microscopy Services Laboratory were always there to answer questions about microscopy of any type, and without them none of the images in my work would have been possible. I always knew if I had an

imaging question there would be an answer, and probably a fresh loaf of bread to go along with it in the basement of Brinkhous-Bullitt.

Kirk McNaughton and Ashley Ezzell sectioned every single piece of tissue I worked with for this work, and have been an invaluable resource for a graduate student just starting out through the end of my graduate career.

Jess Nesmith, for all of the freelance editing of papers, abstracts, award applications, emails, and everything in between. I came to graduate school to earn my Ph.D. and found a wife as a bonus. Your help and willingness to listen to often half-formed ideas in the middle of the night was instrumental in my ability to finish this project.

PREFACE

Chapter 1 is adapted in part from the introduction to a paper published in Nature Communications as well as a review article published in Current Angiogenesis. Chapter 2 and 3 are adapted from the same Nature Communications paper.

TABLE OF CONTENTS

LIST OF FIGURES

LIST OF TABLES

LIST OF ABBREVIATIONS

5-aza	5-azacytidine
Akt	protein kinase B
Ang2	angiopoeitin 2
AP-2α	activating protein 2α
ARMD	age related macular degeneration
BMDC	bone marrow derived cell
BMDEC	bone marrow derived endothelial cell
cAMP	cyclic adenosine monophosphate
CREB	cAMP response element-binding protein
CRISPR	clustered regularly-interspaced short palindromic repeat
CSC	cancer stem cell
Dct	dopachrome tautomerase
DLL4	delta-like 4
EC	endothelial cell
ECFC	endothelial colony forming cell
eNOS	endothelial nitric oxide synthase
EPC	endothelial progenitor cell
EphA2	ephrin A2
Epo	erythropoeitin
FGF2	fibroblast growth factor 2
Flk1	fetal liver kinase 1
GEO	Gene Expression Omnibus

GFP	green fluorescent protein
gPCR	G-protein coupled receptor
H & E	hemotoxylin and eosin
HIF	hypoxia inducible factor
ICAM1	intercellular adhesion molecule 1
Id1	DNA-binding protein inhibitor ID-1
IMG	intussussceptive microvascular growth
ITIM	immunoreceptor tyrosine-based inhibitory motif
KD	knockdown
kD/kDa	kilodaltons
KO	knockout
MART-1	melanoma antigen recognized by T cells 1
MCAM	melanoma cell adhesion molecule
MHz	megahertz
miRNA	microRNA
MITF	micropthalmia induced transcription factor
NOD/SCID	non obese diabatic/severely immunodeficient
NSG	NOD/SCID Il2rγ null
OE	overexpression
Pai-1/Serpine1	plasminogen activator inhibitor-1
PAR-1	protease-activated receptor 1
PCR	polymerase chain reaction
PDGF-β	platelet derived growth factor β

PECAM-1	platelet endothelial cell adhesion molecule-1
PFA	paraformaldehyde
PI3K	phosphoinositide 3-kinase
PKA	protein kinase A
RBC	red blood cells
RBV	relative blood volume
RGP	radial growth phase
RIPA	radioimmunoprecipitation
RT-qPCR	reverse transcription-quantitative polymerase chain reaction
s.e.m	standard error of the mean
SHP2	tyrosine-protein phosphatase non-receptor type 11
siRNA	small interfering ribonucleic acid
Slpi	secretory leukocyte protease inhibitor
TAF	tumor angiogenesis factor
TEC	tumor endothelial cell
TEM	transmission electron microscopy
Thbs1	thrombospondin 1
TIL	tumor infiltrating lympocyte
TNFα	tumor necrosis factor α
TSA	trichostatin A
Tyr	Tyrosinase
VEGF	vascular endothelial growth factor
VEGFR1	vascular endothelial growth factor receptor 1

VEGFR2	vascular endothelial growth factor receptor 2, see also Flk1
VEGFR3	vascular endothelial growth factor receptor 3
VGP	vertical growth phase
VM	vascular mimicry/vasculogenic mimicry
WT	wildtype

CHAPTER 1: Introduction[1]

Tumor angiogenesis as a therapeutic target: A brief history

Solid tumors require blood vessels for growth, access to oxygen and nutrients, and the removal of waste products; and the development of the tumor vasculature has been identified as a hallmark of cancer (Hanahan and Weinberg 2000; Hanahan and Weinberg 2011). Early research in the 1940s-1960s found that in avascular tumor models, without the development of new blood vessels through sprouting angiogenesis. tumor growth was held in check and tumors remained <4 mm (Folkman, Cole, and Zimmerman 1966; Algire and Chalkley 1945). This observation led Dr. Judah Folkman in 1970 to describe a tumor angiogenesis factor (TAF) which was released from tumor cells and elicited strong angiogenic effects in the rat dorsal air sac model (Folkman et al. 1971). The observations of the need for vascular development in tumors of almost every type led Folkman to propose that "if neovascularization is prevented many solid tumors might remain fixed at this [2-3 mm] tiny diameter" (Folkman 1972). Folkman continued studying tumor angiogenesis, and in the decades following his proposal the identification of key pro-angiogenic molecules including bFGF (Shing et al. 1985), PDGF-β and most notably VEGF (Ferrara and Henzel 1989) which was also shown to be secreted by tumor cells shortly after its discovery (Rosenthal et al. 1990). The discovery of the pathways responsible for initiating and maintaining angiogenesis raised interest in the possibility of targeting the molecules in these pathways to blockade angiogenesis. Prevailing theories suggested that as the endothelial cells of

[1] Chapter 1 is adapted in part from Dunleavey, J.M. and Dudley, A.C. "Vascular mimicry: concepts and implications for anti-angiogenic therapy. *Current Angiogenesis*. **1.** 133-138 (2012)

the tumor vasculature are derived from the genetically stable host stroma, anti-angiogenic therapies should not elicit resistance to treatment as is seen with commonly used cytotoxic chemotherapies. Development of anti-angiogenic agents proceeded rapidly through the 1990's and in 2004 the Federal Drug Administration approved bevacizumab, a VEGF ligand-binding antibody for metastatic colorectal cancer following a promising phase III clinical trial (Hurwitz et al. 2004). Subsequent drugs targeted the tyrosine kinase receptors responsible for binding VEGF, primarily VEGFR2, which is largely responsible for the induction of proliferation and migration necessary for endothelial cells to form new stable sprouts. However, despite initial promising results in preclinical trials, introduction of anti-angiogenic agents to cancer patients has shown minor survival benefits compared to control cohorts (Jain 2014; Ellis and Hicklin 2008; Ellis and Fidler 2010; Y. Cao et al. 2011; Carmeliet and Jain 2011). In contrast, a modified antibody fragment of bevacizumab, ranibizumab, has shown high efficacy in treatment of age-related macular degeneration, where aberrant vascular proliferation causes blindness (Stone 2006). These results taken together have led the field to conclude that targeting the VEGF axis may be effective in non-tumor-related neovascularization, but that the tumor vasculature has additional modes of resistance to VEGF blockade and other anti-angiogenesis strategies (Bergers and Hanahan 2008; Carmeliet and Jain 2011).

Modes of tumor vascular development

Decades of work on tumor blood vessels have confirmed at least six routes by which tumors develop a vascular network (Carmeliet and Jain 2011). Most of these processes are conserved between physiologic and pathologic vessel development, but several tumor-specific modes of neovascularization have been described. These processes: vasculogenesis,

angiogenesis, intususceptive branching, vessel cooption, cancer stem cell-derived endothelium, and vascular or vasculogenic mimicry will be summarized in brief.

Vasculogenesis

Vasculogenesis, the de novo creation of nascent vessel beds, is thought to contribute to tumor vessel development (Carmeliet and Jain 2011). Vasculogenesis is best understood in the embryo, where the earliest stages of vascular development occur. Initial studies using embryonic stem cells from mouse blastocysts observed the differentiation of stem cells to cystic embryoid bodies containing "blood islands", or nascent vascular beds, which organized into a differentiated primitive vascular network (Risau et al. 1988). The derivation of these vasculogenic networks from endothelial cell progenitors, termed angioblasts in the embryo, is governed by many of the same factors as angiogenesis, including FGF2 (Cox and Poole 2000), but primarily is thought to be controlled through VEGF signaling, as *Flk1* is prominently upregulated in the angioblast population early in vasculogenesis (Risau and Flamme 1995). Furthermore, *Flk1*-deficient stem cells used to generate *Flk1* chimeric embryos showed a necessity for VEGF signaling through *Flk1*, as $Flk1^{-/-}$ cells failed to contribute to blood islands or nascent vascular beds (Shalaby et al. 1997). In addition to its role in neovascularization in embryogenesis, vasculogenesis has been suggested to occur postnatally through the recruitment of what were initially termed endothelial progenitor cells (EPCs), and more recently termed endothelial colony forming cells (ECFCs). Initial studies identified cells from the mononuclear fraction of human peripheral blood expressing the cell surface antigen CD34 which displayed endothelial phenotypes when cultured (Asahara et al. 1997). However, there remains a controversy whether circulating endothelial cells or their progenitors are involved in tumor vascular development. Gao et al. used GFP-labeled bone marrow introduced to mice following

irradiation, and using immunohistochemistry claimed to find 13% of tumor blood vessels derived from GFP^+ bone marrow (Gao et al. 2008). Furthermore, sex-specific FISH probes in human subjects who had received cross-sex bone marrow transplants revealed marrow-derived cells from donor marrow expressing endothelial markers in tumor blood vessels, albeit at low percentages of total blood vessels examined (Peters et al. 2005). In contrast, previous work from our group found that GFP-labeled bone marrow, when transplanted into irradiated mice failed to adopt endothelial phenotypes by flow cytometry analysis (Dudley et al. 2010). Furthermore, other studies have found little evidence for the incorporation of BMDEC in tumor vessels (Purhonen et al. 2008), although they were met with fierce criticism (Kerbel et al. 2008). The disparity in these data may be explained by a lack of defining markers for BMDEC (Yoder 2009) and the methodologies used. IHC for endothelial markers has a possibility for close overlap with non-endothelial BMDC, while the cytometry experiments performed by our group examined individual cells. Whether bone marrow-derived progenitor cells actively contribute to tumor neovascularization remains one of the major questions facing the field.

Intussusceptive microvascular growth

Intussusception, or intussusceptive microvascular growth (IMG), is a process by which vessel complexity is thought to increase without the need for endothelial cell proliferation or activation. Elegant electron microscopy experiments in 1986 in the rat lung suggested that as the lung develops, vessel complexity increases through the formation of "transcapillary pillars" which divide pre-existing large vessels into separate capillaries, which was thought to allow rapidly growing tissues to increase vascular supply without exponential expansion of the endothelium (Caduff, Fischer, and Burri 1986). The rapidity of intussusception in embryogenesis, which observational microscopy revealed occurred much more quickly than

sprouting angiogenesis, led to the proposal that rapid increases in vessel complexity could aid tumor growth. Indeed, early studies in mouse ascites tumors as well as in human tumor xenografts demonstrated the formation of tumor blood vessels through pre-existing vessel remodeling (Nagy et al. 1995; Patan, Munn, and Jain 1996; Patan et al. 2001), and was observed to take place in human glioblastoma patients (Nico et al. 2009). One study has found a correlation between resistance to anti-VEGF therapy and increases in transcapillary pillars in the tumor vasculature, suggesting a link between IMG and anti-VEGF resistance (Hlushchuk et al. 2010). Interestingly, IMG has been shown to be upregulated by exposure to erythropoietin (Epo), which has been shown to be upregulated in multiple tumor types. However, relatively little is known about the role intussusception plays in tumor vascular development, with less than 20 articles appearing in PubMed on the topic (as of February 2016). It remains to be seen what role this process plays in tumor angiogenesis, and whether discrete pathways independent of those regulating angiogenesis exist for potential therapeutic targeting.

Vessel cooption

Perhaps the simplest way for tumors to enhance their vascular network is to take advantage of pre-tumor physiologic angiogenesis in what has become known as vessel cooption. Simply put, tumors grow along and engulf host blood vessels without the need for generating new vessels. Vessel cooption was initially described in 1999, where it was found that in a rat glioma model, early grade tumors >1mm grew along what appeared to be normal blood vessels and had used these vessels to become perfused. As the tumors progressed, however, these vessels regressed and were partially supplanted by sprouting angiogenesis, which was suggested to be driven by antagonism of Tie2 by angiopoetin-2 (Ang2), triggering erosion of pre-existing vessels followed by VEGF-driven sprouting. Notably, Ang2 has been shown to be upregulated in the

coopted vessels of early tumors (Holash et al. 1999). Ang2 was shown to inhibit tumor angiogenesis when overexpressed, which would support a role for it contributing to erosion of pre-existing vessels in wild-type tumor models (Lee et al. 2006; Y. Cao et al. 2007). Donnem and colleagues surveyed the literature recently and found a large number of studies identifying vessel cooption by tumors, largely in those tumors which originate in highly vascular organs such as the brain and lung (Donnem et al. 2013). They and others have suggested that vessel cooption represents a potent mechanism by which tumors can obtain access to the blood vasculature without initiating angiogenesis (Donnem et al. 2013; Carmeliet and Jain 2011). Interestingly, murine and human studies in glioblastoma have shown that VEGF blockade decreases blood vessel density but vessels remaining post-treatment morphologically resemble those of the normal brain, suggesting that angiogenesis-independent cooption of normal vasculature might contribute to resistance to conventional anti-angiogenic therapies (Rubenstein et al. 2000; Norden et al. 2008). Therefore, to truly inhibit vascularization of tumors, it may be necessary to target mature, nonangiogenic vessels within the tumor in addition to blocking neoangiogenesis. Supporting the theory that cooption is a "fallback" absent angiogenesis, recent data implicating a microRNA cluster (miR-143/145) in tumor neoangiogenesis found that in the absence of tumor angiogenesis tumor vessels have the characteristic honeycomb structure of alveolar blood vessels. This phenotype suggests that impairment of the angiogenic switch may be ameliorated by vascular cooption (Dimitrova et al. 2016). Studies are currently underway testing antagonism of Ang2, and initial reports suggest dual targeting of Ang2 alongside VEGF may improve the efficacy of anti-angiogenesis strategies, but clinical data has not yet been shown to validate Ang2 antagonists as a valid strategy in human cancer patients. Better understanding of

the gene signatures and complexity of mature coopted vessels could perhaps yield new druggable targets in conjunction with existing targeting strategies.

Angiogenesis

Perhaps the best studied of any mode of tumor vessel development is sprouting angiogenesis. Since the initial description of branched sprouts in tumors implanted in the avascular corneal pocket tumor model, the formation of vessels through the extension of sprouts from the pre-existing vasculature to perfuse the tumor has been one of the most intensively studied aspects of tumor biology, and targeting angiogenesis has seen dozens of new drugs brought through clinical trials (Jain 2014). The basic biology of tumor angiogenesis is thought to mirror normal physiologic angiogenic vessel development.

Folkman observed that tumors without a vessel network could only reach a volume of ~4mm. Once a tumor reaches this size, it is proposed that the core of the tumor cannot be sustained by the diffusion of oxygen and nutrients from the peripheral blood vessels. The formation of this hypoxic core stimulates hypoxic response factors, notably the HIF family of proteins, which drive the upregulation and subsequent release of potent endothelial mitogens including VEGF-A (VEGF) (Dor, Porat, and Keshet 2001), and bFGF (Calvani 2006; Krock, Skuli, and Simon 2012) among many others (reviewed in depth by M.C. Simon and colleagues (Krock, Skuli, and Simon 2012)). These soluble factors create gradients of chemokines which work in concert to stimulate the process of sprouting angiogenesis, which I will summarize in brief. The most studied and best understood pathway for neoangiogenesis is mediated through the VEGF pathway. Sprout initiation is thought to begin by upregulation of VEGF ligand in the extracellular environment leading to ligand binding of VEGFR2, which is enhanced by the binding of VEGF co-receptors neuropilin 1 and 2 (Soker et al. 1998). As an alternative or

perhaps as an additive process, VEGF-C has been shown to bind VEGFR3/Flt4 along with NRP2 to trigger sprouting in lymphatic vessels. While VEGFR3 signaling is not sufficient to induce angiogenesis in tumors, if activated alongside VEGFR2 it is sufficient to sustain tumor angiogenesis even after VEGFR2 blockade (Tammela et al. 2008). However VEGF-VEGFR2 signaling is thought to be the primary pro-angiogenic signal from tumors, and will henceforth be referred to as VEGF signaling. Following phosphorylation of the tyrosine kinase receptor, endothelial cells initiate signaling programs which increase cell motility and proliferation while also stimulating upregulation of Notch ligand DLL4, allowing for lateral signaling to neighboring endothelial cells inhibiting further sprouts from forming (Siekmann and Lawson 2007). Notch has been shown to downregulate VEGFR2, suggesting that following the activation of a sprout initiating cell, lateral inhibition through Notch/Dll4 could prevent neighboring cells from receiving VEGF signals, allowing spatial regulation of tip formation (Williams et al. 2006). This selectivity allows an individual sprout to form, wherein the tip cell degrades the basement membrane and migrates towards the VEGF gradient. Furthermore, the VEGF gradient is continually refined in part through secretion of a soluble form of VEGFR1/Flt1 (sFlt1), which binds and sequesters the VEGF ligand without inducing signaling events (Chappell et al. 2009). The specificity of the VEGF gradient allows for a high degree of targeting by the nascent sprout, which can extend into the avascular space and later fuse with other sprouts or mature vessels through anastomosis.

It should be stressed that VEGF is by no means the only factor governing angiogenesis. Dozens of extracellular and intracellular cues regulate sprout initiation and maintenance. However, VEGF occupies a unique position in the field of anti-angiogenesis strategies due to several factors. Perhaps the most striking reason for the focus on VEGF can be traced to initial

loss-of-function genetic experiments wherein inactivation of just one allele of *Vegf* resulted in embryonic lethality and striking vascular defects (Ferrara et al. 1996; Carmeliet et al. 1996). These discoveries led Napoleone Ferrara and others to target the VEGF pathway in tumors, that in preclinical models showed striking success at inhibiting tumor vascular development and growth (Borgström et al. 1996; Borgström et al. 1998; Warren et al. 1995; Ferrara 2002). The success of agents specifically designed to target angiogenesis in preclinical models led to a boom of drugs targeting both VEGF ligand (bevacizumab, aflibercept, ranibizimab, pegaptanib) and receptors (sunitinib, sorafenib, pazaponib, vandetanib). With the introduction of these drugs there have been great successes in treatment of vascular-associated pathologies. Notably, ranibizimab and aflibercept were both approved for treatment of age-related macular degeneration (ARMD) (while bevacizumab has been used off-label for this condition), and have been highly successful at restoring vision in patients with this condition (Rodriguez et al. 2012; Michels et al. 2005). While the results for ARMD have been generally positive, it has been shown that VEGF is necessary for maintenance of Müller cells as well as the photoreceptors of the eye, which casts doubt on the long term efficacy of blockading VEGF (Saint-Geniez et al. 2008). If non-endothelial ocular cells rely on VEGF, sustained blockade of VEGF ligand could damage vision independent of the aberrant neoangiogenesis seen in ARMD. Therefore, even in conditions where anti-angiogenic therapies have been seen as unadulterated successes, there are important considerations to be made about efficacy and long term strategies using these drugs.

The successes at targeting neoangiogenesis in ARMD are tempered by the relative lack of success of anti-VEGF therapies in tumor patients. While the initial phase III clinical trial for bevacizumab in colorectal cancer resulted in ~3 month increases in patient progression free survival (Hurwitz et al. 2004), subsequent clinical trials and clinical data have revealed that the

benefit of anti-angiogenic therapies in patients is modest (Jain 2014). The question posed by the lack of success in anti-angiogenesis research boils down to: is the tumor vasculature more complex than initially thought? Numerous studies following the introduction of anti-VEGF therapies have confirmed that there are multiple ways in which tumors can resist blockade of neoangiogenesis. One major hypothesis to explain the discrepancy between preclinical modeling of anti-VEGF agents and patient responses is the lack of predictive capability of non-human modeling of tumor growth (Ellis and Fidler 2010). Ellis and Fidler suggest that the prevailing models of cancer used for decades fail to physiologically capture the complexity of human tumors. Notably, the injection of boluses of tumor cells fails to recapitulate the potentially decades-long evolution of a tumor from a distinct originating cell. More importantly for anti-angiogenesis modeling, the implantation of a large mass of tumor cells would be predicted to immediately induce hypoxic signaling through HIF-1α and HIF-2β, and that the resulting tumor would be more reliant on neoangiogenesis than other modes of vascularization which may be more common in human patients. Therefore, preclinical modeling in mice, especially those preclinical models used in the early stages of anti-angiogenesis testing, may have generated results that did not accurately forecast patient responses. Fortunately, there have been advances in mouse models of cancer which might improve pre-clinical modeling, although whether the complexity of the decades of tumor development in human patients can be accurately modeled on a shorter time scale remains to be seen (Eklund, Bry, and Alitalo 2013; M. Singh and Ferrara 2012; Francia and Kerbel 2010).

Tumor-specific vascular development

It should be noted there is no clear delineation between the acquisition of endothelial characteristics by tumor cells (vascular mimicry) and the differentiation of multipotent cancer

stem cells (CSCs) into endothelial cells. It is possible that the two processes are in fact stages on a sliding scale of tumor self-vascularization. However, there is no clear linkage of the these two concepts and the field currently treats them as separate modes of tumor vascular development (Carmeliet and Jain 2011), therefore I will discuss them individually.

Cancer stem cell differentiation into endothelial cells

The existence of cancer stem cells or tumor initiating cells has been demonstrated in multiple models, although controversy has existed as to the rarity and consequences of tumor cells differentiating into multiple cell lineages. Initially it was proposed that these tumor-initiating cells were rare, self-renewing cells which mirrored tissue specific stem cells seen in non-tumor conditions. Multiple studies identified rare, tumor initiating cells in colon (Ricci-Vitiani et al. 2006), brain (S. K. Singh et al. 2004), breast (Ponti et al. 2005), skin (Schatton et al. 2008), pancreatic (Adikrisna et al. 2012), head and neck (Prince et al. 2007), ovarian (S. Zhang, Balch, et al. 2008), lung (Eramo et al. 2007), and prostate (Collins et al. 2005) cancers, and have been proposed to be extremely rare (between 1:980 cells to >1:100,000 cells) (Ishizawa et al. 2010) using immunocompromised mice xenograft studies. In contrast, one study found that using NOD/SCID *Il2rg*$^{-/-}$ (NSG) mice, melanoma tumor initiating cells were relatively common (up to 1:5 cells), and suggested that older studies reliant on different mouse models may be flawed (Quintana et al. 2008), while concurrent studies in pancreatic xenografts in NSG recapitulated the rare cell phenotype in NSG mice (Ishizawa et al. 2010). These competing hypotheses may be explained by variations between cancers with different cells-of-origin or through experimental variations, but the rarity of tumor stem cells does not necessarily correlate with the sustained growth of tumors, leading one group to distinguish between tumor initiating stem-like cells and "tumor-propagating cells" that allow for the continued growth of the tumor (Kelly et al. 2007).

Regardless of the rarity of cancer stem cells, it has been shown in several seminal studies that $CD133^+$ tumor stem cells are capable of transdifferentiating into endothelial or endothelial-like cells, and they form part of the vasculature in tumors, notably glioblastoma and breast cancer (Wang et al. 2010; Ricci-Vitiani et al. 2010; Bussolati et al. 2008). To what degree these endothelial cells are in fact bona fide endothelium and whether they retain tumorigenicity and other tumor-specific properties remains unknown. Importantly, one group found that *in vitro*, tumor derived endothelial cells were unresponsive to VEGF stimulation or blockade, suggesting there are fundamental differences between bona fide EC and their tumor-derived counterparts (Soda et al. 2011).

Vascular mimicry

Discovery and controversy

Vascular or vasculogenic mimicry (VM) was initially described in aggressive, uveal forms of melanoma as a process of "dedifferentiation" of tumor cells into an "endothelial-like" phenotype (Maniotis et al. 1999). In these tumors, VM was identified as periodic acid-Schiff (PAS) positive, matrix-associated channels devoid of bona fide endothelium. VM channels appeared to contain erythrocytes and were therefore hypothesized to connect with the existing vasculature. Notably, patients displaying the presence of PAS-positive networks in their tumors had an increased mortality compared to those patients which did not. Following this observation, it was suggested that some tumors were capable of forming their own vascular channels which could carry blood, oxygen and nutrients in collaboration with blood vessels formed by conventional routes of tumor angiogenesis (i.e. sprouting). The clinical implications for VM were clear: VM-forming tumors were more virulent than their non-VM counterparts and VM-lined channels might not respond predictably to conventional anti-angiogenic therapies.

These seminal VM studies were met with criticism at two fronts (McDonald, Munn, and Jain 2010). First, the novelty of the findings was challenged. For example, tumor cell-lined "blood lakes", were identified in uveal melanoma over 40 years prior to the work by Hendrix (Francois 1963; Jensen 1964; Jensen 1976; Francois and Neetens 1967). However, it was not understood at that time that these "blood lakes" were not always physically connected with the vasculature; instead, "blood lakes" were typically formed by erythrocytes which had leaked from poorly formed tumor vessels into the surrounding area (Prause and Jensen 1980; Hammersen, Endrich, and Messmer 1985). Second, the relevance of these findings was questioned, considering the possibility that VM channels were not functional. Moreover, there were serious technical limitations in identifying VM channels using conventional immunohistochemistry, which was prone to artifacts and not entirely objective.

At the same time VM was identified by Hendrix, an alternative mode of tumor cell-originated vasculature was proposed. "Mosaic vessels", whereby tumor cells enter the luminal space of host-derived vasculature were initially described in mouse xenografts of labeled human colon cancer specimens (Chang et al. 2000). Like VM, the concept of mosaic vessels was controversial. It was unclear whether tumor cells were functioning within the vessel wall or were merely an artifact of tumor cells closely positioned near blood vessels or shed into the circulation. Mosaic vessels contrasted the concept of VM, where an entire vascular channel is lined solely by tumor cells, masquerading as endothelium. As concepts, VM and mosaic vessels are not mutually exclusive, and it is possible that both modes of tumor angiogenesis can co-exist within the same tumor (Fig. 1.1).

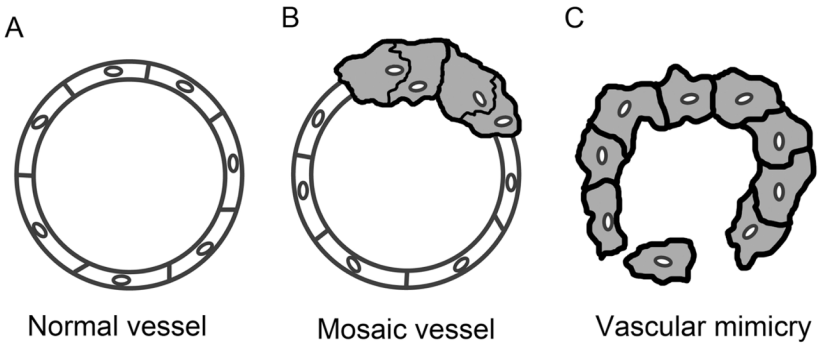

Figure 1.1: Models for tumor-cell-derived vasculature
A) a normal tumor blood vessel lined by vascular endothelial cells **B**) mosaic vessels where tumor cells collaborate with pre-existing endothelium. Tumor cells (shaded) participating as mosaic vessels passively fill in gaps within blood vessel walls. Mosaic tumor cells may co- opt the anti-coagulant properties of existing endothelium and may not express endothelial cell-selective markers **C**) vascular mimicry, whereby tumor cells actively and autonomously create new vessels in the absence of vascular endothelium. These channels are comprised of tumor cells which may acquire features of endothelial cells including expression of endothelial-selective markers, some anti-coagulant properties and ability to transport blood and fluid. Tumor cells, with properties of VM, may also collaborate with co-opted, pre- existing vessels to form hybrid tumor blood vessels.

Recently, VM has re-entered the spotlight in angiogenesis research following the publication of several high-profile research articles on this topic (Wagenblast et al. 2015; Soda et al. 2011) ; see also commentaries by Bautch and Hendrix (Bautch 2010; Hendrix 2015). Importantly, the presence of VM channels in patient samples has recently been shown to predict poor clinical outcomes (Yang et al. 2016; Z. Cao et al. 2013). Irrespective of the advances made in VM research, relatively little is known about the molecular mechanisms and clinical manifestations of VM. Moreover, how VM might impact the effectiveness of anti-angiogenic therapies is not understood.

Characteristics of vascular mimicry

Tumors of vascular origin including hemangioma, angiosarcoma, and Kaposi's sarcoma originate from transformed vascular cells. These tumors, as expected, are highly vascularized,

they are pathologically "bloody," and they are characterized by tangles of poorly formed, atypical vascular structures. In contrast, VM typically designates expression of endothelial factors and acquisition of vascular cell characteristics by tumor cells of a non-vascular origin. Following its initial discovery in uveal melanoma, VM has now been identified in breast (Shirakawa et al. 2002; Wagenblast et al. 2015), ovarian (Sood et al. 2010; Sood et al. 2002), prostate (Sharma et al. 2002), Ewings sarcoma (van der Schaft 2005), hemangiopericytoma (Z. Zhang et al. 2011), astrocytoma (Liu et al. 2011), hepatocellular carcinoma (Guzman et al. 2007), glioblastoma (Wang et al. 2010; Soda et al. 2011; Ricci-Vitiani et al. 2010; Hallani et al. 2010) and lung (Passalidou et al. 2002) cancers. Thus, VM has been described in tumors originating from all three germ layers: ectoderm, mesoderm and endoderm. These findings suggest there may be strong selection pressure for VM within the pool of malignant cells irrespective of cellular ontogeny. Supporting this, in a recent high-profile study of breast cancer heterogeneity, the presence of VM-competent clones in a tumor allowed for efficient intravasation by tumor cells (Wagenblast et al. 2015). A survival advantage may be afforded to tumor cells with greater plasticity and the ability to form their own vascular networks in the face of nutrient and oxygen scarcity characteristic of the tumor microenvironment. Indeed, hypoxic-conditioning of tumor cells promoted their alignment into structures resembling blood vessels and upregulated expression of the endothelial markers vWF and CD31 (Soda et al. 2011). Additionally, hypoxic culturing of VM tumor cell lines increases the expression of a number of endothelial-like factors, including laminin 5 γ2-chain, laminin 411, and EphA2 (R. E. Seftor et al. 2001; Hess et al. 2006; Larson et al. 2014).

Here, I have identified three common characteristics of VM networks in cancer that I consider to be cardinal features of the VM phenotype: expression of endothelial-selective

makers, expression of anti-coagulant factors, and anastomosis/perfusion with the existing vasculature. While these defining characteristics may be common, unifying features of VM, this list is not all-inclusive. Furthermore, VM tumors need not simultaneously display each of these characteristics. For example, tumor-derived channels which connect with the circulation and carry fluid, even without expression of endothelial-selective markers, would embody the definition.

Expression of endothelial-selective markers

Some tumor cells which participate in VM express typical vascular cell markers (E. A. Seftor, Meltzer, Schatteman, et al. 2002; E. A. Seftor, Meltzer, Kirschmann, et al. 2002; Bittner et al. 2000). Expression of VE-cadherin (Hendrix et al. 2001), EphA2 (Hess et al. 2006), CD34 (Soda et al. 2011), and CD31 (Soda et al. 2011) have been described in VM tumors. However, these markers are all selective for and not specific to the vascular endothelium. For example, cells of hematopoietic origin including monocytes, neutrophils, and lymphocytes also express CD31 and CD34. In some cases, expression of these markers by tumor cells may be a "rough attempt" at tumor cell differentiation into vascular-like cells (Pisacane, Picciotto, and Risio 2007). In support of this possibility, VM tumors do not behave predictably in response to treatment with typical endothelial cell mitogens. For example glioblastoma, with features of VM, lack expression of VEGF and bFGF receptors (Soda et al. 2011). The ligands for these receptors are potent endothelial cell mitogens and are indispensable for the survival of bona fide endothelium but may not be necessary for survival of VM tumor cells whose growth is driven by oncogenes. Furthermore, VEGF and bFGF failed to elicit the formation of VM channels, suggesting that factors which are ordinarily pro-angiogenic during development and pathological neovascularization do not necessarily control VM responses (Maniotis et al. 1999). On the other

hand, recent work from the Ellis lab demonstrated expression of VEGFR-2 in ovarian cancer, although it was not determined whether this played a direct role in VM (Spannuth et al. 2009). More recently Rong Shao's group found that VEGFR-2 was involved in VM in a VEGF-independent manner (Francescone et al. 2012; Scully et al. 2012), although the mechanism was unclear. However, expression of VEGF receptors (and other "vascular-like" factors) by tumor cells may not necessarily confer a VM phenotype but may instead reflect acquisition of a survival pathway normally related to endothelial function and development. Good examples are members of the Notch/Nodal pathway commonly involved in embryonic morphogenesis but also involved in the regulation of cellular plasticity in aggressive forms of uveal melanoma (Topczewska et al. 2006; Conway, Collen, and Carmeliet 2001; Khalkhali-Ellis et al. 2014).

Expression of anti-coagulant factors

A major function of vascular endothelium is control of hemostasis, which is achieved by the expression of anticoagulant proteins including tissue factor pathway inhibitors (TFPIs), heparin sulfate proteoglycans, and thrombomodulin at the luminal surface (Pober and Sessa 2007). Blood will coagulate instantaneously when in contact with most tumor cells in the absence of anti-clotting factors (Shoji et al. 1998). Thus, it might be predicted that tumor cells which participate in VM would express anticoagulant factors, or otherwise inhibit clotting by another mechanism. Indeed, some aggressive VM-forming tumors, but not their non-VM counterparts, express proteins involved in the coagulation cascade including TFPI-1 and TFPI-2 (Ruf et al. 2003). Expression of these factors has been detected in VM networks where it is assumed their activity is necessary to allow blood to flow freely by preventing tissue factor-mediated clotting. The presence of anti-coagulant cell-surface markers, coupled with the identification of circulating erythrocytes in the initial discovery of VM, suggests that these

channels may play an active rather than a passive role in fluid transport. While it may be essential that VM channels lined entirely by tumor cells express some proteins of the anti-coagulant system, it is less certain if VM tumor cells which collaborate with host endothelium (e.g. mosaic vessels) require their own anti-coagulant proteins to conduct fluid, or if they can co-opt those of the tumor endothelium. Furthermore, in a study examining breast cancer heterogeneity, the expression of two anti-coagulant genes, *Slpi* and *Serpine2* was sufficient to allow tumor cells to engage in vascular mimicry, and the authors found this VM was able to allow for efficient intravasation and escape of tumor cells from the primary tumor site as well as maintain tumor blood flow (Wagenblast et al. 2015).

Anastomosis with perfused vasculature

Initial discoveries of VM were met with skepticism because it was not believed that tumor cell-lined channels were physically connected with perfused tumor blood vessels. Instead, VM was mostly dismissed as an artifact of tissue sectioning or was ascribed to pooling of erythrocytes in "blood lakes" which were not physically connected with the vasculature. Definitive proof for functioning VM channels has been difficult to establish due to the low fidelity of imaging systems which does not allow for sufficient resolution. For example, the tumor endothelium is typically "squeezed" by the overlying mass of tumor cells resulting in thin, flattened endothelial nuclei which can be difficult to view under standard microscopy (Jain, Munn, and Fukumura 2002). One common approach for demonstrating VM is through the use of fluorescent dyes injected via the tail vein. In one study, fluorophore-conjugated lectin injected intravenously co-localized with $GFAP^+$ glioblastoma cells which is good evidence that the tumor cells were in contact with flowing blood (Soda et al. 2011). Recently, several studies have used advanced imaging techniques including MRI and fluorescent dyes to demonstrate that VM

channels are definitively anastomosed with the vasculature and they exhibit blood flow (Clarijs et al. 2002; Kobayashi et al. 2002; Frenkel et al. 2007). Additionally, injected microbubbles viewed with Doppler imaging revealed a functional connection between host vasculature and VM channels (Ruf et al. 2003).

Origins of vascular mimicry

Highly aggressive, uveal forms of melanoma have served as the VM prototype. These tumors display a high degree of plasticity and cellular heterogeneity which has often been interpreted as a recapitulation of the embryonic stages of development related to the de-differentiation of tumor cells into a more primitive phenotype (E. A. Seftor, Meltzer, Schatteman, et al. 2002; E. A. Seftor, Meltzer, Kirschmann, et al. 2002; Bittner et al. 2000). Evidence for this is given by the genetic signature of some uveal melanoma tumors which reveal loss of melanoma-specific markers including melanoma-cell adhesion molecule and micropthalmia-associated transcription factor and gained expression of markers for cells of diverse origins, especially vascular cells. Remarkably, this plasticity is reversible and reprogrammable by transplanting melanoma cells into an embryonic microenvironment (Hendrix et al. 2007). For example, melanoma cells implanted *in ovo* adjacent to the neuronal crest of embryonic chicks did not form tumors and regained expression of a melanocyte-specific phenotype marker (MART-1) and the neuronal marker Tuj1 (Kulesa et al. 2006). Thus, cues within the microenvironment are capable of instructing melanoma cells to reacquire features of cell types derived from the neural crest, their ancestral cell-of-origin. Furthermore, activation of CD44, which has been implicated in tumor endothelial cell activation (Griffioen et al. 1997), has been shown to activate VM phenotypes in Ewings sarcoma, which suggests there may be parallels between tumor EC and tumor cells engaging in VM (Paulis et al. 2015).

A second possibility is that CSCs, which are not lineage restricted, are the cell-of-origin for some tumor cells with VM characteristics. Theoretically, CSCs would have the potential to differentiate to form cells with multiple phenotypes and multiple functions. For example, many of the factors associated with stem cell maintenance and renewal such as Notch, Wnt, ABCB5, CD133, CD166, nestin, and c-kit, are over-expressed in aggressive cancers displaying a VM phenotype (Hendrix et al. 2003; Hoek et al. 2004; Weeraratna et al. 2002; Klein et al. 2006; Frank et al. 2005).

Similar to melanoma, CSC or "CSC-like" cells are reported to form blood vessels in aggressive glioblastoma. For example, CD133+/CD144+ glioblastoma stem-like cells (GSC) were reported to undergo differentiation into endothelium which was blocked by γ-secretase inhibitors or Notch1 silencing (Wang et al. 2010). These tumor-derived endothelial cells carried glioblastoma-specific chromosomal aberrations, were not sensitive to VEGF inhibition, and contributed substantially to the tumor vasculature (range of 20–90% of TEC). Moreover, GSC-derived blood vessels were functional because their selective depletion dramatically impaired tumor growth. Because a significant proportion of the vasculature may be of neoplastic origin in some tumor types, it is possible that these tumors would not respond predictably to conventional angiogenesis inhibitors. Moreover, rare CSC with an inherent ability to differentiate and form endothelial-like cells may be selected for in response to angiogenesis inhibition. Thus, it is feasible that VM may underlie tumor escape and vascular rebound following an initial vessel pruning response after treatment with drugs such as bevacizumab.

Can VM underlie resistance to anti-angiogenic therapies?

Anti-angiogenic therapy advocates posited that if the tumor's "plumbing" could be selectively eliminated, so could access to oxygen and nutrients. Inhibition of tumor-associated

blood vessels would also eliminate the principal routes of metastasis. However as outlined above, inhibitors of angiogenesis have demonstrated limited efficacy at inhibiting tumor growth while effectively blocking angiogenesis in non-tumor diseases. VM offers one attractive and feasible mechanism for a drug resistance paradigm following the use of angiogenesis inhibitors. Indeed, melanoma tube-forming ability was completely unaltered by the prototypical angiogenesis inhibitor, endostatin, whereas normal endothelial cells were strongly inhibited (van der Schaft et al. 2004).

Initially, anti-angiogenic treatment is thought to be successful because it targets and destroys bona fide endothelium. One consequence of angiogenesis inhibition is the exacerbation of hypoxia, which creates selection pressure for hypoxia-tolerant tumor cells and stimulates expression of factors (e.g. VEGF) which support vessel regrowth. Interestingly, VM-positive Ewings sarcoma were closely localized with areas of hypoxia, suggesting the VM may be a response to inadequate vascularization by normal angiogenic processes (van der Schaft 2005). Indeed, knockdown of VEGF-A in melanoma xenografts reduced tumor growth in some cell lines but increased the frequency of VM, which was attributed to increased hypoxic signaling (Schnegg et al. 2015). Whereas vascular endothelium may be responsive to VEGF inhibition, some tumor cells participating in VM may not be dependent on VEGF for survival, so it is unlikely that therapies which trap and inactivate VEGF would be very effective at targeting these cells. In fact, the initial discovery of VM revealed that it was insensitive to VEGF stimulation (Maniotis et al. 1999). In further support of this theory, AG28262 (a selective inhibitor of VEGFR-1, R-2 and R-3) had no effect on *in vitro* tube formation or percentage of glioblastoma tumor-derived vessels *in vivo* (Soda et al. 2011). On the other hand, thalidomide, an angiogenic

inhibitor which is not believed to interfere with the VEGF pathway, could eradicate VM channels in melanoma *in vivo* (S. Zhang, Li, et al. 2008).

Perspective

The concept of VM, initially met with skepticism, has received renewed attention in the field of angiogenesis research. As studies highlight the disappointing, and unexpected consequences of angiogenesis inhibition in tumors, it is tempting to speculate that VM may be an underlying, perhaps overlooked mechanism of escape to these therapies (Ruf et al. 2003; Jain, Munn, and Fukumura 2002; Bergers and Hanahan 2008). A PubMed search of "vascular mimicry" returns ~419 articles dating back to 1999, with almost 300 articles being published in the last 5 years and recently a burst of high profile studies provide new evidence supporting the existence of VM. Furthermore, while VM was initially described in aggressive forms of uveal melanoma, the list of tumor types displaying characteristics of VM is growing. Still, there are many remaining questions. For example, does VM play a substantial role in metastasis? Do tumor cells form their own lymphatic vessels using processes similar to VM (lymphangiogenic mimicry)? And finally, if tumors can self-vascularize, is an anti-angiogenic approach for shrinking solid tumors feasible?

As we learn more about the molecular mechanisms and genetic signature of VM, it is possible that tumors could be segregated as likely or unlikely to respond to angiogenesis inhibition. Moreover, it is not expected that all tumor types would have the intrinsic ability to carry out VM and these tumors might respond favorably to anti-VEGF or other anti-angiogenic inhibitors. Thus, VM may not be an intractable problem for cancer therapy but yet another complex adaptation of cancer cells struggling to survive in the face of nutrient and oxygen scarcity. Interestingly, a recent publication by the discoverer of vascular mimicry, Mary Hendrix,

describes a novel therapeutic aimed at targeting VM with a small molecule inhibitor, which could be used in conjunction with anti-angiogenic strategies to block tumor vascular development on multiple axes (Hendrix, Seftor et al.. 2016).

REFERENCES

Adikrisna, Rama, Shinji Tanaka, Shunsuke Muramatsu, Arihiro Aihara, Daisuke Ban, Takanori Ochiai, Takumi Irie, et al. 2012. "Identification of Pancreatic Cancer Stem Cells and Selective Toxicity of Chemotherapeutic Agents.." Gastroenterology 143 (1): 234–37. doi:10.1053/j.gastro.2012.03.054.

Algire, Glenn H, and Harold W Chalkley. 1945. "Vascular Reactions of Normal and Malignant Tissues in Vivo. I. Vascular Reactions of Mice to Wounds and to Normal and Neoplastic Transplants." Journal of the National Cancer Institute 6 (73): 73–85.

Asahara, T, T Murohara, A Sullivan, M Silver, R van der Zee, T Li, B Witzenbichler, G Schatteman, and J M Isner. 1997. "Isolation of Putative Progenitor Endothelial Cells for Angiogenesis.." Science 275 (5302): 964–67.

Bautch, Victoria L. 2010. "Tumour Stem Cells Switch Sides.." Nature 468 (7325): 770–71. doi:10.1038/468770a.

Bergers, Gabriele, and Douglas Hanahan. 2008. "Modes of Resistance to Anti-Angiogenic Therapy." Nature Reviews Cancer 8 (8): 592–603. doi:10.1038/nrc2442.

Bittner, M, P Meltzer, Y Chen, Y Jiang, E Seftor, M Hendrix, M Radmacher, et al. 2000. "Molecular Classification of Cutaneous Malignant Melanoma by Gene Expression Profiling.." Nature 406 (6795): 536–40. doi:10.1038/35020115.

Borgström, P, K J Hillan, P Sriramarao, and N Ferrara. 1996. "Complete Inhibition of Angiogenesis and Growth of Microtumors by Anti-Vascular Endothelial Growth Factor Neutralizing Antibody: Novel Concepts of Angiostatic Therapy From Intravital Videomicroscopy.." Cancer Research 56 (17): 4032–39.

Borgström, P, M A Bourdon, K J Hillan, P Sriramarao, and N Ferrara. 1998. "Neutralizing Anti-Vascular Endothelial Growth Factor Antibody Completely Inhibits Angiogenesis and Growth of Human Prostate Carcinoma Micro Tumors in Vivo.." The Prostate 35 (1): 1–10.

Bussolati, Benedetta, Cristina Grange, Anna Sapino, and Giovanni Camussi. 2008. "Endothelial Cell Differentiation of Human Breast Tumour Stem/Progenitor Cells." Journal of Cellular and Molecular Medicine 13 (2): 309–19. doi:10.1111/j.1582-4934.2008.00338.x.

Caduff, J H, L C Fischer, and P H Burri. 1986. "Scanning Electron Microscope Study of the Developing Microvasculature in the Postnatal Rat Lung.." The Anatomical Record 216 (2): 154–64. doi:10.1002/ar.1092160207.

Calvani, M. 2006. "Hypoxic Induction of an HIF-1 -Dependent bFGF Autocrine Loop Drives Angiogenesis in Human Endothelial Cells." Blood 107 (7): 2705–12. doi:10.1182/blood-2005-09-3541.

Cao, Y, P Sonveaux, S Liu, Y Zhao, J Mi, B M Clary, C Y Li, C D Kontos, and M W Dewhirst. 2007. “Systemic Overexpression of Angiopoietin-2 Promotes Tumor Microvessel Regression and Inhibits Angiogenesis and Tumor Growth.” Cancer Research 67 (8): 3835–44. doi:10.1158/0008-5472.CAN-06-4056.

Cao, Yihai, Jack Arbiser, Robert J D'Amato, Patricia A D'Amore, Donald E Ingber, Robert Kerbel, Michael Klagsbrun, et al. 2011. “Forty-Year Journey of Angiogenesis Translational Research..” Science Translational Medicine 3 (114): 114rv3. doi:10.1126/scitranslmed.3003149.

Cao, Zhifei, Meimei Bao, Lucio Miele, Fazlul H Sarkar, Zhiwei Wang, and Quansheng Zhou. 2013. “Tumour Vasculogenic Mimicry Is Associated with Poor Prognosis of Human Cancer Patients: a Systemic Review and Meta-Analysis.” European Journal of Cancer 49 (18). Elsevier Ltd: 3914–23. doi:10.1016/j.ejca.2013.07.148.

Carmeliet, P, V Ferreira, G Breier, S Pollefeyt, L Kieckens, M Gertsenstein, M Fahrig, et al. 1996. “Abnormal Blood Vessel Development and Lethality in Embryos Lacking a Single VEGF Allele..” Nature 380 (6573): 435–39. doi:10.1038/380435a0.

Carmeliet, Peter, and Rakesh K Jain. 2011. “Molecular Mechanisms and Clinical Applications of Angiogenesis.” Nature 473 (7347): 298–307. doi:10.1038/nature10144.

Chang, Y S, E di Tomaso, D M McDonald, R Jones, R K Jain, and L L Munn. 2000. “Mosaic Blood Vessels in Tumors: Frequency of Cancer Cells in Contact with Flowing Blood..” Proceedings of the National Academy of Sciences 97 (26): 14608–13. doi:10.1073/pnas.97.26.14608.

Chappell, John C, Sarah M Taylor, Napoleone Ferrara, and Victoria L Bautch. 2009. “Local Guidance of Emerging Vessel Sprouts Requires Soluble Flt-1.” Developmental Cell 17 (3). Elsevier Ltd: 377–86. doi:10.1016/j.devcel.2009.07.011.

Clarijs, Ruud, Irene Otte-Höller, Dirk J Ruiter, and Robert M W de Waal. 2002. “Presence of a Fluid-Conducting Meshwork in Xenografted Cutaneous and Primary Human Uveal Melanoma..” Investigative Ophthalmology & Visual Science 43 (4): 912–18.

Collins, Anne T, Paul A Berry, Catherine Hyde, Michael J Stower, and Norman J Maitland. 2005. “Prospective Identification of Tumorigenic Prostate Cancer Stem Cells..” Cancer Research 65 (23): 10946–51. doi:10.1158/0008-5472.CAN-05-2018.

Conway, E M, D Collen, and P Carmeliet. 2001. “Molecular Mechanisms of Blood Vessel Growth..” Cardiovascular Research 49 (3): 507–21.

Cox, C M, and T J Poole. 2000. “Angioblast Differentiation Is Influenced by the Local Environment: FGF-2 Induces Angioblasts and Patterns Vessel Formation in the Quail Embryo..” Developmental Dynamics : an Official Publication of the American Association of Anatomists 218 (2): 371–82. doi:10.1002/ (SICI)1097-0177 (200006)218:2.

Dimitrova, N, V Gocheva, A Bhutkar, R Resnick, R M Jong, K M Miller, J Bendor, and T Jacks. 2016. “Stromal Expression of miR-143/145 Promotes Neoangiogenesis in Lung Cancer Development.” Cancer Discovery 6 (2): 188–201. doi:10.1158/2159-8290.CD-15-0854.

Donnem, Tom, Jiangting Hu, Mary Ferguson, Omanma Adighibe, Cameron Snell, Adrian L Harris, Kevin C Gatter, and Francesco Pezzella. 2013. “Vessel Co-Option in Primary Human Tumors and Metastases: an Obstacle to Effective Anti-Angiogenic Treatment?.” Cancer Medicine 2 (4): 427–36. doi:10.1002/cam4.105.

Dor, Y, R Porat, and E Keshet. 2001. “Vascular Endothelial Growth Factor and Vascular Adjustments to Perturbations in Oxygen Homeostasis..” American Journal of Physiology. Cell Physiology 280 (6): C1367–74.

Dudley, A C, T Udagawa, J M Melero-Martin, S C Shih, A Curatolo, M A Moses, and M Klagsbrun. 2010. “Bone Marrow Is a Reservoir for Proangiogenic Myelomonocytic Cells but Not Endothelial Cells in Spontaneous Tumors.” Blood 116 (17): 3367–71. doi:10.1182/blood-2010-02-271122.

Eklund, Lauri, Maija Bry, and Kari Alitalo. 2013. “Mouse Models for Studying Angiogenesis and Lymphangiogenesis in Cancer.” Molecular Oncology 7 (2). Elsevier B.V: 259–82. doi:10.1016/j.molonc.2013.02.007.

Ellis, L M, and D J Hicklin. 2008. “Pathways Mediating Resistance to Vascular Endothelial Growth Factor-Targeted Therapy.” Clinical Cancer Research 14 (20): 6371–75. doi:10.1158/1078-0432.CCR-07-5287.

Ellis, Lee M, and Isaiah J. Fidler. 2010. “Finding the Tumor Copycat. Therapy Fails, Patients Don't..” Nature Medicine 16 (9): 974–75. doi:10.1038/nm0910-974.

Eramo, A, F Lotti, G Sette, E Pilozzi, M Biffoni, A Di Virgilio, C Conticello, L Ruco, C Peschle, and R De Maria. 2007. “Identification and Expansion of the Tumorigenic Lung Cancer Stem Cell Population.” Cell Death and Differentiation 15 (3): 504–14. doi:10.1038/sj.cdd.4402283.

Ferrara, N, and W J Henzel. 1989. “Pituitary Follicular Cells Secrete a Novel Heparin-Binding Growth Factor Specific for Vascular Endothelial Cells..” Biochemical and Biophysical Research Communications 161 (2): 851–58.

Ferrara, N, K Carver-Moore, H Chen, M Dowd, L Lu, K S O'Shea, L Powell-Braxton, K J Hillan, and M W Moore. 1996. “Heterozygous Embryonic Lethality Induced by Targeted Inactivation of the VEGF Gene..” Nature 380 (6573): 439–42. doi:10.1038/380439a0.

Ferrara, Napoleone. 2002. “VEGF and the Quest for Tumour Angiogenesis Factors..” Nature Reviews Cancer 2 (10): 795–803. doi:10.1038/nrc909.

Folkman, J, E Merler, C Abernathy, and G Williams. 1971. “Isolation of a Tumor Factor Responsible for Angiogenesis..” The Journal of Experimental Medicine 133 (2): 275–88.

Folkman, J, P Cole, and S Zimmerman. 1966. “Tumor Behavior in Isolated Perfused Organs: in Vitro Growth and Metastases of Biopsy Material in Rabbit Thyroid and Canine Intestinal Segment..” Annals of Surgery 164 (3): 491–502.

Folkman, Judah. 1972. “Anti-Angiogenesis: New Concept for Therapy of Solid Tumors..” Annals of Surgery 175 (3): 409–16.

Francescone, Ralph, Steve Scully, Brooke Bentley, Wei Yan, Sherry L Taylor, Dennis Oh, Luis Moral, and Rong Shao. 2012. “Glioblastoma-Derived Tumor Cells Induce Vasculogenic Mimicry Through Flk-1 Protein Activation..” Journal of Biological Chemistry 287 (29): 24821–31. doi:10.1074/jbc.M111.334540.

Francia, Giulio, and Robert S Kerbel. 2010. “Raising the Bar for Cancer Therapy Models..” Nature Biotechnology 28 (6): 561–62. doi:10.1038/nbt0610-561.

Francois, J. 1963. “Malignant Melanomata of the Choroid.” The British Journal of Ophthalmology 47 (December): 736–43.

Francois, J, and A Neetens. 1967. “Physico-Anatomical Studies of Spontaneous and Experimental Intraocular Newgrowths: Vascular Supply..” Bibliotheca Anatomica 9: 403–11.

Frank, Natasha Y, Armen Margaryan, Ying Huang, Tobias Schatton, Ana Maria Waaga-Gasser, Martin Gasser, Mohamed H Sayegh, Wolfgang Sadee, and Markus H Frank. 2005. “ABCB5-Mediated Doxorubicin Transport and Chemoresistance in Human Malignant Melanoma..” Cancer Research 65 (10): 4320–33. doi:10.1158/0008-5472.CAN-04-3327.

Frenkel, S, I Barzel, J Levy, A Y Lin, D-U Bartsch, D Majumdar, R Folberg, and J Pe'er. 2007. “Demonstrating Circulation in Vasculogenic Mimicry Patterns of Uveal Melanoma by Confocal Indocyanine Green Angiography.” Eye 22 (7): 948–52. doi:10.1038/sj.eye.6702783.

Gao, Dingcheng, Daniel J Nolan, Albert S Mellick, Kathryn Bambino, Kevin McDonnell, and Vivek Mittal. 2008. “Endothelial Progenitor Cells Control the Angiogenic Switch in Mouse Lung Metastasis..” Science 319 (5860): 195–98. doi:10.1126/science.1150224.

Griffioen, A W, M J Coenen, C A Damen, S M Hellwig, D H van Weering, W Vooys, G H Blijham, and G Groenewegen. 1997. “CD44 Is Involved in Tumor Angiogenesis; an Activation Antigen on Human Endothelial Cells..” Blood 90 (3): 1150–59.

Guzman, Grace, Scott J Cotler, Amy Y Lin, Andrew J Maniotis, and Robert Folberg. 2007. “A Pilot Study of Vasculogenic Mimicry Immunohistochemical Expression in Hepatocellular Carcinoma..” Archives of Pathology & Laboratory Medicine 131 (12): 1776–81.

doi:10.1043/1543-2165 (2007)131[1776:APSOVM]2.0.CO;2.

Hallani, El, S, B Boisselier, F Peglion, A Rousseau, C Colin, A Idbaih, Y Marie, et al. 2010. "A New Alternative Mechanism in Glioblastoma Vascularization: Tubular Vasculogenic Mimicry." Brain 133 (4): 973–82. doi:10.1093/brain/awq044.

Hammersen, F, B Endrich, and K Messmer. 1985. "The Fine Structure of Tumor Blood Vessels. I. Participation of Non-Endothelial Cells in Tumor Angiogenesis" 4 (1): 31–43.

Hanahan, Douglas, and Robert A Weinberg. 2000. "The Hallmarks of Cancer." Cell 100 (1): 57–70.

Hanahan, Douglas, and Robert A Weinberg. 2011. "Hallmarks of Cancer: the Next Generation." Cell 144 (5). Elsevier Inc.: 646–74. doi:10.1016/j.cell.2011.02.013.

Hendrix, M J, E A Seftor, P S Meltzer, L M Gardner, A R Hess, D A Kirschmann, G C Schatteman, and R E Seftor. 2001. "Expression and Functional Significance of VE-Cadherin in Aggressive Human Melanoma Cells: Role in Vasculogenic Mimicry.." Proceedings of the National Academy of Sciences of the United States of America 98 (14): 8018–23. doi:10.1073/pnas.131209798.

Hendrix, Mary J C, Elisabeth A Seftor, Richard E B Seftor, Jun-Tzu Chao, Du-Shieng Chien, and Yi-Wen Chu. 2016. "Pharmacology & Therapeutics." Pharmacology and Therapeutics, February. Elsevier Inc., 1–10. doi:10.1016/j.pharmthera.2016.01.006.

Hendrix, Mary J C. 2015. "Cancer: an Extravascular Route for Tumour Cells.." Nature 520 (7547): 300–302. doi:10.1038/nature14382.

Hendrix, Mary J C, Elisabeth A Seftor, Angela R Hess, and Richard E B Seftor. 2003. "Vasculogenic Mimicry and Tumour-Cell Plasticity: Lessons From Melanoma.." Nature Reviews Cancer 3 (6): 411–21. doi:10.1038/nrc1092.

Hendrix, Mary J C, Elisabeth A Seftor, Richard E B Seftor, Jennifer Kasemeier-Kulesa, Paul M Kulesa, and Lynne-Marie Postovit. 2007. "Reprogramming Metastatic Tumour Cells with Embryonic Microenvironments." Nature Reviews Cancer 7 (4): 246–55. doi:10.1038/nrc2108.

Hess, Angela R, Elisabeth A Seftor, Lynn M Gruman, Michael S Kinch, Richard E B Seftor, and Mary J C Hendrix. 2006. "VE-Cadherin Regulates EphA2 in Aggressive Melanoma Cells Through a Novel Signaling Pathway: Implications for Vasculogenic Mimicry.." Cancer Biology & Therapy 5 (2): 228–33.

Hlushchuk, Ruslan, Oliver Riesterer, Oliver Baum, Jeanette Wood, Guenther Gruber, Martin Pruschy, and Valentin Djonov. 2010. "Tumor Recovery by Angiogenic Switch From Sprouting to Intussusceptive Angiogenesis After Treatment with PTK787/ZK222584 or Ionizing Radiation." The American Journal of Pathology 173 (4). American Society for

Investigative Pathology: 1173–85. doi:10.2353/ajpath.2008.071131.

Hoek, Keith, David L Rimm, Kenneth R Williams, Hongyu Zhao, Stephan Ariyan, Aiping Lin, Harriet M Kluger, et al. 2004. "Expression Profiling Reveals Novel Pathways in the Transformation of Melanocytes to Melanomas.." Cancer Research 64 (15): 5270–82. doi:10.1158/0008-5472.CAN-04-0731.

Holash, J, P C Maisonpierre, D Compton, P Boland, C R Alexander, D Zagzag, G D Yancopoulos, and S J Wiegand. 1999. "Vessel Cooption, Regression, and Growth in Tumors Mediated by Angiopoietins and VEGF.." Science 284 (5422): 1994–98.

Hurwitz, Herbert, Louis Fehrenbacher, William Novotny, Thomas Cartwright, John Hainsworth, William Heim, Jordan Berlin, et al. 2004. "Bevacizumab Plus Irinotecan, Fluorouracil, and Leucovorin for Metastatic Colorectal Cancer.." New England Journal of Medicine 350 (23): 2335–42. doi:10.1056/NEJMoa032691.

Ishizawa, Kota, Zeshaan A Rasheed, Robert Karisch, Qiuju Wang, Jeanne Kowalski, Erica Susky, Keira Pereira, et al. 2010. "Tumor-Initiating Cells Are Rare in Many Human Tumors.." Cell Stem Cell 7 (3): 279–82. doi:10.1016/j.stem.2010.08.009.

Jain, Rakesh K. 2014. "Perspective." Cancer Cell 26 (5). Elsevier Inc.: 605–22. doi:10.1016/j.ccell.2014.10.006.

Jain, Rakesh K, Lance L Munn, and Dai Fukumura. 2002. "Dissecting Tumour Pathophysiology Using Intravital Microscopy.." Nature Reviews Cancer 2 (4): 266–76. doi:10.1038/nrc778.

Jensen, O A. 1964. "Malignant Melanoma of the Choroid of a Peculiar Cavernous Type. Clinical Manifestation by Hemorrhage of the Vitreous Body." Archives of Ophthalmology 72 (September): 337–40.

Jensen, O A. 1976. "The "Knapp-Ronne" Type of Malignant Melanoma of the Choroid. a Haemangioma-Like Melanoma with a Typical Clinical Picture. So-Called "Preretinal Malignant Choroidal Melanoma"." Acta Opthalmoliogica 54 (January).

Kelly, P N, A Dakic, J M Adams, S L Nutt, and A Strasser. 2007. "Tumor Growth Need Not Be Driven by Rare Cancer Stem Cells." Science 317 (5836): 337–37. doi:10.1126/science.1142596.

Kerbel, Robert S, Robert Benezra, David C Lyden, Koichi Hattori, Beate Heissig, Daniel J Nolan, Vivek Mittal, et al. 2008. "Endothelial Progenitor Cells Are Cellular Hubs Essential for Neoangiogenesis of Certain Aggressive Adenocarcinomas and Metastatic Transition but Not Adenomas.." Proceedings of the National Academy of Sciences of the United States of America 105 (34): E54–E55. doi:10.1073/pnas.0804876105.

Khalkhali-Ellis, Zhila, Dawn A Kirschmann, Elisabeth A Seftor, Alina Gilgur, Thomas M Bodenstine, Andrew P Hinck, and Mary J C Hendrix. 2014. "Divergence (S) in Nodal

Signaling Between Aggressive Melanoma and Embryonic Stem Cells." International Journal of Cancer 136 (5): E242–51. doi:10.1002/ijc.29198.

Klein, Walter M, Bryan P Wu, Shuping Zhao, Hong Wu, Andres J P Klein-Szanto, and Steven R Tahan. 2006. "Increased Expression of Stem Cell Markers in Malignant Melanoma." Modern Pathology 20 (1): 102–7. doi:10.1038/modpathol.3800720.

Kobayashi, Hisataka, Kazuo Shirakawa, Satomi Kawamoto, Tsuneo Saga, Noriko Sato, Akira Hiraga, Ichiro Watanabe, et al. 2002. "Rapid Accumulation and Internalization of Radiolabeled Herceptin in an Inflammatory Breast Cancer Xenograft with Vasculogenic Mimicry Predicted by the Contrast-Enhanced Dynamic MRI with the Macromolecular Contrast Agent G6- (1B4M-Gd) (256).." Cancer Research 62 (3): 860–66.

Krock, B L, N Skuli, and M C Simon. 2012. "Hypoxia-Induced Angiogenesis: Good and Evil." Genes & Cancer 2 (12): 1117–33. doi:10.1177/1947601911423654.

Kulesa, Paul M, Jennifer C Kasemeier-Kulesa, Jessica M Teddy, Naira V Margaryan, Elisabeth A Seftor, Richard E B Seftor, and Mary J C Hendrix. 2006. "Reprogramming Metastatic Melanoma Cells to Assume a Neural Crest Cell-Like Phenotype in an Embryonic Microenvironment.." Proceedings of the National Academy of Sciences 103 (10): 3752–57. doi:10.1073/pnas.0506977103.

Larson, Allison R, Chung-Wei Lee, Cecilia Lezcano, Qian Zhan, John Huang, Andrew H Fischer, and George F Murphy. 2014. "Melanoma Spheroid Formation Involves Laminin-Associated Vasculogenic Mimicry.." The American Journal of Pathology 184 (1): 71–78. doi:10.1016/j.ajpath.2013.09.020.

Lee, Ok-Hee, Juan Fueyo, Jing Xu, W K Alfred Yung, Michael G Lemoine, Frederick F Lang, B Nebiyou Bekele, et al. 2006. "Sustained Angiopoietin-2 Expression Disrupts Vessel Formation and Inhibits Glioma Growth." Neoplasia 8 (5). Neoplasia Press, Inc.: 419–28. doi:10.1593/neo.06109.

Liu, Zhengcao, Yue Li, Wei Zhao, Ying Ma, and Xianghong Yang. 2011. "Pathology – Research and Practice." Pathology -- Research and Practice 207 (10). Elsevier GmbH.: 645–51. doi:10.1016/j.prp.2011.07.012.

Maniotis, A J, R Folberg, A Hess, E A Seftor, L M Gardner, J Pe'er, J M Trent, P S Meltzer, and M J Hendrix. 1999. "Vascular Channel Formation by Human Melanoma Cells in Vivo and in Vitro: Vasculogenic Mimicry.." Ajpa 155 (3): 739–52. doi:10.1016/S0002-9440 (10)65173-5.

McDonald, Donald M, Lance Munn, and Rakesh K Jain. 2010. "Vasculogenic Mimicry: How Convincing, How Novel, and How Significant?." The American Journal of Pathology 156 (2). American Society for Investigative Pathology: 383–88. doi:10.1016/S0002-9440 (10)64740-2.

Michels, Stephan, Philip J Rosenfeld, Carmen A Puliafito, Erin N Marcus, and Anna S Venkatraman. 2005. "Systemic Bevacizumab (Avastin) Therapy for Neovascular Age-Related Macular Degeneration Twelve-Week Results of an Uncontrolled Open-Label Clinical Study.." Ophthalmology 112 (6): 1035–47. doi:10.1016/j.ophtha.2005.02.007.

Nagy, J A, E S Morgan, K T Herzberg, E J Manseau, A M Dvorak, and H F Dvorak. 1995. "Pathogenesis of Ascites Tumor Growth: Angiogenesis, Vascular Remodeling, and Stroma Formation in the Peritoneal Lining.." Cancer Research 55 (2): 376–85.

Nico, Beatrice, Enrico Crivellato, Diego Guidolin, Tiziana Annese, Vito Longo, Nicoletta Finato, Angelo Vacca, and Domenico Ribatti. 2009. "Intussusceptive Microvascular Growth in Human Glioma." Clinical and Experimental Medicine 10 (2): 93–98. doi:10.1007/s10238-009-0076-7.

Norden, A D, G S Young, K Setayesh, A Muzikansky, R Klufas, G L Ross, A S Ciampa, et al. 2008. "Bevacizumab for Recurrent Malignant Gliomas: Efficacy, Toxicity, and Patterns of Recurrence.." Neurology 70 (10): 779–87. doi:10.1212/01.wnl.0000304121.57857.38.

Passalidou, E, M Trivella, N Singh, M Ferguson, J Hu, A Cesario, P Granone, et al. 2002. "Vascular Phenotype in Angiogenic and Non-Angiogenic Lung Non-Small Cell Carcinomas.." British Journal of Cancer 86 (2): 244–49. doi:10.1038/sj.bjc.6600015.

Patan, S, L L Munn, and R K Jain. 1996. "Intussusceptive Microvascular Growth in a Human Colon Adenocarcinoma Xenograft: a Novel Mechanism of Tumor Angiogenesis.." Microvascular Research 51 (2): 260–72. doi:10.1006/mvre.1996.0025.

Patan, S, S Tanda, S Roberge, R C Jones, R K Jain, and L L Munn. 2001. "Vascular Morphogenesis and Remodeling in a Human Tumor Xenograft: Blood Vessel Formation and Growth After Ovariectomy and Tumor Implantation.." Circulation Research 89 (8): 732–39.

Paulis, Yvette W J, Elisabeth J M Huijbers, Daisy W J van der Schaft, Patricia M M B Soetekouw, Patrick Pauwels, Vivianne C G Tjan-Heijnen, and Arjan W Griffioen. 2015. "CD44 Enhances Tumor Aggressiveness by Promoting Tumor Cell Plasticity.." Oncotarget 6 (23): 19634–46. doi:10.18632/oncotarget.3839.

Peters, Brock A, Luis A Diaz, Kornelia Polyak, Leslie Meszler, Kathy Romans, Eva C Guinan, Joseph H Antin, et al. 2005. "Contribution of Bone Marrow–Derived Endothelial Cells to Human Tumor Vasculature." Nature Medicine 11 (3): 261–62. doi:10.1038/nm1200.

Pisacane, A M, F Picciotto, and M Risio. 2007. "CD31 and CD34 Expression as Immunohistochemical Markers of Endothelial Transdifferentiation in Human Cutaneous Melanoma." Cellular Oncology : the Official Journal of the International Society for Cellular Oncology 29 (1): 59–66.

Pober, Jordan S, and William C Sessa. 2007. "Evolving Functions of Endothelial Cells in Inflammation." Nature Reviews Immunology 7 (10): 803–15. doi:10.1038/nri2171.

Ponti, Dario, Aurora Costa, Nadia Zaffaroni, Graziella Pratesi, Giovanna Petrangolini, Danila Coradini, Silvana Pilotti, Marco A Pierotti, and Maria Grazia Daidone. 2005. "Isolation and in Vitro Propagation of Tumorigenic Breast Cancer Cells with Stem/Progenitor Cell Properties.." Cancer Research 65 (13): 5506–11. doi:10.1158/0008-5472.CAN-05-0626.

Prause, J U, and O A Jensen. 1980. "Scanning Electron Microscopy of Frozen-Cracked, Dry-Cracked and Enzyme-Digested Tissue of Human Malignant Choroidal Melanomas.." Albrecht Von Graefes Archiv Für Klinische Und Experimentelle Ophthalmologie. Albrecht Von Graefe's Archive for Clinical and Experimental Ophthalmology 212 (3-4): 217–25.

Prince, M E, R Sivanandan, A Kaczorowski, G T Wolf, M J Kaplan, P Dalerba, I L Weissman, M F Clarke, and L E Ailles. 2007. "Identification of a Subpopulation of Cells with Cancer Stem Cell Properties in Head and Neck Squamous Cell Carcinoma.." Proceedings of the National Academy of Sciences 104 (3): 973–78. doi:10.1073/pnas.0610117104.

Purhonen, Susanna, Jarmo Palm, Derrick Rossi, Nina Kaskenpää, Iiro Rajantie, Seppo Ylä-Herttuala, Kari Alitalo, Irving L Weissman, and Petri Salven. 2008. "Bone Marrow-Derived Circulating Endothelial Precursors Do Not Contribute to Vascular Endothelium and Are Not Needed for Tumor Growth.." Proceedings of the National Academy of Sciences of the United States of America 105 (18): 6620–25. doi:10.1073/pnas.0710516105.

Quintana, Elsa, Mark Shackleton, Michael S Sabel, Douglas R Fullen, Timothy M Johnson, and Sean J Morrison. 2008. "Efficient Tumour Formation by Single Human Melanoma Cells." Nature 456 (7222): 593–98. doi:10.1038/nature07567.

Ricci-Vitiani, Lucia, Dario G Lombardi, Emanuela Pilozzi, Mauro Biffoni, Matilde Todaro, Cesare Peschle, and Ruggero De Maria. 2006. "Identification and Expansion of Human Colon-Cancer-Initiating Cells." Nature 445 (7123): 111–15. doi:10.1038/nature05384.

Ricci-Vitiani, Lucia, Roberto Pallini, Mauro Biffoni, Matilde Todaro, Gloria Invernici, Tonia Cenci, Giulio Maira, et al. 2010. "Tumour Vascularization via Endothelial Differentiation of Glioblastoma Stem-Like Cells." Nature 468 (7325). Nature Publishing Group: 824–28. doi:10.1038/nature09557.

Risau, W, and I Flamme. 1995. "Vasculogenesis.." Annual Review of Cell and Developmental Biology 11: 73–91. doi:10.1146/annurev.cb.11.110195.000445.

Risau, W, H Sariola, H G Zerwes, J Sasse, P Ekblom, R Kemler, and T Doetschman. 1988. "Vasculogenesis and Angiogenesis in Embryonic-Stem-Cell-Derived Embryoid Bodies.." Development 102 (3): 471–78.

Rodriguez, Fausto J, Brent A Orr, Keith L Ligon, and Charles G Eberhart. 2012. "Neoplastic Cells Are a Rare Component in Human Glioblastoma Microvasculature.." Oncotarget 3 (1): 98–106.

Rosenthal, Rosalind A, Joseph F Megyesi, William J Henzel, Napoleone Ferrara, and Judah Folkman. 1990. “Conditioned Medium From Mouse Sarcoma 180 Cells Contains Vascular Endothelial Growth Factor.” Growth Factors 4 (1): 53–59. doi:10.3109/08977199009011010.

Rubenstein, J L, J Kim, T Ozawa, M Zhang, M Westphal, D F Deen, and M A Shuman. 2000. “Anti-VEGF Antibody Treatment of Glioblastoma Prolongs Survival but Results in Increased Vascular Cooption..” Neoplasia 2 (4): 306–14.

Ruf, Wolfram, Elisabeth A Seftor, Ramona J Petrovan, Robert M Weiss, Lynn M Gruman, Naira V Margaryan, Richard E B Seftor, Yohei Miyagi, and Mary J C Hendrix. 2003. “Differential Role of Tissue Factor Pathway Inhibitors 1 and 2 in Melanoma Vasculogenic Mimicry..” Cancer Research 63 (17): 5381–89.

Saint-Geniez, Magali, Arindel S R Maharaj, Tony E Walshe, Budd A Tucker, Eiichi Sekiyama, Tomoki Kurihara, Diane C Darland, Michael J Young, and Patricia A D'Amore. 2008. “Endogenous VEGF Is Required for Visual Function: Evidence for a Survival Role on Müller Cells and Photoreceptors.” Edited by Tailoi Chan-Ling. PLoS ONE 3 (11): e3554. doi:10.1371/journal.pone.0003554.s005.

Schatton, Tobias, George F Murphy, Natasha Y Frank, Kazuhiro Yamaura, Ana Maria Waaga-Gasser, Martin Gasser, Qian Zhan, et al. 2008. “Identification of Cells Initiating Human Melanomas.” Nature 451 (7176): 345–49. doi:10.1038/nature06489.

Schnegg, C I, M H Yang, S K Ghosh, and M Y Hsu. 2015. “Induction of Vasculogenic Mimicry Overrides VEGF-a Silencing and Enriches Stem-Like Cancer Cells in Melanoma.” Cancer Research 75 (8): 1682–90. doi:10.1158/0008-5472.CAN-14-1855.

Scully, S, R Francescone, M Faibish, B Bentley, S L Taylor, D Oh, R Schapiro, L Moral, W Yan, and R Shao. 2012. “Transdifferentiation of Glioblastoma Stem-Like Cells Into Mural Cells Drives Vasculogenic Mimicry in Glioblastomas.” Journal of Neuroscience 32 (37): 12950–60. doi:10.1523/JNEUROSCI.2017-12.2012.

Seftor, Elisabeth A, Paul S Meltzer, Dawn A Kirschmann, Jacob Pe’er, Andrew J Maniotis, Jeffrey M Trent, Robert Folberg, and Mary J C Hendrix. 2002. “Molecular Determinants of Human Uveal Melanoma Invasion and Metastasis..” Clinical & Experimental Metastasis 19 (3): 233–46.

Seftor, Elisabeth A, Paul S Meltzer, Gina C Schatteman, Lynn M Gruman, Angela R Hess, Dawn A Kirschmann, Richard E B Seftor, and Mary J C Hendrix. 2002. “Expression of Multiple Molecular Phenotypes by Aggressive Melanoma Tumor Cells: Role in Vasculogenic Mimicry..” Critical Reviews in Oncology/Hematology 44 (1): 17–27.

Seftor, R E, E A Seftor, N Koshikawa, P S Meltzer, L M Gardner, M Bilban, W G Stetler-Stevenson, V Quaranta, and M J Hendrix. 2001. “Cooperative Interactions of Laminin 5 Gamma2 Chain, Matrix Metalloproteinase-2, and Membrane Type-1-

Matrix/Metalloproteinase Are Required for Mimicry of Embryonic Vasculogenesis by Aggressive Melanoma.." Cancer Research 61 (17): 6322–27.

Shalaby, F, J Ho, W L Stanford, K D Fischer, A C Schuh, L Schwartz, A Bernstein, and J Rossant. 1997. "A Requirement for Flk1 in Primitive and Definitive Hematopoiesis and Vasculogenesis.." Cell 89 (6): 981–90.

Sharma, Navesh, Richard E B Seftor, Elisabeth A Seftor, Lynn M Gruman, Paul M Heidger, Michael B Cohen, David M Lubaroff, and Mary J C Hendrix. 2002. "Prostatic Tumor Cell Plasticity Involves Cooperative Interactions of Distinct Phenotypic Subpopulations: Role in Vasculogenic Mimicry." The Prostate 50 (3): 189–201. doi:10.1002/pros.10048.

Shing, Y, J Folkman, C Haudenschild, D Lund, R Crum, and M Klagsbrun. 1985. "Angiogenesis Is Stimulated by a Tumor-Derived Endothelial Cell Growth Factor.." Journal of Cellular Biochemistry 29 (4): 275–87. doi:10.1002/jcb.240290402.

Shirakawa, Kazuo, Hiro Wakasugi, Yuji Heike, Ichiro Watanabe, Shigeki Yamada, Ken Saito, and Fumio Konishi. 2002. "Vasculogenic Mimicry and Pseudo-Comedo Formation in Breast Cancer." International Journal of Cancer 99 (6): 821–28. doi:10.1002/ijc.10423.

Shoji, M, W W Hancock, K Abe, C Micko, K A Casper, R M Baine, J N Wilcox, et al. 1998. "Activation of Coagulation and Angiogenesis in Cancer: Immunohistochemical Localization in Situ of Clotting Proteins and Vascular Endothelial Growth Factor in Human Cancer.." Ajpa 152 (2): 399–411.

Siekmann, Arndt F, and Nathan D Lawson. 2007. "Notch Signalling Limits Angiogenic Cell Behaviour in Developing Zebrafish Arteries." Nature 445 (7129): 781–84. doi:10.1038/nature05577.

Singh, Mallika, and Napoleone Ferrara. 2012. "Modeling and Predicting Clinical Efficacy for Drugs Targeting the Tumor Milieu." Nature Biotechnology, July. Nature Publishing Group, 1–10. doi:10.1038/nbt.2286.

Singh, Sheila K, Cynthia Hawkins, Ian D Clarke, Jeremy A Squire, Jane Bayani, Takuichiro Hide, R Mark Henkelman, Michael D Cusimano, and Peter B Dirks. 2004. "Identification of Human Brain Tumour Initiating Cells.." Nature 432 (7015): 396–401. doi:10.1038/nature03128.

Soda, Yasushi, Tomotoshi Marumoto, Dinorah Friedmann-Morvinski, Mie Soda, Fei Liu, Hiroyuki Michiue, Sandra Pastorino, Meng Yang, Robert M Hoffman, and Santosh Kesari. 2011. "Transdifferentiation of Glioblastoma Cells Into Vascular Endothelial Cells." Proceedings of the National Academy of Sciences 108 (11). National Acad Sciences: 4274–80. doi:10.1073/pnas.1016030108.

Soker, S, S Takashima, H Q Miao, G Neufeld, and M Klagsbrun. 1998. "Neuropilin-1 Is Expressed by Endothelial and Tumor Cells as an Isoform-Specific Receptor for Vascular

Endothelial Growth Factor..” Cell 92 (6): 735–45.

Sood, Anil K, Elisabeth A Seftor, Mavis S Fletcher, Lynn M G Gardner, Paul M Heidger, Richard E Buller, Richard E B Seftor, and Mary J C Hendrix. 2010. “Molecular Determinants of Ovarian Cancer Plasticity.” The American Journal of Pathology 158 (4). American Society for Investigative Pathology: 1279–88. doi:10.1016/S0002-9440(10)64079-5.

Sood, Anil K, Mavis S Fletcher, Chris M Zahn, Lynn M Gruman, Jeremy E Coffin, Elisbeth A Seftor, and Mary J C Hendrix. 2002. “The Clinical Significance of Tumor Cell-Lined Vasculature in Ovarian Carcinoma: Implications for Anti-Vasculogenic Therapy..” Cancer Biology & Therapy 1 (6): 661–64.

Spannuth, Whitney A, Alpa M Nick, Nicholas B Jennings, Guillermo N Armaiz-Pena, Lingegowda S Mangala, Christopher G Danes, Yvonne G Lin, et al. 2009. “Functional Significance of VEGFR-2 on Ovarian Cancer Cells.” International Journal of Cancer 124 (5): 1045–53. doi:10.1002/ijc.24028.

Stone, Edwin M. 2006. “A Very Effective Treatment for Neovascular Macular Degeneration..” New England Journal of Medicine 355 (14): 1493–95. doi:10.1056/NEJMe068191.

Tammela, Tuomas, Georgia Zarkada, Elisabet Wallgard, Aino Murtomäki, Steven Suchting, Maria Wirzenius, Marika Waltari, et al. 2008. “Blocking VEGFR-3 Suppresses Angiogenic Sprouting and Vascular Network Formation.” Nature 454 (7204): 656–60. doi:10.1038/nature07083.

Topczewska, Jolanta M, Lynne-Marie Postovit, Naira V Margaryan, Anthony Sam, Angela R Hess, William W Wheaton, Brian J Nickoloff, Jacek Topczewski, and Mary J C Hendrix. 2006. “Embryonic and Tumorigenic Pathways Converge via Nodal Signaling: Role in Melanoma Aggressiveness.” Nature Medicine 12 (8): 925–32. doi:10.1038/nm1448.

van der Schaft, D W J. 2005. “Tumor Cell Plasticity in Ewing Sarcoma, an Alternative Circulatory System Stimulated by Hypoxia.” Cancer Research 65 (24): 11520–28. doi:10.1158/0008-5472.CAN-05-2468.

van der Schaft, D W J, R E B Seftor, E A Seftor, A R Hess, L M Gruman, D A Kirschmann, Y Yokoyama, A W Griffioen, and M J C Hendrix. 2004. “Effects of Angiogenesis Inhibitors on Vascular Network Formation by Human Endothelial and Melanoma Cells.” JNCI Journal of the National Cancer Institute 96 (19): 1473–77. doi:10.1093/jnci/djh267.

Wagenblast, Elvin, Mar Soto, Sara Gutiérrez-Ángel, Christina A Hartl, Annika L Gable, Ashley R Maceli, Nicolas Erard, et al. 2015. “A Model of Breast Cancer Heterogeneity Reveals Vascular Mimicry as a Driver of Metastasis.” Nature, April. doi:10.1038/nature14403.

Wang, Rong, Kalyani Chadalavada, Jennifer Wilshire, Urszula Kowalik, Koos E Hovinga, Adam Geber, Boris Fligelman, Margaret Leversha, Cameron Brennan, and Viviane Tabar. 2010.

"Glioblastoma Stem-Like Cells Give Rise to Tumour Endothelium." Nature 468 (7325). Nature Publishing Group: 829–33. doi:10.1038/nature09624.

Warren, R S, H Yuan, M R Matli, N A Gillett, and N Ferrara. 1995. "Regulation by Vascular Endothelial Growth Factor of Human Colon Cancer Tumorigenesis in a Mouse Model of Experimental Liver Metastasis.." Journal of Clinical Investigation 95 (4): 1789–97. doi:10.1172/JCI117857.

Weeraratna, Ashani T, Yuan Jiang, Galen Hostetter, Kevin Rosenblatt, Paul Duray, Michael Bittner, and Jeffrey M Trent. 2002. "Wnt5a Signaling Directly Affects Cell Motility and Invasion of Metastatic Melanoma.." Cancer Cell 1 (3): 279–88.

Williams, Cassin Kimmel, Ji-Liang Li, Matilde Murga, Adrian L Harris, and Giovanna Tosato. 2006. "Up-Regulation of the Notch Ligand Delta-Like 4 Inhibits VEGF-Induced Endothelial Cell Function.." Blood 107 (3): 931–39. doi:10.1182/blood-2005-03-1000.

Yang, J P, Y D Liao, D M Mai, P Xie, Y Y Qiang, L S Zheng, M Y Wang, et al. 2016. "Tumor Vasculogenic Mimicry Predicts Poor Prognosis in Cancer Patients: a Meta-Analysis." Angiogenesis, February. Springer Netherlands, 1–10. doi:10.1007/s10456-016-9500-2.

Yoder, Mervin C. 2009. "Defining Human Endothelial Progenitor Cells." Journal of Thrombosis and Haemostasis 7 (July): 49–52. doi:10.1111/j.1538-7836.2009.03407.x.

Zhang, S, C Balch, M W Chan, H C Lai, D Matei, J M Schilder, P S Yan, T H-M Huang, and K P Nephew. 2008. "Identification and Characterization of Ovarian Cancer-Initiating Cells From Primary Human Tumors." Cancer Research 68 (11): 4311–20. doi:10.1158/0008-5472.CAN-08-0364.

Zhang, Shiwu, Man Li, Yanjun Gu, Zhiyong Liu, Shaoyan Xu, Yanfeng Cui, and Baocun Sun. 2008. "Thalidomide Influences Growth and Vasculogenic Mimicry Channel Formation in Melanoma." Journal of Experimental & Clinical Cancer Research 27 (1): 60. doi:10.1186/1756-9966-27-60.

Zhang, Zhen, Yun Han, Keke Zhang, and Liangzhu Teng. 2011. "Investigation of Vasculogenic Mimicry in Intracranial Hemangiopericytoma.." Molecular Medicine Reports 4 (6): 1295–98. doi:10.3892/mmr.2011.567.

CHAPTER 2: Identification of PECAM-1$^+$ subpopulations of melanoma[2]

Introduction

As introduced in **CHAPTER ONE**, the development of anti-angiogenic therapies to attack tumor-associated blood vessels has been a large field of study for several decades. As anti-angiogenic drugs are designed to target vascular endothelial cells, they should be active against a spectrum of cancers. While preclinical modeling has shown success in blocking tumor growth with these agents, data from clinical trials has shown less success in patients. VM, initially described in aggressive forms of uveal melanoma, has been documented in multiple tumor types. However, the different molecular mechanisms which generate VM-competent tumor cells are unclear, and how tumor cell-lined conduits are formed and connected with host vasculature is undetermined. Furthermore, it remains controversial whether tumor cells actively engage tumor blood vessels or if they simply fill in gaps between neighboring EC in a passive manner. Bona fide TEC may be identified and isolated from collagenase-dispersed tumors using intercellular adhesion molecule 2 (ICAM2) or platelet EC adhesion molecule (PECAM-1, also known as CD31) antibodies followed by immunomagnetic separation (Dudley et al. 2008). Using this methodology I uncovered a novel subpopulation of PECAM1$^+$ tumor cells in melanoma that participate in a PECAM-1-dependent form of VM. Unlike previous models suggesting that tumor cells contribute to neovascularization through endothelial-like differentiation or recapitulation of developmental plasticity, I demonstrate the VM-competent tumor cells exist as

[2] Chapter 2 is adapted in part from Dunleavey, J.M. et al. Vascular channels formed by subpopulations of PECAM1$^+$ melanoma cells. *Nature Comm*. **5.** 1-16. (2014)

stable, yet hidden subpopulations in heterogeneous melanomas (Wang et al. 2010, Hendrix et al. 2003, Francescone et al. 2012). Clean separation of PECAM-1^{+} and PECAM-1^{-} clonal populations from the same tumor has allowed us to compare and contrast the differential role these two populations have during tumor growth, angiogenesis, and responses to anti-angiogenic therapy.

Results

Identification of PECAM-1^{+} tumor cells from B16F10 melanoma

Using PECAM-1 immunomagnetic separation of collagenase-dispersed B16F10 melanoma allograft (Dudley et al., 2008; Xiao, Harrell, Perou, & Dudley, 2013; Xiao, McCann, & Dudley, 2015), we enriched a PECAM-1^{+} population to ~ 98% purity, as determined by flow cytometry (Fig. 2.1a, b). Compared to the PECAM-1^{-} fraction, the enriched PECAM-1^{+} population expressed abundant *PECAM-1* mRNA by semi-quantitative RT-PCR (Fig. 2.1c). Unexpectedly, *VE-cadherin* mRNA was not detected in the PECAM-1^{+} fraction, in contrast to mouse dermal endothelial cells (mEC) used as a positive control (Fig. 2.1c) (Dudley et al., 2008). However, the PECAM-1^{+} fraction strongly expressed the melanocyte marker tyrosinase (*Tyr*) leading us to suspect we had enriched a previously unidentified PECAM-1^{+} subpopulation of melanoma cells from the B16F10 cell line. To test this possibility, we engrafted parental B16F10-GFP tumor cells into wild type, C57BL/6 mice and unlabeled B16F10 cells into C57BL/6-Tg$^{(CAG–EGFP)}$1Osb/J mice. We then used PECAM-1 immunomagnetic separation to retrieve highly purified fractions as before. The results showed that B16F10-GFP tumor cells in a wild type host generated PECAM-1^{+}/GFP^{+} cells whereas wild type tumors in a GFP host generated PECAM-1^{+}/GFP^{-} cells (Fig. 2.1d). These results are consistent with a tumor cell-of-origin for the PECAM-1^{+} cells we have isolated. Furthermore, these results appear to rule out the

possibility of fusion between tumor cells and PECAM-1$^+$ vascular EC in this particular mouse tumor model.

Next, we determined the proportion of PECAM-1$^+$ tumor cells in B16F10 tumors in vivo using flow cytometry. Tumors were harvested once they had reached ~ 0.4 g (+/– 0.26 g, s.e.m.) or ~ 1.0 g (+/– 0.22 g, s.e.m.) in size. The proportion of PECAM-1$^+$ tumor cells remained at ~ 0.2% of the total cellular pool, irrespective of tumor size. After gating out CD45$^+$ hematopoietic cells, the ratio of PECAM-1$^+$ vascular EC to PECAM-1$^+$ tumor cells was approximately 10:1 (Fig. 2.1e, f). Taken together, these results suggest that subpopulations of melanoma cells may express the vascular cell adhesion molecule PECAM-1 in vivo.

Isolation of PECAM-1$^+$ clonal populations from B16F10 melanoma

PECAM-1$^+$ cells comprised a minor fraction of B16F10 cultures and could not be easily detected by flow cytometry. However, occasional clusters of PECAM-1$^+$ cells could be found under fluorescence microscopy when B16F10 cultures were directly stained with PECAM-1 antibodies (Supplementary Fig. 2.1a). To further explore the significance and biological functions of PECAM-1$^+$ melanoma cells, we prepared clonal populations using limiting dilution assays from highly enriched PECAM-1$^+$ fractions (Fig. 2.2a). In 50% enriched fractions, PECAM-1$^+$ tumor cells were visible as large, flattened colonies that were distinct in appearance from spindle-shaped, PECAM-1$^-$ tumor cells (Supplementary Fig. 2.1b). These PECAM-1$^+$ tumor cells could be cleanly separated from their PECAM-1$^-$ counterparts using cloning rings or multiple rounds of immunomagnetic separation with PECAM-1 antibodies followed by limiting dilution assays. qPCR using clonally-derived populations revealed robust *PECAM-1* mRNA expression in clones A2 and A5 but not in clone A1 (Fig. 2.2b). No mRNAs were detected for *VE-cadherin* or *Vegfr-2* in PECAM-1$^-$ or PECAM-1$^+$ tumor cells. *Tyr* was expressed

by all melanoma cells but not mEC, as expected. Confocal microscopy revealed that PECAM-1 was concentrated at the cell membrane in mEC but was diffusely localized at the membrane and throughout the cytoplasm in PECAM-1^+ tumor cells (Supplementary Fig. 2.1c). Western blotting confirmed a migrating band at the expected size for murine PECAM-1 in PECAM-1^+ clones (Fig. 2.2c). PECAM-1 was tyrosine phosphorylated in PECAM-1^+ tumor cells suggesting it may have similar signaling abilities in both EC and tumor cells (Supplementary Fig. 2.1d).

PECAM-1^+ melanoma cells generate PECAM-1^+ progeny

We found that PECAM-1 expression in PECAM-1^+ clones was stable in vitro and was not diminished by growth in different culture media (Supplementary Fig. 2.2a). However, cell-surface PECAM-1 was reduced by > 50% when PECAM-1^+ tumor cells were detached from tissue culture dishes using trypsin as opposed to accutase which does not affect PECAM-1 surface expression (Supplementary Fig. 2.2b). Additionally, routine passaging of cells did not diminish PECAM-1 expression (Supplementary Fig. 2.2c). Interestingly, PECAM-1^+ tumor cells displayed a slight growth delay in vitro and in vivo when engrafted into mice (Supplementary Fig. 2.2d). Long-term in vitro propagation of PECAM-1^- and PECAM-1^+ tumor cells revealed that PECAM-1^+ tumor cells generally give rise to PECAM-1^+ progeny and vice versa (Supplementary Fig. 2.2e). To determine the fate of PECAM-1^- and PECAM-1^+ tumor cells in vivo, we transduced PECAM-1^+ and PECAM-1^- tumor cells with GFP using lentivirus to generate PECAM-1^+/GFP^+ (clone A5) or PECAM-1^-/GFP^+ (clone A1) lines. We then injected 1.0×10^6 tumor cells subcutaneously in wild type C57BL/6 mice. Flow cytometry of collagenase-dispersed tumors revealed that, in general, PECAM-1^+ tumor cells generate PECAM-1^+ progeny whereas PECAM-1^- tumor cells generate mostly PECAM-1^- progeny (Supplementary Fig. 2.2f). When quantified by flow cytometry, PECAM-1^- tumors generated a mixed population consisting

of ~ 2% PECAM-1$^+$ progeny and ~ 98% PECAM-1$^-$ progeny. These results suggest that PECAM-1$^-$ and PECAM-1$^+$ melanoma cells are stable subpopulations but may generate their counterparts at low frequencies with a tendency for PECAM-1$^-$ tumor cells to generate PECAM-1$^+$ progeny. Finally, karyotypes performed on PECAM-1$^+$ and PECAM-1$^-$ clones showed that PECAM-1$^-$ tumor cells were more variable in chromosome counts with a median chromosome number of 70 whereas PECAM-1$^+$ tumor cells had a median chromosome count of 64 (Supplementary Fig. 2.3a, b). Both PECAM-1$^-$ and PECAM-1$^+$ clones displayed similar marker chromosomes to those observed in previously published reports of the B16 cell line (Hu, Wang, & Hsu, 1987; Kendal, Wang, Hsu, & Frost, 1987). This result, in addition to the shared chromosomal aberrations between the two populations, suggests that the PECAM-1$^+$ fraction may have persisted and been continuously generated at a low frequency within the B16F10 cell line for decades.

In vitro vascular properties of PECAM$^+$ melanoma

To further characterize established PECAM-1$^+$ clones, we carried out a microarray analysis using an Affymetrix mouse gene ST1.0 platform. A complete microarray dataset showing differentially expressed genes in PECAM-1$^-$ and PECAM-1$^+$ tumor cells has been uploaded to the Gene Expression Omnibus (GEO). Notably, microarray analysis showed an enrichment of additional candidate genes associated with known vascular functions in PECAM-1$^+$ clones (A2, A3, A4, A5) compared to parental B16F10 tumor cells. These genes included *Ephb4*, *Bmpr2*, *Pdgfa*, *Icam1 (CD54)*, *Thbs1*, *Bmp1*, *Rbpj1*, and *Notch2* (Fig. 2.2d). Expression of these genes was confirmed by qPCR (Supplementary Fig. 2.4 and see Supplementary Table 2.1 for a complete list of PCR primer sets).

Because PECAM-1 is a cell adhesion molecule known to mediate in vitro tube formation of bona fide EC, we assessed whether PECAM-1$^+$ melanoma cells might also undergo in vitro tube formation (Cao et al., 2002; DeLisser et al., 1997). PECAM-1$^+$ tumor cells displayed a 4–5 fold increase in branching tube-like networks compared to their PECAM-1$^-$ counterparts. PECAM-1$^-$ tumor cells only formed occasional tube-like structures which were not stable in culture. Tube like-structures in PECAM-1$^+$ tumor cells could be inhibited by ~ 50% using a PECAM-1 blocking antibody indicating a functional role for PECAM-1 in this assay (Fig. 2.2e) (DeLisser et al., 2010). Gain of function experiments showed that PECAM-1 over-expression (OE) in PECAM-1$^-$ tumor cells (clone A1) stimulated in vitro tube formation ~ 4-fold whereas PECAM-1 shRNA in PECAM-1$^+$ tumors cells (clone A5) diminished tube formation by ~ 50% (Fig. 2.2f, g, h, i). These results suggest that PECAM-1 is a marker of a unique subpopulation of B16F10 tumor cells and it plays a functional role in the establishment and stability of in vitro tube-like networks.

PECAM-1$^+$ tumor cells exist in spontaneous murine melanoma

Next, we turned to the ΔBraf/Pten$^{-/-}$ genetically-engineered mouse model of melanoma to assess whether PECAM-1$^+$ tumor cells were present in spontaneous tumors (Fig. 2.3a) (Dankort et al., 2009). First, we measured *PECAM-1*mRNA expression using qPCR in two cell lines recently derived from tumors in ΔBraf/Pten$^{-/-}$ mice (Hanna et al., 2013). The results showed that *PECAM-1* mRNA levels were above the zero transcript threshold we established using a known PECAM-1$^-$ clone derived from B16F10 (clone A1) (Fig. 2.3b). These results suggested that, similar to B16F10, a minor subpopulation of PECAM-1$^+$ tumor cells might be present within ΔBraf/Pten$^{-/-}$ tumor cells. To address this possibility, we used PECAM-1-mediated immunomagnetic enrichment in PBT2460 tumor cells and found that after six

enrichment steps, about 15% of the population expressed PECAM-1 on the cell surface by flow cytometry. After two additional enrichment steps, about 98% of the population expressed PECAM-1 (Fig. 2.3c). qPCR confirmed an ~ 100-fold increase in *PECAM-1* mRNA in the enriched fraction when compared to the un-enriched parental population but *VE-cadherin* and *Vegfr-2* were absent from both populations (Fig. 2.3d). Notably, these PECAM-1$^+$ cells derived from ΔBraf/Pten$^{-/-}$ tumors were not identical to those obtained from B16F10; namely, unlike PECAM-1$^+$ cells from B16F10 melanoma, they did not express ICAM1 protein or mRNA by qPCR (Supplementary Fig. 2.5a, b).

Using the enriched PECAM-1$^+$ fraction from ΔBraf/Pten$^{-/-}$ tumors, we generated single-cell clones by limiting dilution assays. Similar to PECAM-1$^+$ tumor cells derived from B16F10, single cell clones derived from ΔBraf/Pten$^{-/-}$ tumors maintained PECAM-1 expression in culture that was detectable on the cell surface by flow cytometry (Fig. 2.3e). Furthermore, clonally-derived PECAM-1$^+$ tumor cells from ΔBraf/Pten$^{-/-}$ tumors showed a five-fold increase in the formation of vascular-like networks in vitro compared to their PECAM-1$^-$ counterparts (Fig. 2.3f). As with B16F10-derived PECAM-1$^+$ tumor cells, these tube-like structures were stable over time but could be diminished by ~ 50% using a PECAM-1 neutralizing antibody (Fig. 2.3g, Supplementary Movie 1).

PECAM-1$^+$ melanoma cells integrate into vessel lumens in vivo

To assess whether PECAM-1$^+$ melanoma cells generated vessel-like structures in vivo, we engrafted unlabeled, clonally-derived PECAM-1$^+$ (clone A5) and PECAM-1$^-$ (clone A1) melanoma cells under the skin of C57BL6/J mice. We then stained cryosections with antibodies against PECAM-1 and the melanoma marker S100B (Eyles et al., 2010). Strikingly, in PECAM-1$^+$ tumors, we found intra-tumoral holes and channels lined by PECAM-1$^+$/S100B$^+$ tumor cells

(Fig. 2.4a). These channels appeared to be formed entirely by PECAM-1$^+$/S100B$^+$ tumor cells (top row) or were formed in collaboration with PECAM-1$^+$/S100B$^+$ tumor cells and host endothelium (middle row). In contrast, PECAM-1$^-$ tumors were characterized by host-derived PECAM-1$^+$ vasculature juxtaposed to S100B$^+$ tumor cells (bottom row). Next, we used GFP-labeled PECAM-1$^+$ and PECAM-1$^-$ clonally-derived populations from B16F10 to further assess the localization of PECAM-1$^-$ and PECAM-1$^+$ tumor cells in vivo by immunohistochemistry. Similar to the results above, in PECAM-1$^+$ tumors, co-staining using PECAM-1 and GFP antibodies revealed large openings, intratumoral channels, and vascular-like structures that incorporated GFP$^+$ tumor cells within their lumens (Fig. 2.4b, first row). In contrast, host-derived PECAM-1$^+$ vascular EC were mainly peripheral to GFP$^+$ tumor cells in PECAM-1$^-$ tumors (Fig. 2.4b, second row). We then determined whether PECAM-1$^+$ tumor cells were also incorporated into VE-cadherin$^+$ vascular lumens. Similar to the staining pattern for PECAM-1 above, we found that PECAM-1$^+$ tumor cells formed mosaic vascular structures and were incorporated within occasional VE-cadherin$^+$ lumens (Fig. 2.4b, third row). In contrast, PECAM-1$^-$ counterpart tumor cells were localized to the margins of host-derived VE-cadherin$^+$ blood vessels (Fig. 2.4b, fourth row). Taken together, these results suggest that PECAM-1$^+$ melanoma cells have vascular-like properties including the ability to spontaneously organize into tube-like structures in vitro and incorporate into vascular lumens in vivo.

PECAM-1$^+$ melanoma form perfused vascular structures in mice

To determine whether PECAM-1$^+$ tumor cells were in direct contact with the host circulation, we examined paraffin-embedded tumor sections stained with GFP antibodies visualized using 3,3′ diaminobenzidine (DAB). The results showed numerous channels or "lumens" that were comprised of GFP$^+$ tumor cells in direct contact with erythrocytes (Fig. 2.5a).

H & E stained sections showed large dilated vessels, hemorrhage, and blood-filled channels in PECAM-1$^+$ tumors versus their PECAM-1$^-$ counterparts (Fig. 2.5b). When quantified using the ImageJ software package, the mean hemorrhage area for PECAM-1$^-$ tumors was 46.7 AU +/– 1.3 and 88.3 AU +/– 23.0 for PECAM-1$^+$ tumors (Fig. 2.5b, lower panel). In support of a PECAM-1-dependent form of VM in this model, this increase in hemorrhage area was diminished when PECAM-1$^+$ tumors were engrafted in PECAM-1 KO mice (Supplementary Fig. 2.6a, b, c).

Next, we carried out 3D acoustic angiography and dynamic contrast-enhanced perfusion imaging using lipid-encapsulated micro-bubble contrast agents to measure real-time tumor perfusion and vascular structure in PECAM-1$^-$ and PECAM-1$^+$ tumors (Fig. 2.5c, left) (Gessner, Aylward, & Dayton, 2012). Dual-frequency, 3D acoustic angiography revealed mean volumetric vascular density values of 47.9 +/– 2.9 for PECAM-1$^-$ tumors, whereas PECAM-1$^+$ tumors had mean volumetric vascular density values of 72.3 +/– 5.5 (Fig. 2.5c, middle). The sample means were statistically significant when analyzed using a two tailed t-test. We observed that the acoustic angiography images showed the presence of greater sub-resolution contrast in PECAM-1$^+$compared to PECAM-1$^-$ tumors. This sub-resolution contrast signal likely emanates from pooling blood, which could correspond with the larger hemorrhage areas observed in PECAM-1$^+$ tumors. Additionally, destruction-reperfusion images acquired longitudinally were used to compute the area-normalized relative blood volume (normalized RBV) analyzed using a linear mixed effects model in R. The area-normalized RBV regression intercept was 3.46 +/– 2.95 units for PECAM-1$^-$ tumors and 15.60 +/– 4.76 units for PECAM-1$^+$ tumors which was statistically significant (Fig. 2.5c, right). Overall, these results demonstrate that the normalized RBV of PECAM-1$^+$ tumors was an average of 4.5 times higher than that of PECAM-1$^-$ tumors.

To determine whether PECAM-1$^+$ tumor cells were in contact with the circulation, we injected Texas Red-labeled high molecular weight Dextran (TR-Dextran) by way of the tail vein in mice bearing PECAM-1$^-$/GFP$^+$ or PECAM-1$^+$/GFP$^+$ tumors (Lin et al., 2006). GFP$^+$ tumor cells in direct contact with TR-Dextran were then analyzed using confocal microscopy (Fig. 2.5d). After analyzing multiple sections from 3–4 mice/group, we found a six-fold increase in PECAM-1$^+$ tumor cells in contact with TR-Dextran when compared to their PECAM-1$^-$ counterparts. These results were confirmed in an additional PECAM-1$^+$ clone (clone A2) (Supplementary Fig. 2.7a, b, Supplementary Movies 2, 3). Finally, we carried out transmission electron microscopy (TEM) of engrafted PECAM-1$^-$ and PECAM-1$^+$ tumors. The ultrastructure of vessels in these tumors showed melanoma cells (identified by the presence of melanosomes, a unique feature of melanocytes and melanoma cells) in direct contact with the basal lamina of erythrocyte-containing vessels in PECAM-1$^+$ tumors, but this contact was rarely seen in PECAM-1$^-$ tumors (Supplementary Fig. 2.8). Thus, these results suggest that PECAM-1$^+$ tumor cells organize into primitive vascular channels that may be affiliated with the host circulation and perfused with blood.

AP-2α is reduced in PECAM-1$^+$ tumor cells and represses PECAM-1

Next, we asked how PECAM-1 expression was transcriptionally-regulated in PECAM-1$^+$ tumor cells. Notably, we did not find evidence for epigenetic regulation of *PECAM-1* expression in B16F10 because neither the DNA methyltransferase inhibitor 5-azacytidine nor the pan-HDAC inhibitor TSA could induce *PECAM-1* mRNA (Supplementary Fig. 2.9a). However, PECAM-1 is known to be regulated by the transcription factor GATA2 and additional binding sites in the PECAM-1 promoter for SP1, ETS, and AP-2α are also reported (Gumina, Kirschbaum, Piotrowski, & Newman, 1997). We scanned the PECAM-1 promoter and used

semi-quantitative RT-PCR to measure the expression of these candidate transcription factors in PECAM-1$^-$ and PECAM-1$^+$ clones. The results showed that unsorted B16F10 melanoma and clonally-derived PECAM-1$^-$ or PECAM-1$^+$ tumor cells either did not express or expressed similar levels of most of these transcription factors, including *Ets* (Fig. 2.6a). On the other hand, *Ap-2α* expression was strikingly diminished in PECAM-1$^+$ tumor cells and mEC but was expressed in unsorted B16F10 cells and PECAM-1$^-$ tumor cells. *Ap-2α* expression was similar in parental B16F0, the low-metastatic B16 clone B16F1, B16F10, and two independent PECAM-1$^-$ clones (Supplementary Fig. 2.9b). Expression of the well-characterized melanoma markers dopachrome tautomerase (*Dct)* and micropthalmia-associated transcription factor (*Mitf-m)* were also similar in these same cell lines at the mRNA and protein levels (Supplementary Fig. 2.9b, c). Interestingly, PECAM-1$^+$ clones consistently produced more pigmented cells in vitro and highly pigmented tumors in vivo despite expressing similar levels of *Tyr* and *Dct* compared to PECAM-1$^-$ counterparts (Supplementary Fig. 2.9d, e).

Because AP-2α levels were inversely correlated with PECAM-1, we hypothesized that AP-2α might function as a transcriptional repressor of PECAM-1. We used chromatin immunoprecipitation (ChIP) to confirm that AP-2α occupied the PECAM-1 promoter in B16F10 tumor cells. Immunoprecipitation with an AP-2α antibody followed by PCR using two primer sets unique to the mouse PECAM-1 promoter revealed amplified fragments of the predicted sizes (Fig. 2.6b). Furthermore, PECAM-1$^-$ tumor cells transfected with *Ap-2α* siRNA revealed up-regulation of *PECAM-1* mRNA and protein expression, which was accompanied by a four-fold increase in tube formation in Matrigel (Fig. 2.6c, d). On the other hand, stable lentiviral re-expression of *Ap-2α* into PECAM-1$^+$ tumor cells resulted in down-regulation of *PECAM-1* mRNA and protein expression, and a 6-fold reduction in tube formation (Fig. 2.6e,

f, Supplementary Movie 4). These results suggest that AP-2α may repress PECAM-1 expression and that diminished expression of AP-2α in PECAM-1$^+$ B16F10 cells accompanies their ability to form vascular like structures in vitro.

PECAM-1$^+$ tumor cells are enriched after anti-VEGF therapy

Because PECAM-1$^+$ tumor cells do not express VEGFR-2, but engage in VM, we hypothesized they might form VEGF-independent intratumoral channels in mice. First, we subjected mice bearing B16F10-GFP tumors to MCR84, a neutralizing antibody raised against VEGF-A, and then harvested tumors once they become refractory to further treatment (Fig. 2.7a) (Roland et al., 2009; Sullivan et al., 2010). MCR84-treated mice demonstrated a characteristic delay in tumor growth, followed by tumor regrowth that was resistant to further VEGF inhibition (Fig. 2.7b). We then used flow cytometry to measure the proportion of GFP$^+$/PECAM-1$^+$ tumor cells in size-matched tumors. We found that in size-matched, MCR84-resistant tumors, the number of PECAM-1$^+$ tumor cells was enriched ~ 6 fold whereas PECAM-1$^-$ tumor cells and bona fide EC were marginally reduced (Fig. 2.7c, d). To examine the specific role of PECAM-1$^+$ tumor cells in tumor responses to anti-angiogenic therapy, we engrafted GFP-labeled clonally-derived populations of either PECAM-1$^+$ or PECAM-1$^-$ tumor cells into C57BL6/J mice. Mice were then treated with MCR84 as described above. We found that PECAM-1$^-$ tumors demonstrated an expected delay in tumor growth and reduction in tumor volume (~ two-fold decrease in tumor volume at day 15) when challenged with MCR84. On the other hand, PECAM-1$^+$ tumors showed no appreciable growth inhibition compared to controls (Fig. 2.7e). H & E and GFP-stained tissue sections revealed striking differences in blood vessel morphology and numerous blood-filled "channels" encapsulated by GFP$^+$ tumor cells in the PECAM-1$^+$ tumors challenged with MCR84 (Fig. 2.7f). Taken together, VEGF blockade induces

expansion of a minor subpopulation of PECAM-1^{+}melanoma cells; furthermore, PECAM-1^{+} melanoma cells form tumors that do not respond to VEGF inhibition and they generate aberrant vascular-like structures following challenge with VEGF blocking antibodies.

Human melanoma contains a PECAM-1^{+} subpopulation

We examined *PECAM-1* expression from microarray data generated from > 40 human melanoma cell lines and normal human melanocytes (Carson et al., 2012). From these data, we identified approximately 10 cell lines which fell above a threshold (~ 1.5 adjusted mean fluorescence values from microarray data) established using normal human melanocytes which do not express *PECAM-1* (Fig. 2.8a). A list of normal melanocytes and melanoma cells along with the raw fluorescence values from the microarray are shown in Supplementary Table 2.2. We began by culturing some of the highest *PECAM-1*-expressing cell lines and measuring *PECAM-1* mRNA levels by quantitative RT-PCR. The results showed that, as predicted from the microarray analysis, *PECAM-1* mRNA was detected in the WM2664, MEL505, RPMI7951, WM1158, and SBCl2 cell lines albeit at vey low levels compared to human EC (hEC) (Fig. 2.8b). No *PECAM-1* transcripts were detected in normal melanocytes, RPMI8332, or SKMEL119 which all fell below the established threshold on the microarray. On the other hand, *VE-CADHERIN* mRNA, which is expressed in some uveal forms of melanoma that engage in vasculogenic mimicry, was not detected in most cell lines but was found at very low levels in WM1158 cells (Hendrix et al., 2001). Using flow cytometry, we could detect a minor shift in PECAM-1 fluorescence in RPMI7951 (3.3%) and WM1158 cells (1.6%) but a much larger shift in SBCl2 cells (50%). No PECAM-1 surface expression was detected in normal melanocytes (NHM7) or in RPMI8332, as expected (Fig. 2.8c). Similar to the PECAM-1^{+} fractions derived from murine B16F10 and ΔBraf/Pten$^{-/-}$ cells, SBCl2 melanoma cells formed robust and stable

vessel-like networks in vitro which were inhibited by PECAM-1 neutralizing antibodies (Fig. 2.8d, Supplementary Movie 5).

Because SBCl2 expressed detectable PECAM-1 levels by flow cytometry, we engrafted this cell line subcutaneously in NOD-SCID-Il2γ (NSG) mice. We then stained primary, paraffin-embedded SBCl2 tumors with PECAM-1 antibodies that were verified to be human specific using western blotting and immunohistochemistry (Supplementary Fig. 2.10a, b). While the majority of PECAM-1^+ tumor cells detected with human antibodies appeared randomly scattered throughout the tumor, occasional PECAM-1^+ "lumens" were also visible (Fig. 2.8e). Overall, PECAM-1^+ tumor cells were found at the luminal and abluminal surface of vascular structures (white arrowheads), and were detected in all SBCl2 tumors examined, and were present at an average density of ~ 5 vessel-like structures per mm2 when normalized to tumor size for each tissue section (Fig. 2.8e, far right). Thus, similar to mouse melanoma, a subpopulation of some human melanoma cells express PECAM-1 and engage in the formation of vascular-like structures in vitro and in vivo.

Materials and Methods

Mice

For studies using the B16F10 melanoma cell lines, female C57BL6/J mice were used (Jackson Laboratories, Bar Harbor, ME). Mice were injected with tumor cells at 7-8 weeks of age. For engraftment of human melanoma cells, we used female NSG mice (7-8 weeks of age) provided by the mouse phase I unit at UNC. C57BL/6-Tg (CAG-EGFP)1Osb/J mice were purchased from Jackson Laboratories, (Bar Harbor ME). PECAM-1 knockout mice were kindly provided by Dr. E. Tzima (UNC Chapel Hill), and tumor cells were engrafted in female mice at 7-8 weeks of age. All mouse experiments were carried out in accordance with protocols

approved by the Institutional Animal Care and Use Committee at the University of North Carolina at Chapel Hill.

Cell lines and media

B16F0, B16F1, B16F10 (ATCC), ΔBraf/Pten$^{-/-}$ (derived from B6.Cg-Braf^{tm1Mmcm}Pten^{tm1Hwu}Tg$^{(Tyr- cre/ERT2)}$13Bos/BosJ mice (UNC-Chapel Hill Mouse Phase 1 Unit)) cell lines PBT2460 and PBT2130 (Drs. W. Kim and J. Bear, UNC-Chapel Hill), and human melanoma cell lines WM1158, SBCl2, Sk-Mel-119, Sk-Mel-173, and WM2664 (Dr. J. Shields, UNC-Chapel Hill) were maintained in DMEM with 4.5 g/mL D-Glucose and 10% FBS. Human melanoma cell lines RPMI7951, RPMI8322, and Mel505 (Dr. J Shields, UNC-Chapel Hill) were maintained in RPMI with 10% FBS. The normal human melanocyte line NHM7 (Dr. J Shields, UNC-Chapel Hill) was maintained in Media 254 (Gibco) supplemented with HGMS (Gibco). EC were maintained in Endothelial Cell Media (EC-Media), composed of DMEM with 1g/L glucose, 5 μg/L bFGF, 10 μg/L VEGF, 100 mg/L heparin, antibiotics, and 10% NuSerum IV (BD).

Antibodies

For a complete list of antibodies and dilutions used, please refer to Supplementary Table 3.

Western blotting

Whole cell lysates were prepared in radioimmunoprecipitation assay buffer (RIPA, Boston BioProducts), separated by SDS-PAGE at 100V using a Bio-Rad 4-20% TGX gel (Bio-Rad), blocked with 5% Milk-TBS-T for standard western blotting, 5% BSA for phospo-VEGFR2 blotting , and probed with antibodies overnight at 4°C. Peroxidase-conjugated secondary antibodies were incubated at RT for 1 hour, and bands were exposed with Western

Lightning (PerkinElmer). Blots were imaged on a Fluorchem M (ProteinSimple). All antibodies and dilutions are presented in Supplementary Table 3.

Chromatin immunoprecipitation (ChIP)

ChIP experiments were performed using the ChIPit Express Kit (Active Motif) according to the manufacturer's instructions. 2 μg anti-AP-2α antibodies were used for immunoprecipitation and bound DNA was analyzed using two primer sets designed against the mouse PECAM-1 promoter for sequences see Supplementary Table 2.1).

siRNA Knockdown

Cells were plated at 2.0 x10^5 cells/well in 6-well plates. siRNA SmartPools (Dharmacon) targeting Ap-2α (M-062788-01-0005), PECAM-1 (TRC RMM4534-EG18613), or non-targeting controls (D-001206- 13-05) were added to plates the next day according to the manufacturer's instructions at a concentration of 100 nM. Cells were allowed to grow for 48 hours before harvesting.

Isolation of PECAM-1$^+$ tumor cells

Tumors were harvested and prepared for cell isolation as previously described by us (Dudley et al., 2008; 2010). In brief, tumors were minced in cold DMEM with 1 g/L glucose. Tumors were further digested using a mechanical tissue homogenizer (Miltenyi). Samples were incubated at 37°C with 5 ml Collagenase T2 (2 mg/ml, Worthington), 1 mL neutral buffered protease (2.5 U/ml, Worthington), and 75 μL deoxyribonuclease (1 mg/mL, Worthington) for 75 minutes. Red blood cells were lysed with 1X Pharmlyse B (BD PharMingen). Cells were suspended in FACS Buffer (degassed phosphate-buffered saline containing 2 mM EDTA and 0.5% BSA), Fc receptors were blocked with Fc Block (Miltenyi), and 10 μg PE-conjugated anti-

PECAM-1 antibodies were added for 20 minutes. Cells were washed and resuspended with anti-PE magnetic beads (Miltenyi) for 15 minutes. Cells were then washed and passed over a magnetic column, washed, and then eluted. Eluted cells were washed and plated in EC-Media. Cells were grown for several weeks, and the isolation was repeated until cultures reached ~ 99% PECAM-1 positivity, at which point single cell clones were made by limiting dilutions.

Tumor dissociation and flow cytometry

Single cell suspensions were prepared either from whole tumors as described above or from detached cell cultures as previously described by us (Dudley et al., 2010). Briefly, cells were washed with PBS and detached using accutase (Sigma) and then labeled with fluorophore-tagged antibodies. Cells were then washed and fixed in FACS buffer containing 1% paraformaldehyde. Cells were analyzed by flow cytometry using an Accuri C6 flow cytometer running BD Accuri CFlow Plus Analysis software. Samples were then analyzed using the FloJo software package (version 10).

Immunohistochemistry

Tumors were harvested and fixed in 4% paraformaldehyde overnight at 4°C. Samples were then cryoprotected in 30% sucrose overnight. Samples were frozen in OCT and cut into 7 μm sections. Slides were fixed in methanol for 20 minutes, and washed in PBS. Sections were blocked in 5% BSA with species-specific serum (5%) for one hour, and antibodies were added in blocking buffer. All antibodies and dilutions are described in Supplementary Table 3. Slides were incubated overnight at 4°C. Slides were washed and secondary antibodies were added for one hour at room temperature. Slides were counterstained with Vectashield Hard-set Mounting Medium with DAPI (Vector Labs). Sections were analyzed on a Leica DM-IRB inverted

microscope or a Zeiss 710 laser scanning confocal microscope. Images were globally adjusted using ImageJ analysis software (http://rsb.info.nih.gov/ij) to enhance contrast and sharpness.

Acoustic angiography and perfusion imaging

Two methods of contrast enhanced ultrasonography were employed to quantify perfusion in PECAM-1^{+} and PECAM-1^{-} tumors in vivo. Additionally, non-contrast ultrasound provided reference anatomical information and tumor volume. The lipid encapsulated microbubble contrast agents were prepared as previously described and injected intravenously through a tail-vein catheter (Streeter, Gessner, Miles, & Dayton, 2010). Destruction-reperfusion imaging was performed using a Vevo 2100 ultrasound system (VisualSonics, Toronto, Ontario, Canada), similar to methods used as described previously (Kogan et al., 2011). Dynamic contrast enhanced perfusion imaging sequences were used to compute relative blood volumes (VevoCQ-Advanced Contrast Quantification Software Analysis Tool for the Vevo 2100. VisualSonics. Toronto, Canada, © Bracco Suisse S.A. 2010). Data were normalized by tumor cross-sectional areas as defined by regions of interest (ROIs) drawn manually. Acoustic angiography utilizes a prototype dual- frequency transducer, with a low frequency element to transmit at 4 MHz, exciting microbubbles to produce broadband, superharmonic echoes (at a mechanical index of 0.6). The confocal high frequency element (30 MHz) is used to receive the microbubble response, thus avoiding tissue signal and producing high-contrast, high resolution images of the tumor microvasculature without tissue background, in 3 dimensions (Gessner et al., 2012). Acoustic angiography is acquired near simultaneously with b-mode soft tissue imaging, which provides anatomical reference. These images were used to compute the volumetric vascular density of the tumors using the following procedure in MATLAB (The MathWorks Inc., Natick, MA). First, ROIs were drawn manually to define tumor boundaries based on the b-mode images.

Then, the ROIs were applied to mask the tumor volume in the acoustic angiography images. Finally, the vascular volume was computed by applying an intensity threshold cutoff, to segment the image into vascular and nonvascular regions. The volumetric vascular density is the ratio of the number of voxels classified as vascular volume over the total number of voxels in the tumor ROI. Statistical analysis was carried out using R (http://www.R-project.org).

Transmission electron microscopy

PECAM-1^{+} or PECAM-1- tumors were grown as described above. Tissues were harvested, fixed in 2.5% glutaraldehyde/2% PFA in 0.15M sodium phosphate buffer. Samples were post-fixed for 1 hour in 1% osmium tetroxide in 0.15M sodium phosphate buffer, dehydrated with a graded series of ethanol washes, treated with propylene oxide and embedded in PolyBed 812 epoxy resin (Polysciences, Warrington, PA). Ultrathin sections (70-80 nm) were cut and mounted on copper grids and stained with 4% aqueous uranyl acetate and Reynolds' lead citrate. Sections were mounted to copper grids, OsO4 was used to stain the tissues and sections were imaged on a Zeiss Leo EM910 TEM.

Lentiviral constructs and transduction

All recombinant DNA work was carried out under approval of the Environmental Health Safety Division of UNC-Chapel Hill. Lentiviral expression plasmids were created by E. Campeau and obtained from Addgene: pLenti CMV-GFP-DEST (736-1, Addgene plasmid 19732), pLenti CMV/TO GFP-Zeo DEST (719-1, Addgene 17431). Packaging plasmids psPax2 and pMD2.6 were created by Didier Trono (Addgene plasmids 12259 and 12260). Mouse ORF-eome constructs were acquired from the ATCC I.M.A.G.E Consortium, then cloned into pDONR 221 (Invitrogen) Gateway donor vectors using Clonase BP (Invitrogen). Cloned pDONR 221 vectors were sub-cloned into lentiviral expression vectors by Clonase LR reaction (Invitrogen).

Lentiviral backbones were transfected with 1.5 μg packaging plasmids psPAX2 and pMDG2 with 15 μl Lipofectamine 2000 in 6-well plates into HEK293T cells. Viral particles were harvested at 24 and 48 hours post transfection. Viral particles were used to infect target cells with 10 μg/mL Polybrene in antibiotic-free media.

Tumor studies in mice

B16F10 melanoma cells were grown in appropriate culture medium, detached and resuspended in HBSS (Gibco). 1.0 x 10^6 tumor cells were injected subcutaneously in the right shoulder of C57BL6/J mice. Tumors were allowed to grow to 1 cm3 and were measured daily with calipers. For MCR84 studies, mice were treated with 25 mg/kg/day MCR84 or isotype control antibodies as previously described (Roland et al., 2009; Sullivan et al., 2010). Tumor sizes were measured with calipers each day. At the end of the experiment, mice were euthanized and tumors were harvested and weighed.

Microarray analysis

RNA was harvested from cell lines and run on a Mouse Gene ST1.0 Chip (Affymetrix). Heat maps were generated using the Gene-E software package, version 2.1.134. (http://www.broadinstitute.org/cancer/software/GENE-E/). Microarray dataset is available at the Gene Expression Omnibus, accession number: GSE59564.

Polymerase chain reaction (PCR)

Primers were designed using Invitrogen Primer Perfect Design Software. End-point PCR was completed using a standard PCR kit (NEB). RT-qPCR was completed with Maxima SYBR Green (ThermoFisher) on an Applied Biosystems Step One Plus analyzer. All qPCR experiments were run in triplicate and data are presented as the average with the standard error of the mean (s.e.m.). Primer sequences used are presented in Supplementary Table 1.1.

Tumor hemorrhage quantification

H & E stained sections were imaged using polarized light microscopy which caused red blood cells (RBC) to fluoresce. Images were subsequently converted to a binary image using ImageJ software. The images were then thresholded to only show RBC and the "count particles" tool was used to analyze RBC content. The first 500 observations were binned and plotted.

In vitro tube-forming assays

Briefly, 50 μL Matrigel (BD) was plated in 96-well culture dishes and allowed to polymerize at 37°C for 30 minutes. Next, 2.5 x 10^4 cells/well were plated on the Matrigel layer and grown for 16 hours. Randomized fields were captured using a DM-IRB inverted microscope and tubes were quantified from each image. Data are presented as the average number of tubes per field +/- SEM from multiple fields. For live imaging experiments Matrigel was plated in 24-well plates, and 5 x 10^4 cells/well were seeded on top of the layer. Tube formation was imaged on a Leica IX70 microscope outfitted with an environmental chamber. Data were compiled using ImageJ Analysis Software. Brightfield images were converted to eight-bit black and white and the "find edges" command was used to identify cells. Images were enhanced using sharpen tools and pseudocolored for video analysis.

Dextran perfusion

Dextran perfusion was carried out according to previously-published methods (Lin et al., 2006). GFP labeled tumor cells were injected subcutaneously as described. Once tumors reached 1 cm^3, mice were injected with 100 μL, 70 kD-Texas Red Dextran (Life Technologies) via the tail vein and sacrificed three minutes post-injection. Tumors were prepared for immunohistochemistry as described and imaged with a Zeiss LSM700 scanning laser confocal microscope. Tumor-cell affiliated dextran was quantified by identifying GFP^+ cells abutting on

dextran-lined channels in tumors and are presented as average tumor cells integrated within lumens per field.

XTT Assay

XTT Assay Kit (ATCC) was used to measure growth of cells. 5,000 cells were plated in triplicate in a 96 well plate. XTT reagent was prepared per manufacturers recommendations, added to wells, and absorbance at 475 nm was measured after 4 hours.

5-azacytadine (5-aza) and trichostatin A (TSA) treatment

5-Aza (stock: 819mM) or TSA (stock: 6.6mM) were diluted as indicated and added to media. Cells were harvested seven days later and RNA was purified for semi quantitative RT-PCR analysis.

Karyotypes

Cells were treated with 0.1 mg ml 1 colcemid (Irvine Scientific) for 3 h to accumulate cells in metaphase. Cells were then treated with hypotonic 0.075 M KCl for 25 min at 37°C and fixed in 3:1 methanol/acetic acid. Air-dried slides were stained for G-band analysis and at least 20 metaphase cells were counted for each cell line by the Brigham and Women's Hospital CytoGenomics Core Laboratory, Boston, MA, USA.

Statistical analysis

Statistical power for mouse experiments was calculated using Biomath (biomath.info/power). All samples sizes were equal to or greater than recommended minimum group size. All measurements in mouse studies were done with the assistance of at least one blinded researcher for recording and confirmation. Statistical analysis was carried out using the Graphpad Prism 5.0f statistical analysis package unless otherwise noted. Figure legends list specific n and P values. Data are presented as mean±standard error of the mean (s.e.m.).

Figures

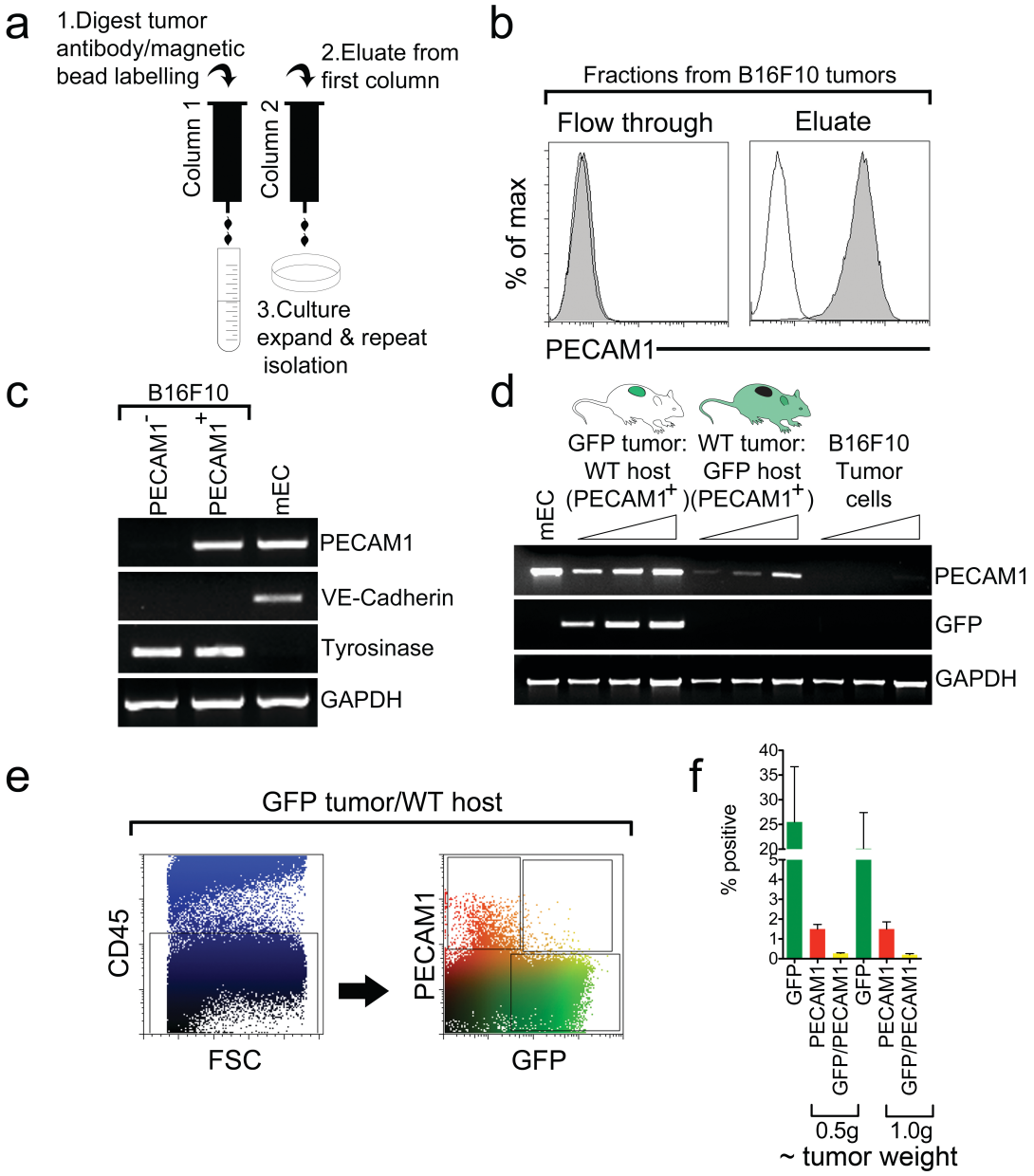
a
1.Digest tumor antibody/magnetic bead labelling
2.Eluate from first column
Column 1
Column 2
3.Culture expand & repeat isolation
b
Fractions from B16F10 tumors
Flow through
Eluate
% of max
PECAM1
c
B16F10
PECAM1-
PECAM1+
mEC
PECAM1
VE-Cadherin
Tyrosinase
GAPDH
d
GFP tumor: WT host (PECAM1+)
WT tumor: GFP host (PECAM1+)
B16F10 Tumor cells
mEC
PECAM1
GFP
GAPDH
e
GFP tumor/WT host
CD45
FSC
PECAM1
GFP
f
% positive
GFP
PECAM1
GFP/PECAM1
GFP
PECAM1
GFP/PECAM1
0.5g
1.0g
~ tumor weight

Figure 2.1. Identification, isolation, and characterization of PECAM-1+ tumor cells from B16F10 melanoma.
(a) PECAM-1 antibodies coupled to immunomagnetic beads were used to enrich PECAM-1^+ tumor cells from collagenase-digested B16F10 tumors. (b) The enriched cells (eluate) are ~ 99% PECAM-1^+ by flow cytometry. (c) Purity of the cells was further confirmed by semi-quantitative RT-PCR. The PECAM-1^+ fraction from B16F10 expresses PECAM-1 and Tyr, but not VE-cadherin. (d) Retrieval of PECAM-1^+/GFP^+ cells from GFP tumors engrafted in WT hosts and PECAM-1+/GFP- cells engrafted in GFP hosts. Following immunomagnetic separation with PECAM-1 antibodies, increasing amounts of cDNA template were analyzed by semi-quantitative RT-PCR, indicated by the wedge. (e) Detection of PECAM-1^+/GFP^+ tumor cells in vivo after injecting B16F10-GFP tumor cells into WT hosts. $CD45^+$ hematopoietic cells were excluded by out-gating. The upper right quadrant are PECAM-1^+ tumor cells which comprise ~ 0.1% of each tumor. (f) The percentage of PECAM-1^+/GFP^+ tumor cells are shown for two time points when tumors were different sizes, n=3 mice/group. (error bars = s.e.m)

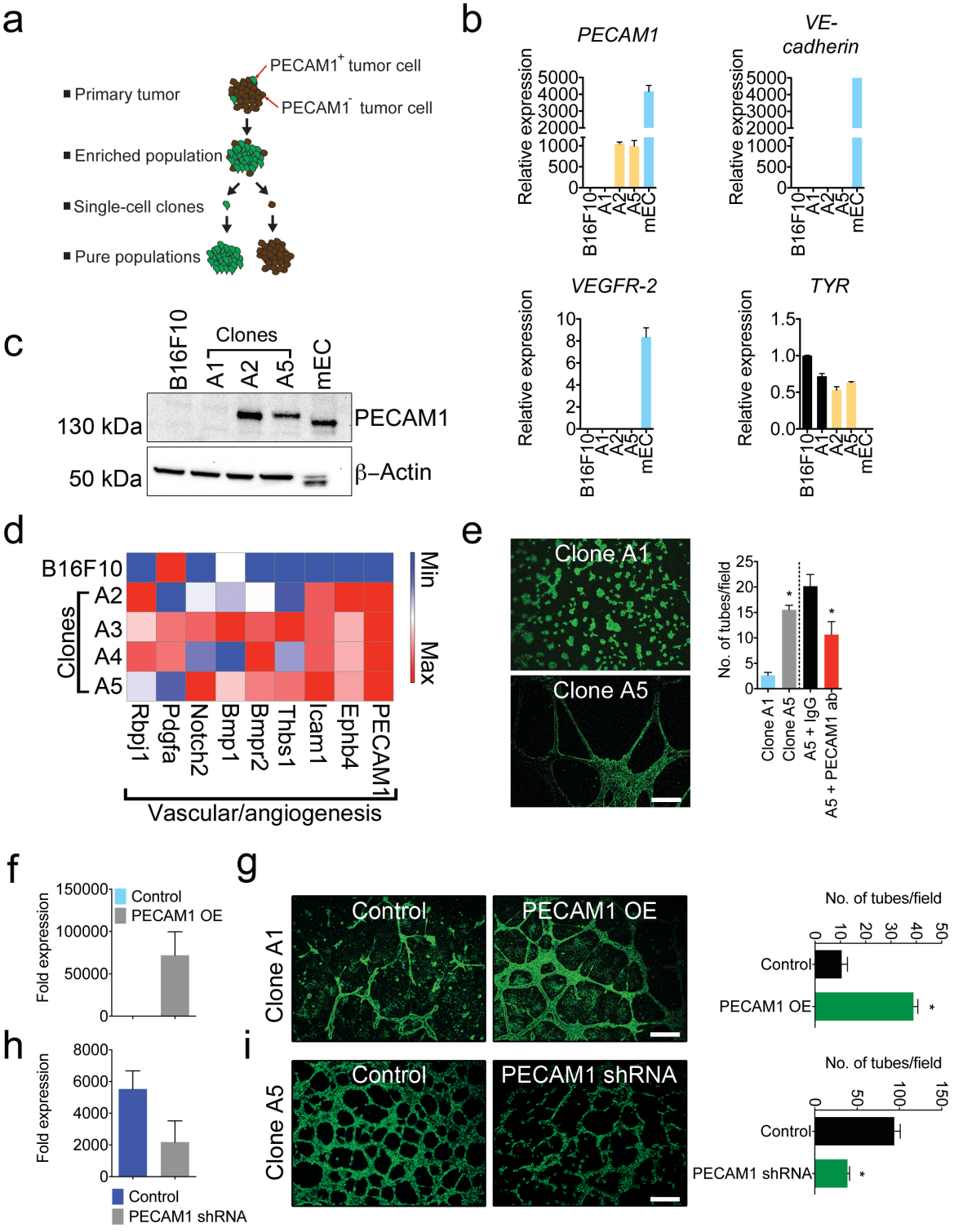
a
Primary tumor
Enriched population
Single-cell clones
Pure populations
PECAM1+ tumor cell
PECAM1- tumor cell
b
PECAM1
VE-cadherin
VEGFR-2
TYR
Relative expression
B16F10
A1
A2
A5
mEC
c
Clones
130 kDa
PECAM1
50 kDa
β–Actin
d
B16F10
Clones
A2
A3
A4
A5
Min
Max
Rbpj1
Pdgfa
Notch2
Bmp1
Bmpr2
Thbs1
Icam1
Ephb4
PECAM1
Vascular/angiogenesis
e
Clone A1
Clone A5
No. of tubes/field
Clone A1
Clone A5
A5 + IgG
A5 + PECAM1 ab
f
Fold expression
Control
PECAM1 OE
g
Clone A1
Control
PECAM1 OE
No. of tubes/field
h
Fold expression
Control
PECAM1 shRNA
i
Clone A5
Control
PECAM1 shRNA
No. of tubes/field

Figure 2.2. PECAM-1$^+$ clonally-derived populations from B16F10 melanoma display vascular characteristics and form PECAM-1-dependent tube-like structures.
(a) Strategy for preparation of PECAM-1$^+$ clonal populations from B16F10 melanoma using limiting dilutions of partially-enriched cellular fractions. (b) Characterization of PECAM-1$^-$ and PECAM-1$^+$ clonal populations using qPCR. (c) Western blotting for PECAM-1 using whole cell extracts from the indicated cell type. PECAM-1 migrates at the expected size of ~ 130 kDa. Blots were stripped and re-probed with β-actin antibodies to show equal loading. (d) Microarray analysis of parental B16F10 and PECAM-1$^+$ clonal populations derived from B16F10. Only known vascular or angiogenesis-related genes shown to be up-regulated in PECAM-1$^+$ clones are shown. (e) Images from tube-forming assay in Matrigel comparing a PECAM-1$^-$ and PECAM-1$^+$ clone. Tube-like structures in high power fields were quantified and plotted. Sample means were statistically significant as determined by a student's t-test ($p<0.02$, $n = 6$ wells per condition). (f) qPCR analysis of PECAM-1 expression in PECAM-1- melanoma cells (clone A1) following ectopic PECAM-1 expression. (g) Images of control-transfected cells and PECAM-1 over-expressing cells (OE) are shown after a 16-hour tube formation assay and quantified at right. Means are statistically significant as determined by a student's t-test ($p<0.001$, $n = 6$-7 wells per condition) (h) qPCR analysis of PECAM-1 expression in PECAM-1$^+$ melanoma cells (clone A5) following shRNA knockdown. (i) Images of empty-vector transfected and PECAM-1 shRNA-transfected cells are shown after a 16-hour tube formation assay and quantified at right. Means are statistically significant as determined by a student's t-test ($p<0.001$, $n = 7$-8 wells per condition). (scale bars = 100 μm, error bars = s.e.m.)

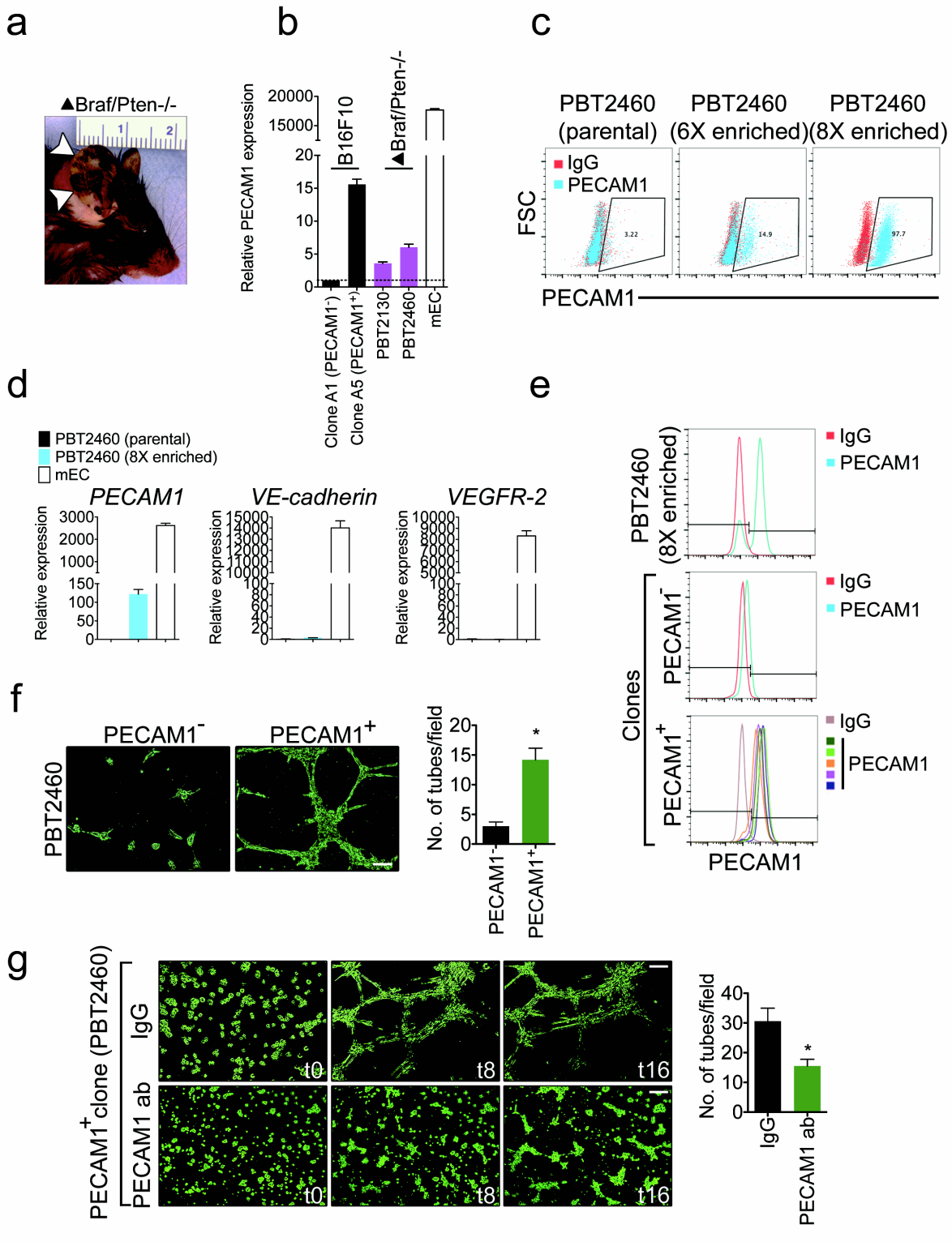
a
▲Braf/Pten-/-
b
Relative PECAM1 expression
B16F10
▲Braf/Pten-/-
Clone A1 (PECAM1-)
Clone A5 (PECAM1+)
PBT2130
PBT2460
mEC
c
PBT2460 (parental)
PBT2460 (6X enriched)
PBT2460 (8X enriched)
IgG
PECAM1
FSC
PECAM1
3.22
14.9
97.7
d
PBT2460 (parental)
PBT2460 (8X enriched)
mEC
PECAM1
VE-cadherin
VEGFR-2
Relative expression
e
PBT2460 (8X enriched)
IgG
PECAM1
Clones
PECAM1-
PECAM1+
PECAM1
f
PECAM1-
PECAM1+
PBT2460
No. of tubes/field
PECAM1-
PECAM1+
g
PECAM1+ clone (PBT2460)
IgG
PECAM1 ab
t0
t8
t16
No. of tubes/field
IgG
PECAM1 ab

Figure 2.3. PECAM-1^{+}/VEGFR-2^{-} tumor cells exist in a genetically engineered mouse model of melanoma and they form vascular-like networks in Matrigel.
(a) Examples of tumors from ΔBraf/Pten$^{-/-}$ mice. (b) qPCR analysis of PECAM-1 expression in PECAM-1^{-} and PECAM-1^{+} B16F10 clonal populations and two additional unsorted cell lines derived from dispersed tumors from ΔBraf/Pten$^{-/-}$mice. mEC are a positive control for PECAM-1 expression. (c) Flow cytometry analysis of unsorted (parental) PBT2460 cells shows ~ 3% positivity for PECAM-1. After six rounds of PECAM-1 selection, this fraction increases to ~ 15% and after eight rounds to ~ 98%. (d) qPCR analysis of the parental PBT2460 population versus the 8X-enriched fraction. Basal PECAM-1 expression is ~ 100-fold higher in the 8X-enriched fraction compared to unsorted PBT2460 cells, while neither population expresses VE-cadherin or Vegfr-2. (e) Using the 8X enriched fraction, single cell clones were prepared by limiting dilution assays and then analyzed by flow cytometry for PECAM-1 expression. (f) Clonally-derived PECAM-1^{+} PBT2460 cells show an ~ 5-fold increase in tube formation as compared to PECAM-1^{-} cells. Sample means were statistically significant as determined by a student's t-test ($p<0.01$). (g) Time-lapse images of tube formation assay using clonally-derived PECAM-1^{+} PBT2460 cells incubated with either a non-specific IgG (top row) or PECAM-1-blocking antibody (bottom row). Elapsed time is shown in hours. (h) PECAM-1 blocking antibodies reduce tube formation by ~ 50% in PECAM-1^{+} PBT2460 cells. (scale bars = 100 μm, error bars = s.e.m.)

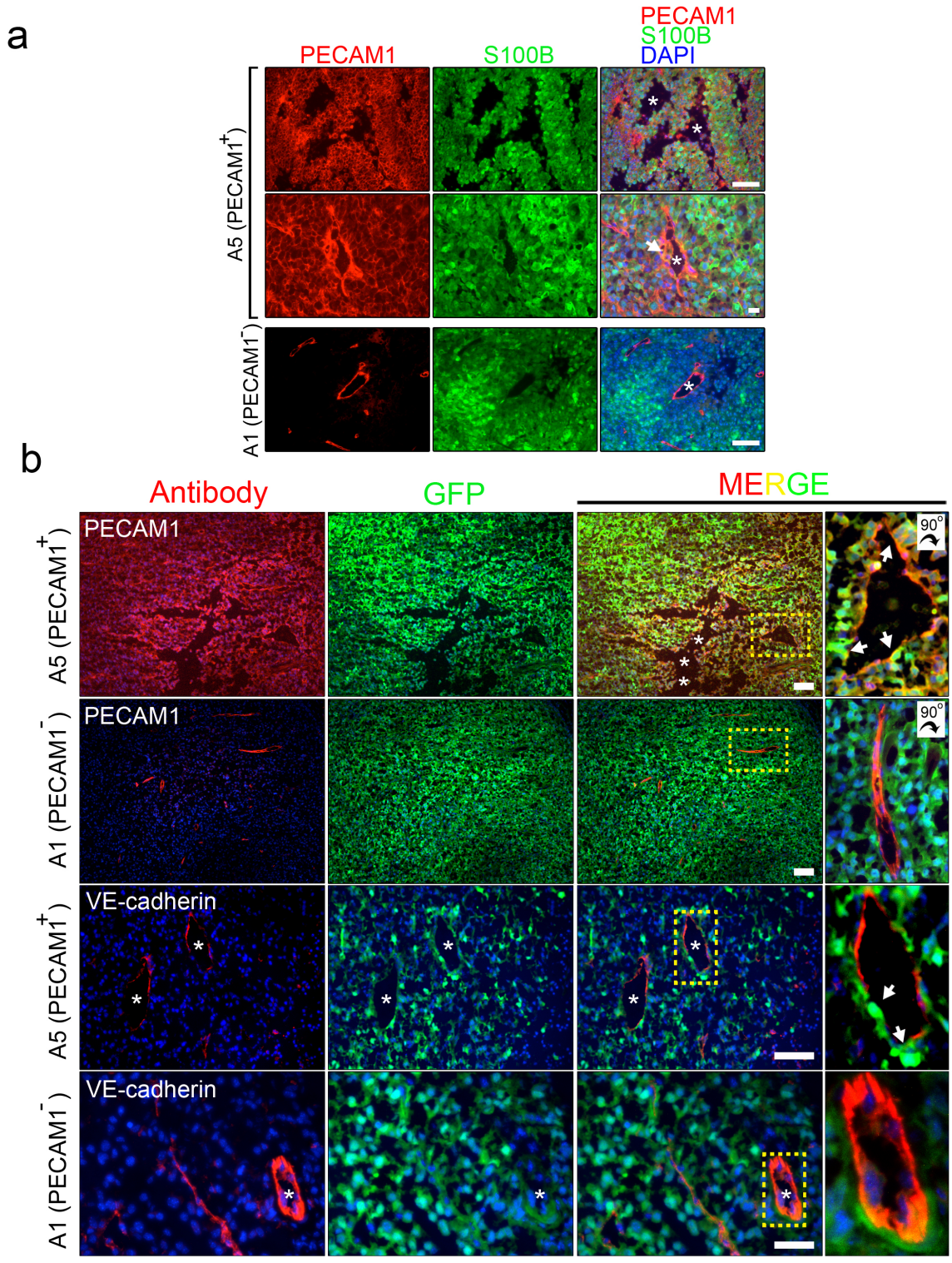
a
PECAM1
S100B
PECAM1
S100B
DAPI
A5 (PECAM1+)
A1 (PECAM1-)
b
Antibody
GFP
MERGE
PECAM1
PECAM1
VE-cadherin
VE-cadherin
A5 (PECAM1+)
A1 (PECAM1-)
A5 (PECAM1+)
A1 (PECAM1-)
90°
90°

Figure 2.4. PECAM-1$^+$ melanoma cells integrate within vessel lumens in vivo.
(a) Engraftment of unlabeled PECAM-1$^-$ (clone A1) and PECAM-1$^+$ (clone A5) tumor cells in C57BL6/J mice. Tumors were implanted subcutaneously and then harvested ~ 3 weeks later. Frozen sections were stained with PECAM-1 and S100b antibodies. (b) Representative GFP-labeled PECAM-1$^+$ and PECAM-1$^-$ tumors are shown. Sections were stained with PECAM-1 or VE-Cadherin antibodies where indicated. The boxed regions shown at far right are zoomed regions taken from these images. In the top panels, asterisks indicated tumor cell-lined "channels". The arrows show luminally-positioned tumor cells. In the bottom panels, the asterisks and arrows indicate where host-derived VE-cadherin$^+$ EC are absent but void space is filled by GFP$^+$/PECAM-1$^+$ tumor cells. In PECAM-1$^-$/GFP$^+$ tumors shown for comparison, PECAM-1$^-$/GFP$^+$ tumor cells surround a host-derived, VE-cadherin+ vessel but do not incorporate into the lumen. (long scale bars = 100 μm, short = 20 μm)

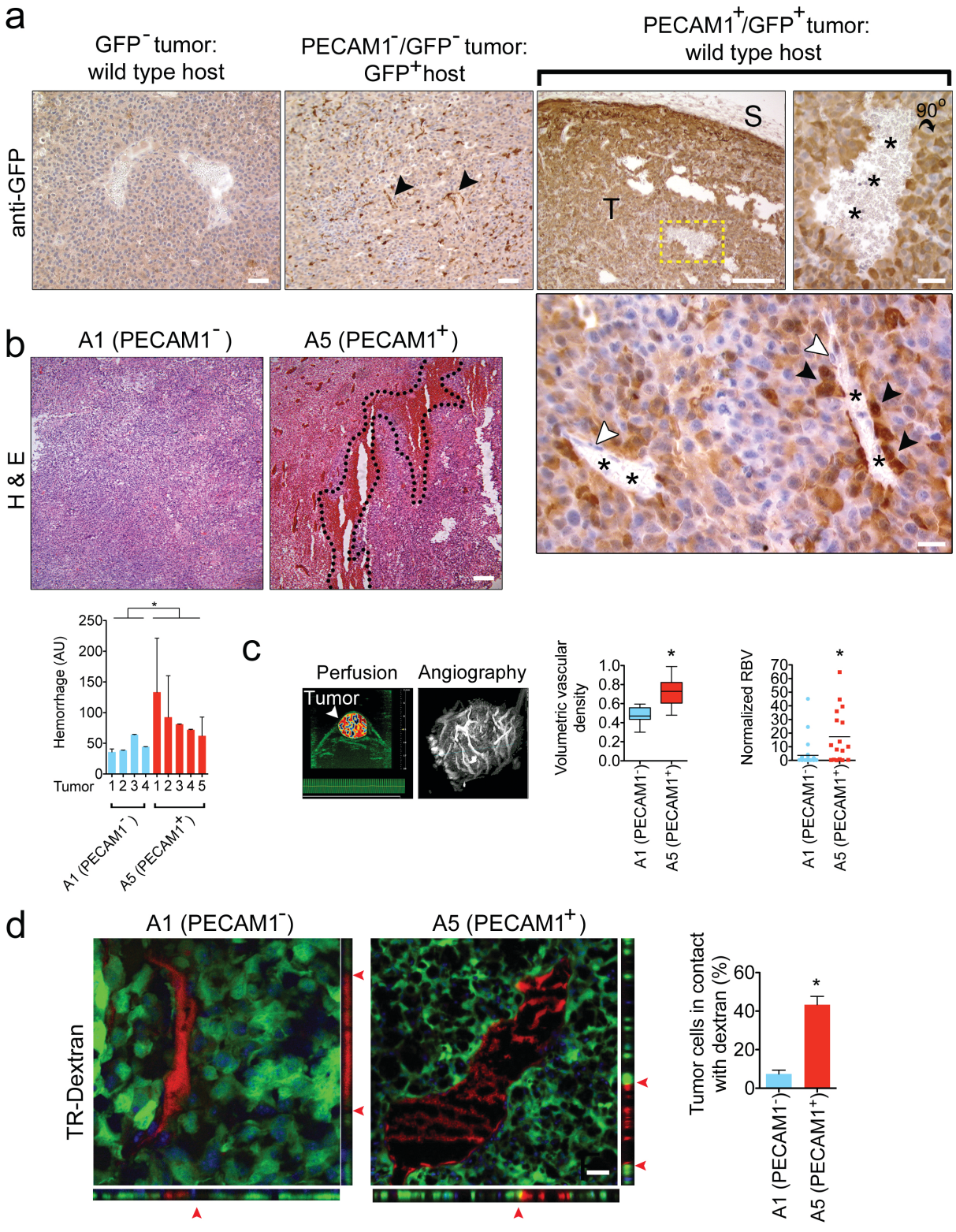
a
GFP- tumor: wild type host
PECAM1-/GFP- tumor: GFP+host
PECAM1+/GFP+ tumor: wild type host
anti-GFP
S
T
90°
b
A1 (PECAM1-)
A5 (PECAM1+)
H & E
Hemorrhage (AU)
Tumor 1 2 3 4 1 2 3 4 5
A1 (PECAM1-)
A5 (PECAM1+)
c
Perfusion
Angiography
Tumor
Volumetric vascular density
Normalized RBV
d
A1 (PECAM1-)
A5 (PECAM1+)
TR-Dextran
Tumor cells in contact with dextran (%)

Figure 2.5. PECAM-1$^+$ melanoma cells form primitive but perfused vascular structures. (a) 3,3' diaminobenzidine (DAB) detection of GFP antibodies used to stain tumors. Unlabeled B16F10 tumors implanted in wild type hosts were used as negative controls. Two large blood vessels are visible in the center of field. Unlabeled PECAM-1$^-$ tumors implanted in a GFP host showed an expected staining pattern of host-derived blood vessels (black arrow heads) and stromal cells. PECAM-1$^+$/GFP$^+$ tumor cells contained large "holes" and channels, some of which were blood-filled. GFP$^+$ tumor cells in right two panels appear to be in direct contact with red blood cells (asterisks). The boxed area in the third panel is magnified on far right. Tumor area is marked with a "T" and the overlying mouse skin (GFP$^-$) is marked with an "S." Lower panel shows a second PECAM-1$^+$ clone (clone A2) with PECAM-1$^+$/GFP$^+$ tumor cells closely aligned with host blood vessels. Some unstained endothelial cell nuclei are also visible and are marked with white arrowheads. (b) H & E stained sections of PECAM-1$^-$ and PECAM-1$^+$ tumors reveals large areas of hemorrhage and vessel dilation. Sections from individual tumors were analyzed using ImageJ and are plotted. Sample means were statistically significant as determined by a student's t-test ($p=0.0384$) ($n = 5$ tumors). (c) Tumor vascularity was measured using 3D acoustic angiography imaging in regions of interest. Means were statistically significant using a Welch two sample t-test ($p=0.003$), $n = 9$ for PECAM-1$^-$ tumors and $n = 8$ for PECAM-1$^+$ tumors. Area-normalized relative blood volume was calculated from 2D destruction-reperfusion imaging. A linear mixed-effects model was used to calculate statistical significance ($p=0.0182$). (d) TR-Dextran was injected intravenously in mice bearing GFP-labeled PECAM-1$^-$ or PECAM-1$^+$ tumors. Harvested tumors were sectioned and imaged on a confocal microscope. Red arrowheads point to GFP$^+$/TR-Dextran$^+$ areas ($n = 4$). Ten separate fields from tissue sections from each mouse were used to quantify number of tumor cells in contact with the circulation as shown. Means were statistically significant using an unpaired two tailed t-test, $p < 0.0001$. (scale bars = 100 μm, short bars in high-magnification panels = 20 μm, error bars = s.e.m.)

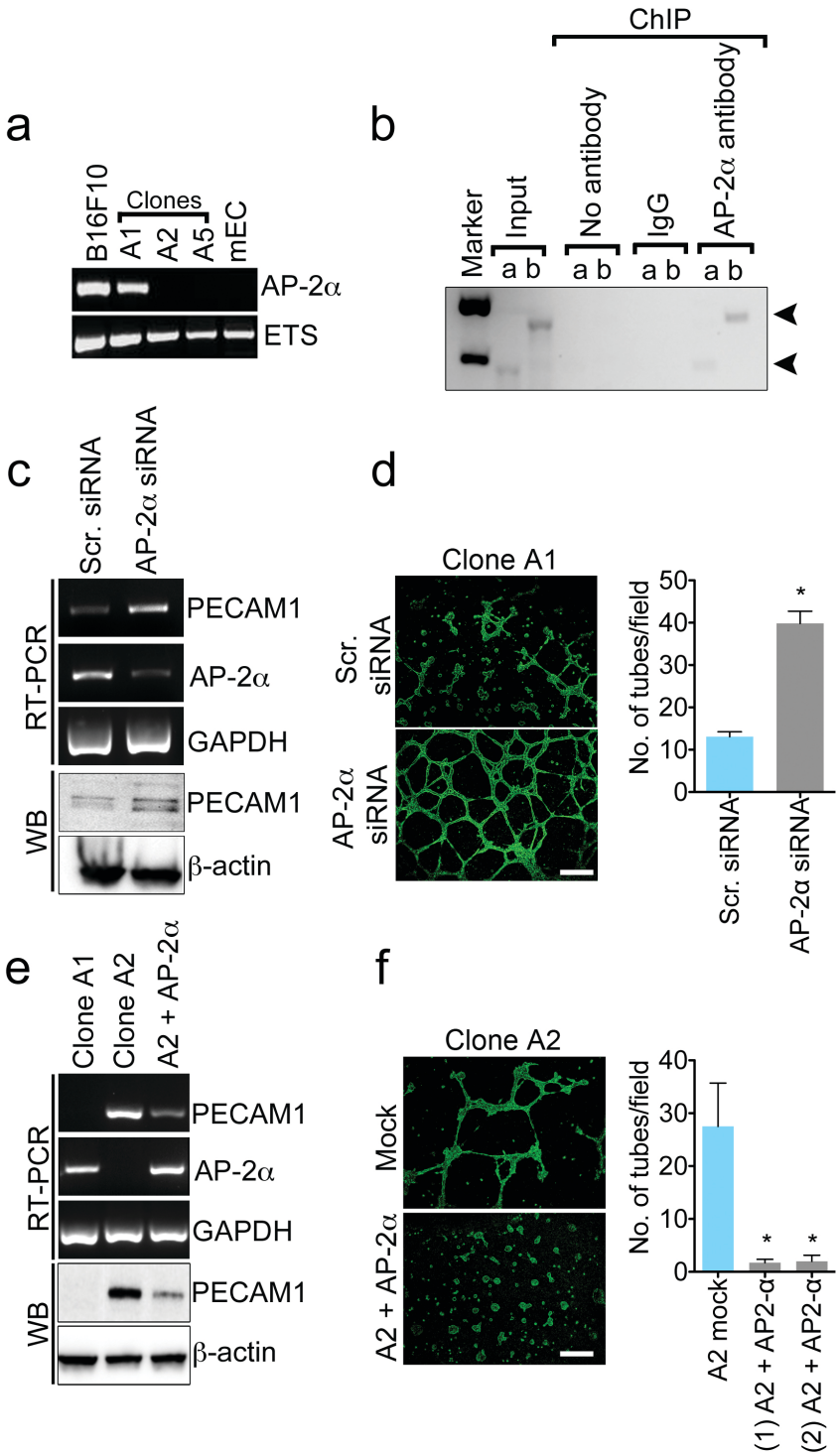
a
B16F10
Clones
A1
A2
A5
mEC
AP-2α
ETS
b
ChIP
Marker
Input
No antibody
IgG
AP-2α antibody
a b
a b
a b
a b
c
Scr. siRNA
AP-2α siRNA
RT-PCR
PECAM1
AP-2α
GAPDH
WB
PECAM1
β-actin
d
Clone A1
Scr. siRNA
AP-2α siRNA
No. of tubes/field
50
40
30
20
10
0
*
Scr. siRNA
AP-2α siRNA
e
Clone A1
Clone A2
A2 + AP-2α
RT-PCR
PECAM1
AP-2α
GAPDH
WB
PECAM1
β-actin
f
Clone A2
Mock
A2 + AP-2α
No. of tubes/field
40
30
20
10
0
*
*
A2 mock
(1) A2 + AP2-α
(2) A2 + AP2-α

Figure 2.6. AP-2α is diminished in PECAM-1$^+$ tumor cells and is a transcriptional repressor of PECAM-1.
(a) Semi-quantitative RT-PCR analysis of Ap-2α and Ets transcription factors in PECAM-1$^-$ and PECAM-1$^+$ clones. (b) Chromatin immunoprecipitation using B16F10 tumor cells. Purified genomic DNA was incubated with AP-2α antibodies followed by capture on protein-G agarose. Samples were analyzed by semiquantitative RT-PCR using two primer sets predicted to amplify different regions of the mouse PECAM-1 promoter (indicated by arrow heads). (c) siRNA knockdown of Ap-2α. Cells were incubated for 48 hours with 100 nM of either scrambled control (Scr. siRNA) or Ap-2α siRNA. Cell extracts were then evaluated by RT-PCR and western blotting. (d) Images of tube forming assay in a PECAM-1- clone following Ap-2α siRNA knockdown. Images were taken approximately 16 hours after seeding on Matrigel. Quantification of tube-forming ability following Ap-2α siRNA knockdown on right. Results are statistically significant where indicated by an asterisk ($p<0.0001$ by unpaired t-test, n = 12 observations from individual wells). (e) Lentiviral over-expression of Ap-2α in PECAM-1$^+$ clones. Stable cell lines were established from clonal populations following Ap- 2α introduction and selection in Zeocin. Cell extracts were evaluated by RT-PCR and western blotting. (f) Images of tube forming assay in a PECAM-1+ clone following Ap-2α lentiviral introduction. Images were taken approximately 16 hours after seeding on Matrigel. Quantification of tube-forming ability following Ap-2α lentiviral introduction on right. Results are statistically significant where indicated by an asterisk and were confirmed using two different derived clones ($p=0.0202$, n = 3-4 observations from individual wells). (scale bars = 100 μm, error bars = s.e.m.)

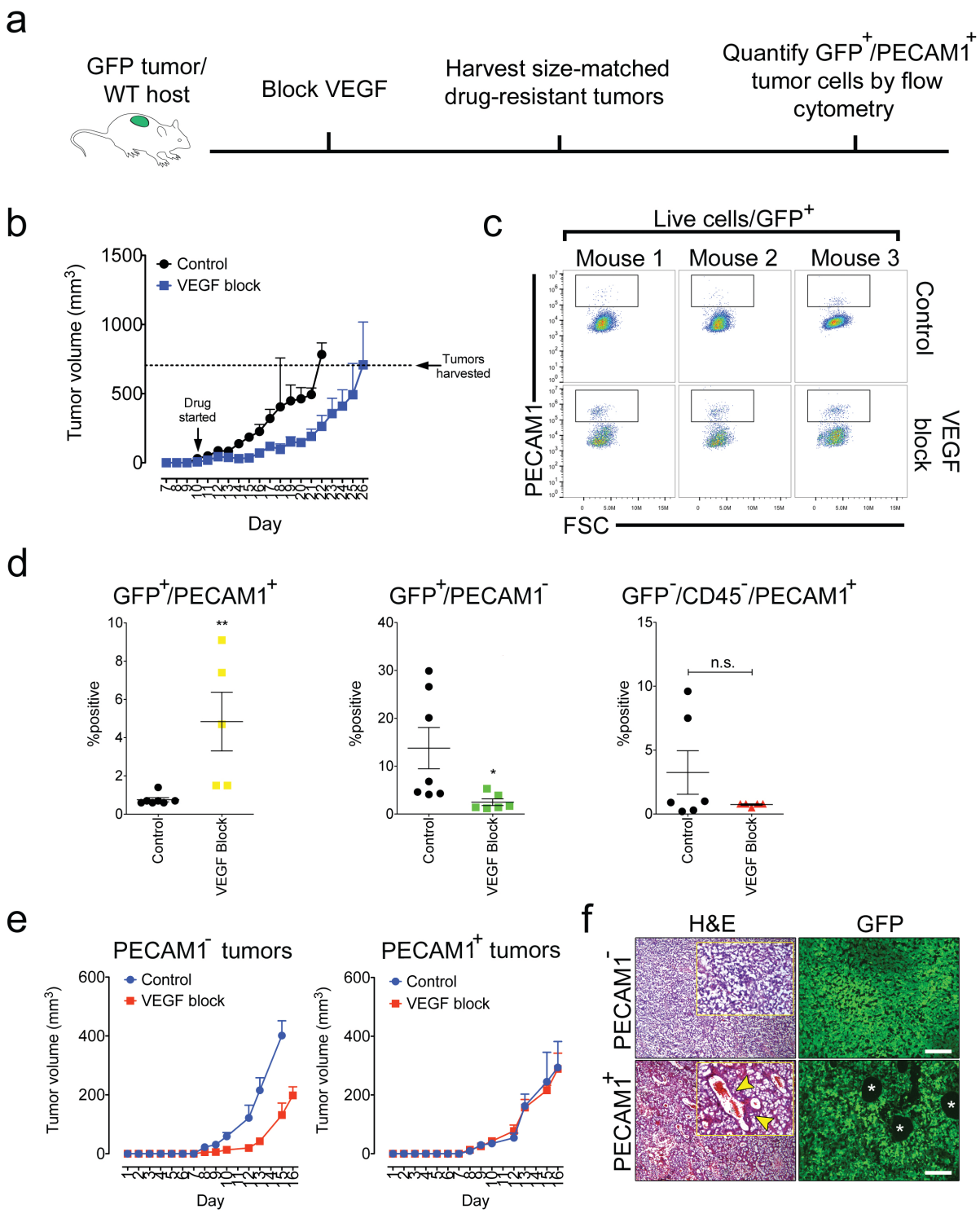
a
GFP tumor/
WT host
Block VEGF
Harvest size-matched
drug-resistant tumors
Quantify GFP+/PECAM1+
tumor cells by flow
cytometry
b
Tumor volume (mm3)
Control
VEGF block
Drug
started
Tumors
harvested
Day
c
Live cells/GFP+
Mouse 1
Mouse 2
Mouse 3
Control
VEGF
block
PECAM1
FSC
d
GFP+/PECAM1+
GFP+/PECAM1-
GFP-/CD45-/PECAM1+
%positive
Control
VEGF Block
n.s.
e
PECAM1- tumors
PECAM1+ tumors
Tumor volume (mm3)
Control
VEGF block
Day
f
H&E
GFP
PECAM1-
PECAM1+

Figure 2.7. PECAM-1$^+$ tumor cells are enriched in tumors challenged with anti-VEGF therapy.
(a) Experimental design. (b) Tumor volumes in control (n = 8) and MCR84-treated (n = 8) mice measured with calipers each day. MCR84 treatment was initiated where indicated. (c) Flow cytometry analysis of collagenase-dispersed tumors from control and MCR84-treated mice. Three representative dot plots from individual mice are shown. Live cells/GFP+ cells were selected and then gated for PECAM-1. The top three panels are controls and the bottom three panels are MCR84-treated mice. (d) Quantification of tumor subpopulations from collagenase-dispersed tumors using flow cytometry (n = 5-7 mice/group). Results are statistically significant where indicated with an asterisk (left, p=0.0095; center, p=0.0361; right, n.s. = not significant) as evaluated by unpaired t-test. (e) Tumor growth in mice bearing PECAM-1$^-$ tumors (clone A1) or PECAM-1$^+$ tumors (clone A5) challenged with MCR84. Drug treatment was initiated on day five and tumor sizes were measured each day with calipers (n = 4-5 mice per group). (f) H & E and GFP-stained tissue sections from MCR84-treated PECAM-1$^-$ and PECAM-1$^+$ tumors. Yellow arrows identify dense pockets of PECAM-1$^+$ tumor cells surrounding a vessel lumen (also identified by asterisks in the accompanying GFP-stained section). (scale bars = 100 μm, error bars = s.e.m.)

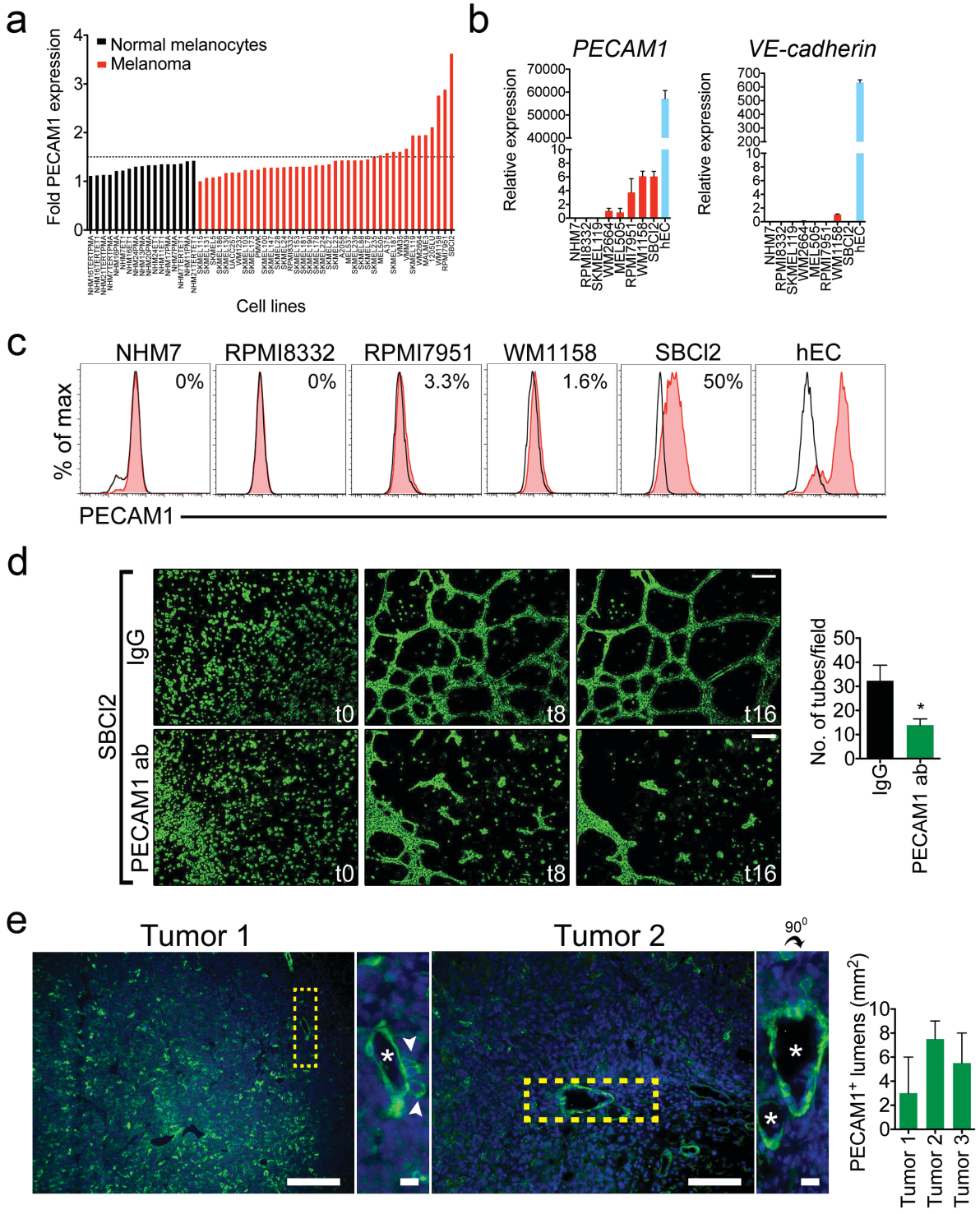
a
Normal melanocytes
Melanoma
Fold PECAM1 expression
Cell lines
b
PECAM1
VE-cadherin
Relative expression
NHM7
RPMI8332
SKMEL119
WM2664
MEL505
RPMI7951
WM1158
SBCl2
hEC
c
NHM7
RPMI8332
RPMI7951
WM1158
SBCl2
hEC
0%
0%
3.3%
1.6%
50%
% of max
PECAM1
d
SBCl2
IgG
PECAM1 ab
t0
t8
t16
No. of tubes/field
IgG
PECAM1 ab
e
Tumor 1
Tumor 2
90⁰
PECAM1⁺ lumens (mm²)
Tumor 1
Tumor 2
Tumor 3

Figure 2.8. Human melanoma contains a PECAM-1$^+$ subpopulation that displays vascular-like characteristics.
(a) Microarray analysis of normal human melanocytes (black bars) and human melanoma (red bars). Each cell line and the raw fluorescence intensity value from the microarray are listed in Supplementary Table 2. The dotted horizontal line on the graph is the threshold below which no PECAM-1 transcripts are detected. (b) Quantitative real-time PCR analysis of PECAM-1 and VE- CADHERIN expression in normal melanocytes and seven of the highest PECAM-1-expressing cell lines predicted from the microarray. Except for WM1158, no VE-CADHERIN transcripts were detected. Human endothelial cells (hEC) were used as a positive control. (c) Flow cytometry of selected cell lines stained with human-specific PECAM-1 antibodies. (d) Time-lapse images of tube formation assay using the PECAM-1$^+$ human melanoma cell line SBCl2 incubated with either a non- specific IgG (top row) or PECAM-1-blocking antibody (bottom row). Far right: PECAM-1 blocking antibodies reduce tube formation by ~ 60% in PECAM-1$^+$ SBCl2 cells. Sample means were statistically significant as determined by a student's t-test ($p=0.02$, $n = 8$ wells per condition). (e) PECAM-1$^+$ lumens formed by SBCl2 tumors. The asterisks mark lumens and white arrow head shows PECAM-1$^+$ tumor cells positioned at the abluminal surface. Two sections from each tumor were scanned for PECAM-1$^+$ lumens and the mean values were plotted on right. (scale bars = 100μm, short bars in high-magnification panels = 20 μm, error bars = s.e.m.)

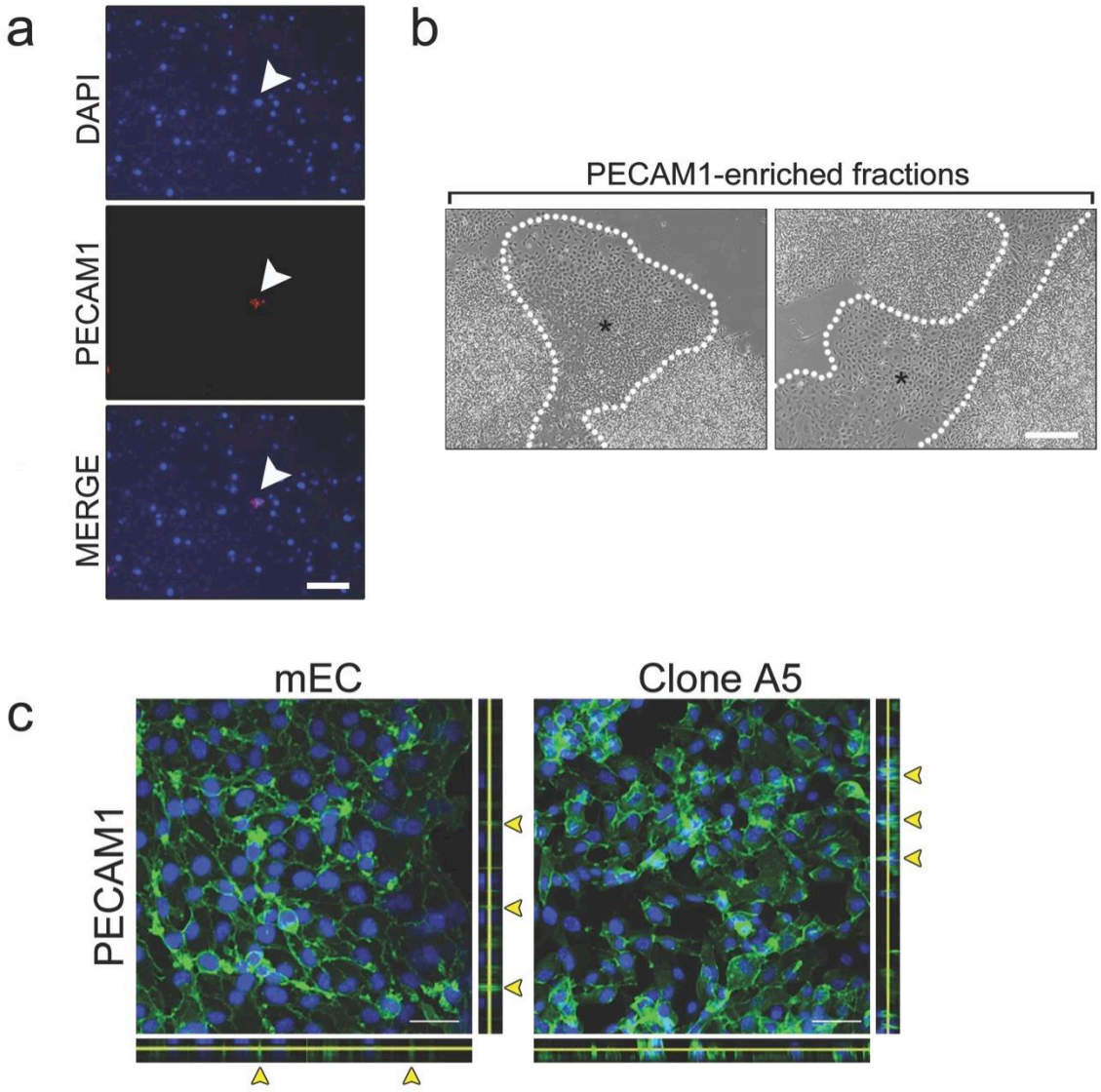
a
DAPI
PECAM1
MERGE
b
PECAM1-enriched fractions
c
mEC
Clone A5
PECAM1
d
Clone A2
Clone A5
mEC
PECAM1 ab IP
- + - + - +
130 kDa
PECAM1
130 kDa
pTYR-
PECAM1

Supplementary Figure 2.1. PECAM-1 is aberrantly expressed in cultured PECAM-1$^+$ melanoma cells.
(a) PECAM-1$^+$ melanoma cells viewed under fluorescence microscopy in un-enriched B16F10 cultures. B16F10 cultures were detached with accutase, washed and then labeled with PE-conjugated PECAM-1 before seeding onto microscope slides. Only rare PECAM-1$^+$ cells are labeled. (b) Light microscopy showing distinct colonies (asterisks) of PECAM-1$^+$ tumor cells that appeared in B16F10 cultures following 3-4 rounds of enrichment using immunomagnetic separation. (c) Confocal analysis of mEC and a PECAM-1$^+$ clone derived from B16F10 melanoma. The yellow arrow heads in the z-plane identify where PECAM-1 expression appears distributed throughout that cytoplasm, rather than concentrated at the cell membrane. (d) PECAM-1 tyrosine phosphorylation in PECAM-1$^+$ tumor cells and mEC. PECAM-1 was immunoprecipitated from whole cell extracts. Western blots were probed with a pan-PECAM-1 antibody followed by a 4G10 antibody which recognizes phosphorylated tyrosine. (scale bar = 100 μm)

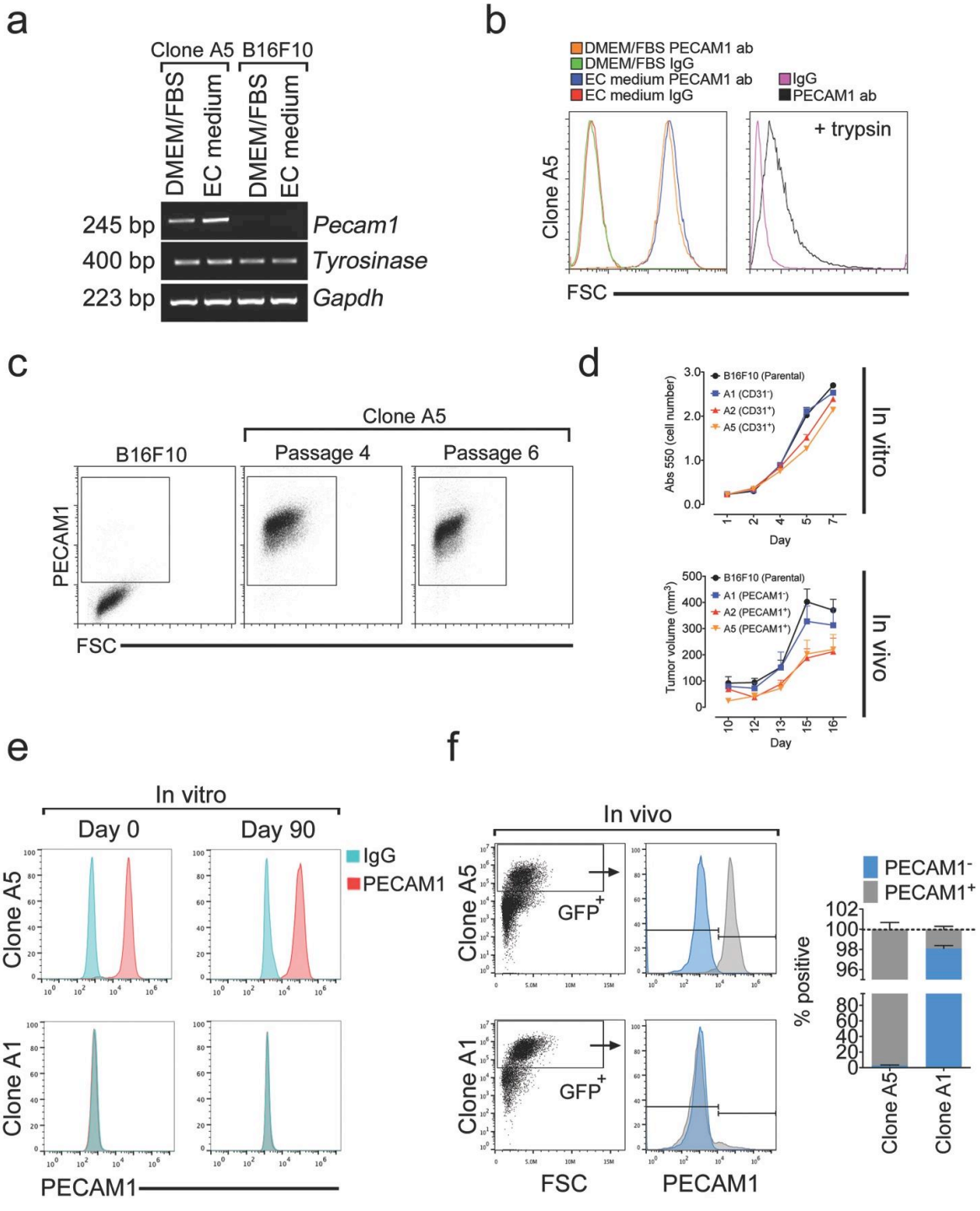
a
Clone A5
B16F10
DMEM/FBS
EC medium
DMEM/FBS
EC medium
245 bp
Pecam1
400 bp
Tyrosinase
223 bp
Gapdh
b
DMEM/FBS PECAM1 ab
DMEM/FBS IgG
EC medium PECAM1 ab
EC medium IgG
IgG
PECAM1 ab
+ trypsin
Clone A5
FSC
c
Clone A5
B16F10
Passage 4
Passage 6
PECAM1
FSC
d
B16F10 (Parental)
A1 (CD31-)
A2 (CD31+)
A5 (CD31+)
Abs 550 (cell number)
Day
In vitro
B16F10 (Parental)
A1 (PECAM1-)
A2 (PECAM1+)
A5 (PECAM1+)
Tumor volume (mm3)
Day
In vivo
e
In vitro
Day 0
Day 90
IgG
PECAM1
Clone A5
Clone A1
PECAM1
f
In vivo
Clone A5
GFP+
Clone A1
GFP+
FSC
PECAM1
PECAM1-
PECAM1+
% positive
Clone A5-
Clone A1-

Supplementary Figure 2.2. Tumor cell PECAM-1 expression is stably maintained in vivo and in vitro.
(a) RT-PCR analysis of PECAM-1 expression in parental B16F10 and in a PECAM-1^+ clone when cells were cultured in standard growth medium (DMEM/FBS) or in an endothelial growth medium (EC medium). (b) Flow cytometry of PECAM-1 expression in clone A5 when cells were cultured in different growth medium and detached with accutase or detached from tissue culture dishes using trypsin. (c) PECAM-1 expression is stable in a PECAM-1^+ clone (clone A5) when cells are serially passaged using accutase for cell detachment. (d) PECAM-1^+ clonal cells show slight growth delay compared to PECAM-1^- counterparts both in vitro (as measured by XTT assay) and in vivo. Tumor growth curves represent one million tumor cells measured daily by calipers (n = 5 mice per group). (e) Flow cytometry for PECAM-1 expression in PECAM-1^+ (clone A5) and PECAM-1^- (clone A1) melanoma cells in vitro. Cells were harvested with accutase and analyzed at day 0 and then again 90 days later after routine culturing. (f) Flow cytometry for PECAM-1 expression by PECAM-1^+/GFP^+ and PECAM-1^-/GFP^+ tumor cells in vivo. Harvested tumors were dispersed with collagenase and then stained with PECAM-1 antibodies. Gating on GFP^+ tumor cells shows that PECAM-1^+ tumor cells generate PECAM-1^+ progeny whereas PECAM-1^- tumor cells generate PECAM-1^- progeny. Results were averaged and graphed from three mice as shown at far right. (error bars = s.e.m.)

a

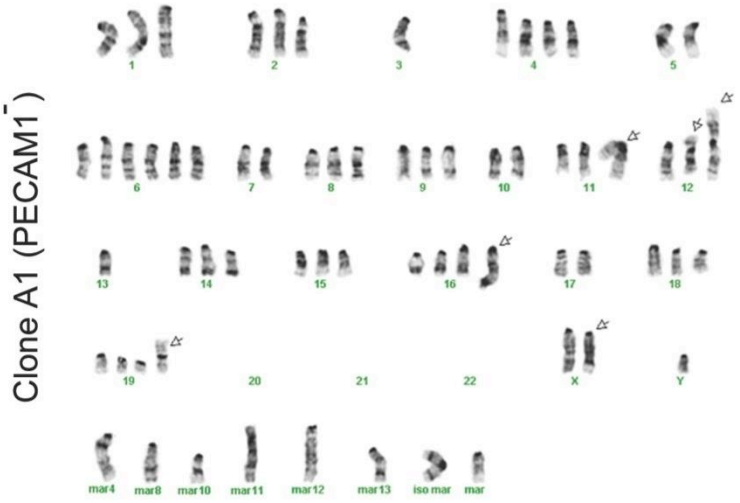
Clone A1 (PECAM1-)
1
2
3
4
5
6
7
8
9
10
11
12
13
14
15
16
17
18
19
20
21
22
X
Y
mar4
mar8
mar10
mar11
mar12
mar13
iso mar
mar

b

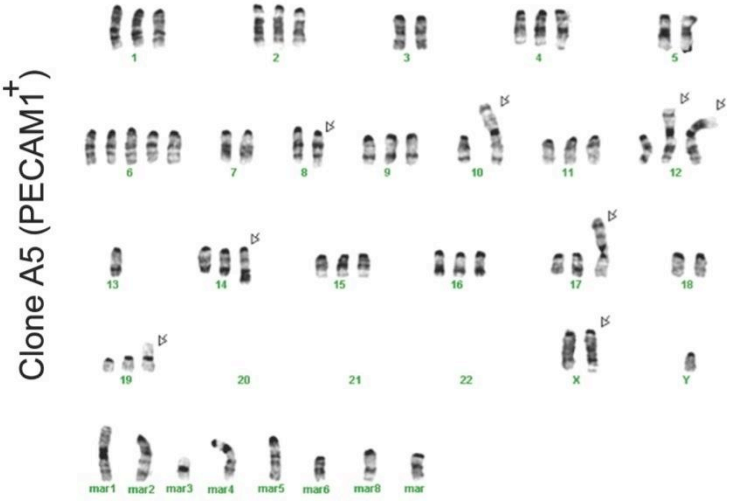
Clone A5 (PECAM1+)
1
2
3
4
5
6
7
8
9
10
11
12
13
14
15
16
17
18
19
20
21
22
X
Y
mar1
mar2
mar3
mar4
mar5
mar6
mar8
mar

Supplementary Figure 2.3. Karyotype analysis of a PECAM-1$^-$ and a PECAM-1$^+$ clone derived from B16F10 melanoma.

Karyotypes were obtained from 21-22 metaphase spreads of PECAM-1$^+$ and PECAM$^-$ clonal populations. Five cells were chosen at random from each cell line. Clone A1 (PECAM-1$^-$) and A5 (PECAM-1$^+$) appear to be related, as seen in their similar ploidies (both are hypertriploid), and numerous shared numerical and structural abnormalities.

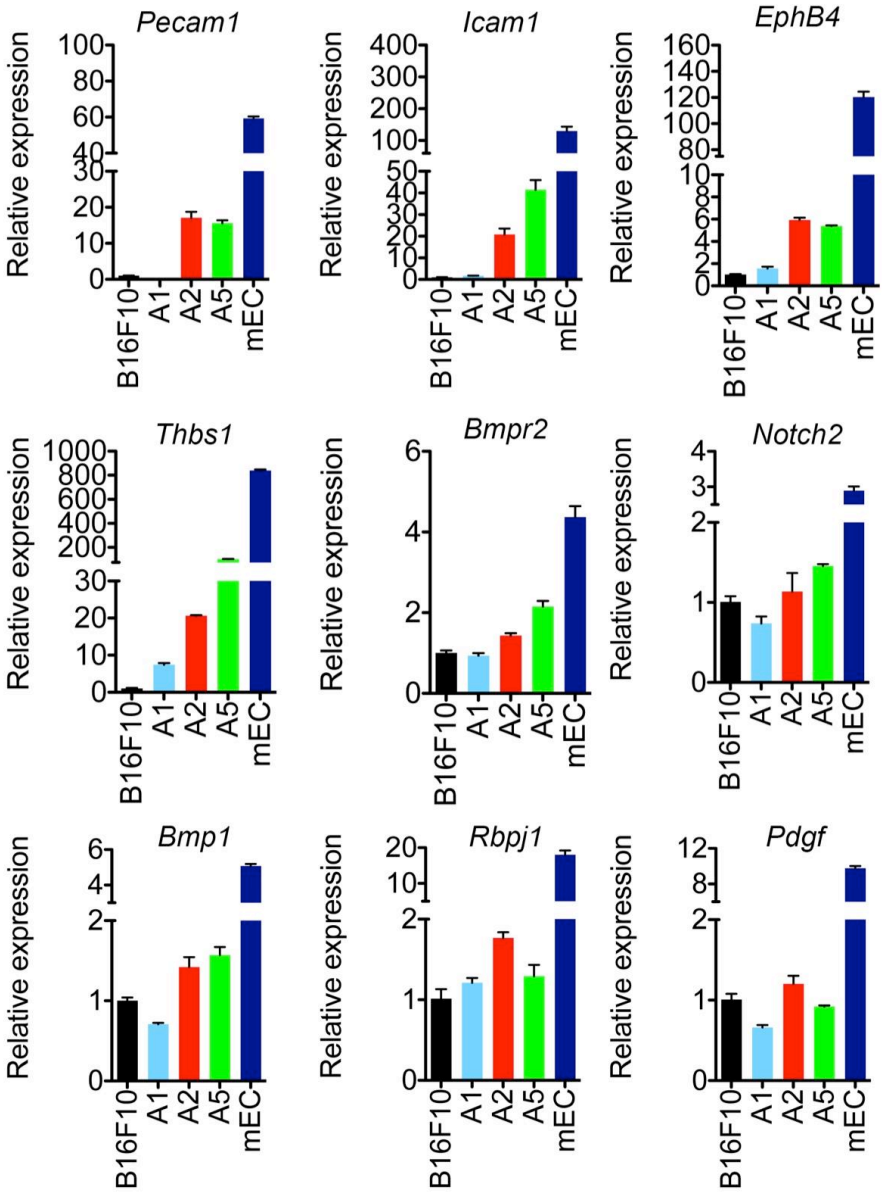
Pecam1
Icam1
EphB4
Thbs1
Bmpr2
Notch2
Bmp1
Rbpj1
Pdgf
Relative expression
B16F10
A1
A2
A5
mEC

Supplementary Figure 2.4. Validation of microarray analysis using qPCR.
Relative expression is indicated for unsorted B16F10, PECAM-1$^-$ (A1), and PECAM-1$^+$ (A2 and A5) clones. mEC were used as a positive control. (error bars = s.e.m.)

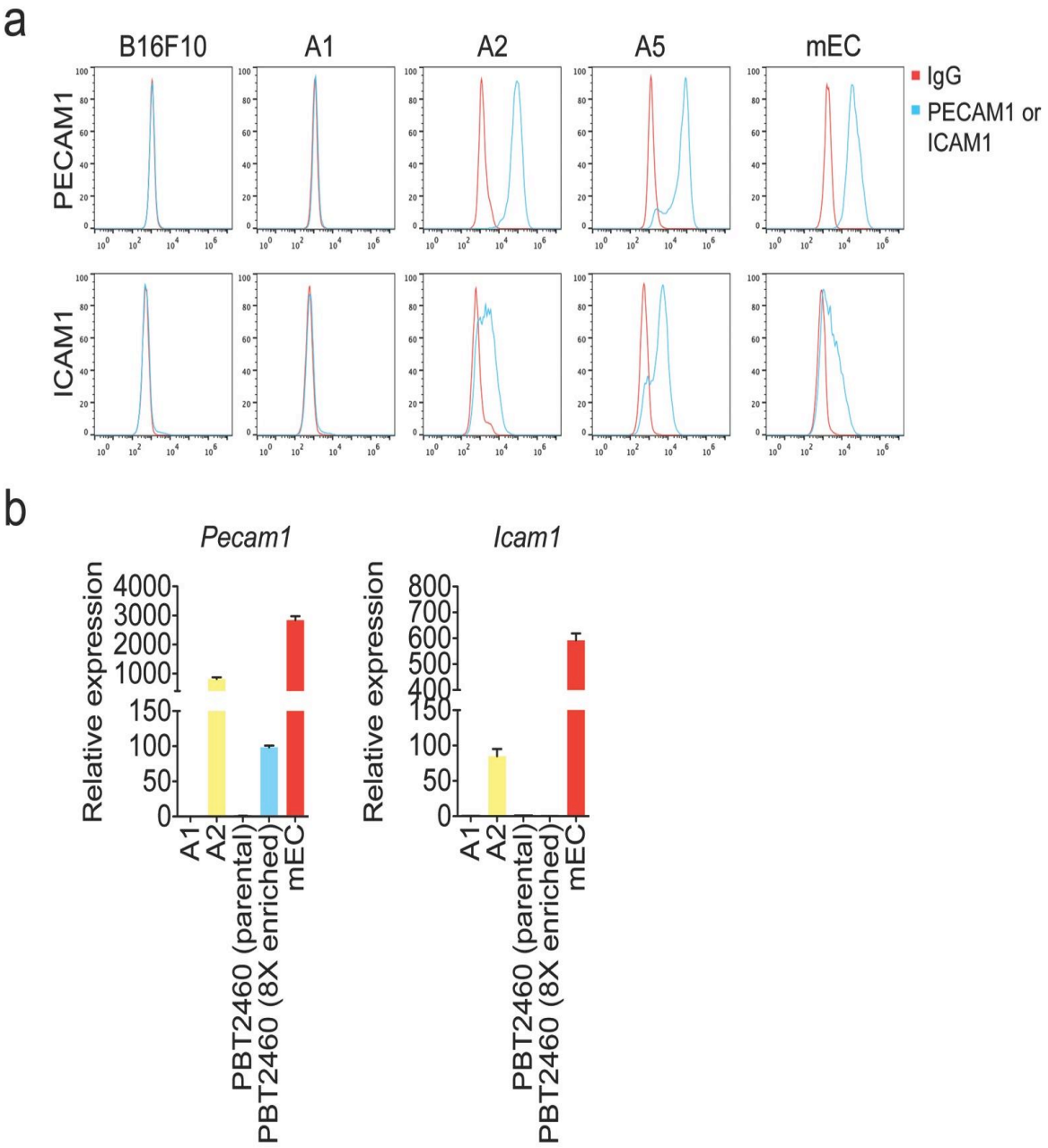
a
B16F10
A1
A2
A5
mEC
PECAM1
ICAM1
IgG
PECAM1 or ICAM1
b
Pecam1
Icam1
Relative expression
A1
A2
PBT2460 (parental)
PBT2460 (8X enriched)
mEC

Supplementary Figure 2.5. PECAM-1^{+} melanoma cells from ΔBraf/Pten$^{-/-}$ tumors do not express ICAM1/CD54.

(a) Flow cytometry analysis for ICAM1 expression in PECAM-1+ clones derived from B16F10.

(b) PECAM-1^{+} cells (clone A2) derived from B16F10 tumors express ICAM1 mRNA whereas PECAM-1^{+} cells derived from ΔBraf/Pten$^{-/-}$ cells do not. (error bars = s.e.m.)

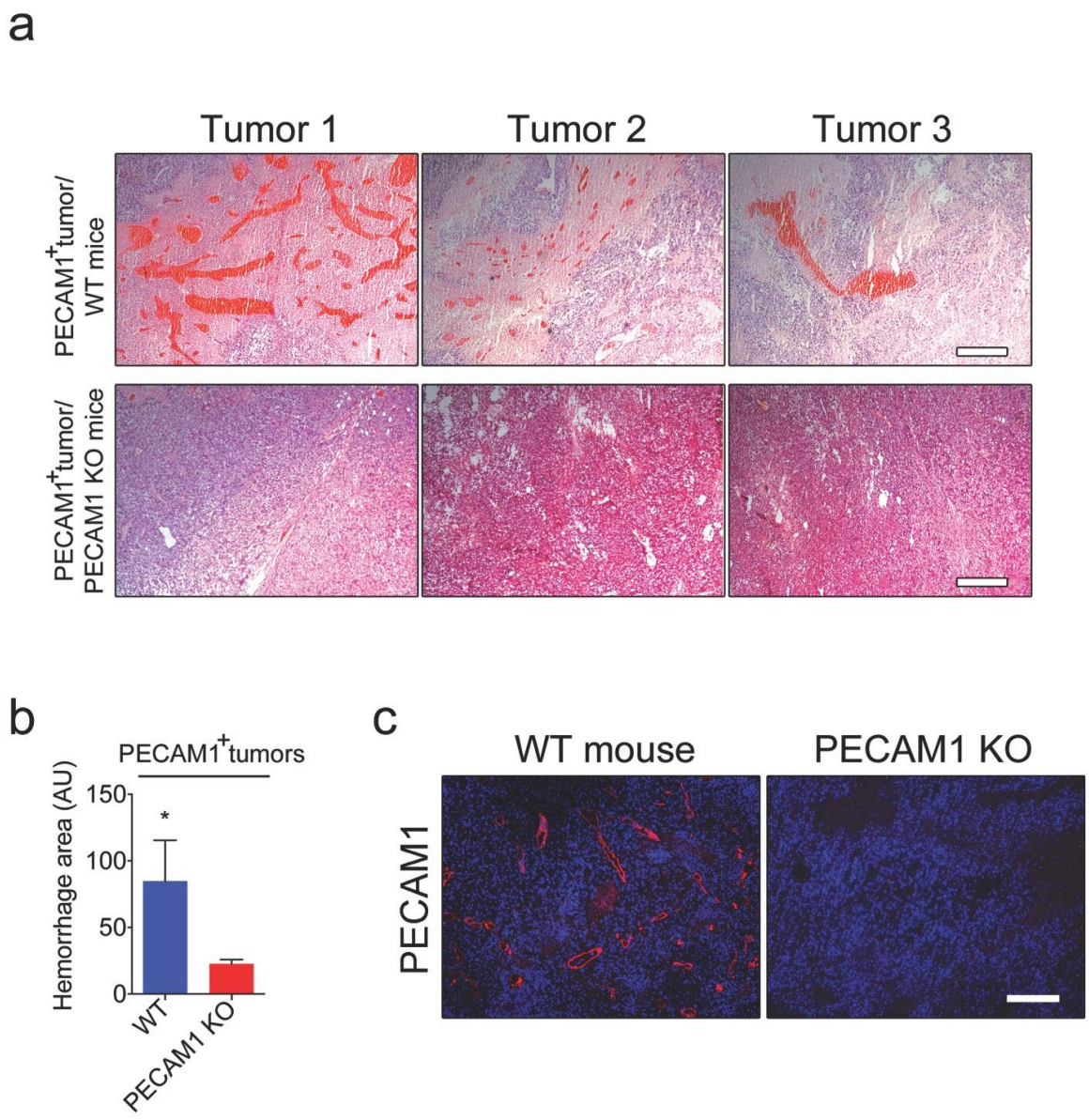
a
Tumor 1
Tumor 2
Tumor 3
PECAM1+tumor/ WT mice
PECAM1+tumor/ PECAM1 KO mice
b
PECAM1+tumors
Hemorrhage area (AU)
150
100
50
0
*
WT
PECAM1 KO
c
WT mouse
PECAM1 KO
PECAM1

Supplementary Figure 2.6. Engraftment of PECAM-1$^+$ tumors in PECAM-1 KO mice reduces vascular hemorrhage.

(a) Three representative images from PECAM-1$^+$ tumors engrafted in WT mice (a-c) or PECAM-1+ tumors engrafted in PECAM-1 KO mice. (b) Hemorrhage area was quantified as described in the methods section (n = 8-9 fields per group, $p < 0.05$ using a one-tailed Student's t-test). (c) Confirmation of PECAM-1 KO using PECAM-1 immunohistochemistry in PECAM-1- tumors engrafted in WT or PECAM-1 KO mice. (scale bar = 100 μm, error bars = s.e.m.)

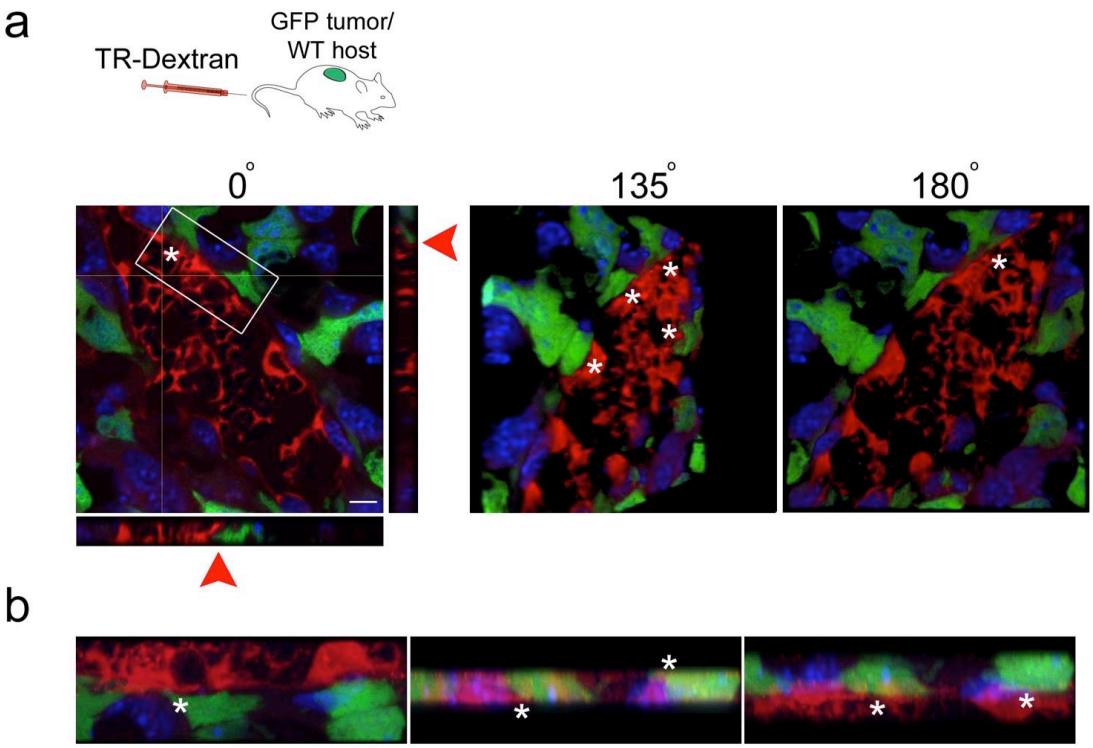
a
TR-Dextran
GFP tumor/
WT host
0°
135°
180°
b

Supplementary Figure 2.7. Confocal analysis of GFP$^+$/TR-Dextran$^+$ vascular structures using an additional PECAM-1$^+$ clone (clone A2).
(a) Clone A2 PECAM-1$^+$ tumors perfused with TR-Dextran. Representative images of vessel-like structures are shown. GFP$^+$/ TR-Dextran cell contact is shown by asterisks and arrows. (b) Still images showing 3D slices through magnified portion of vessel outlined by the white box above. The image was rotated along the z-axis ~ 180 degrees through panels. (scale bar = 20 μm)

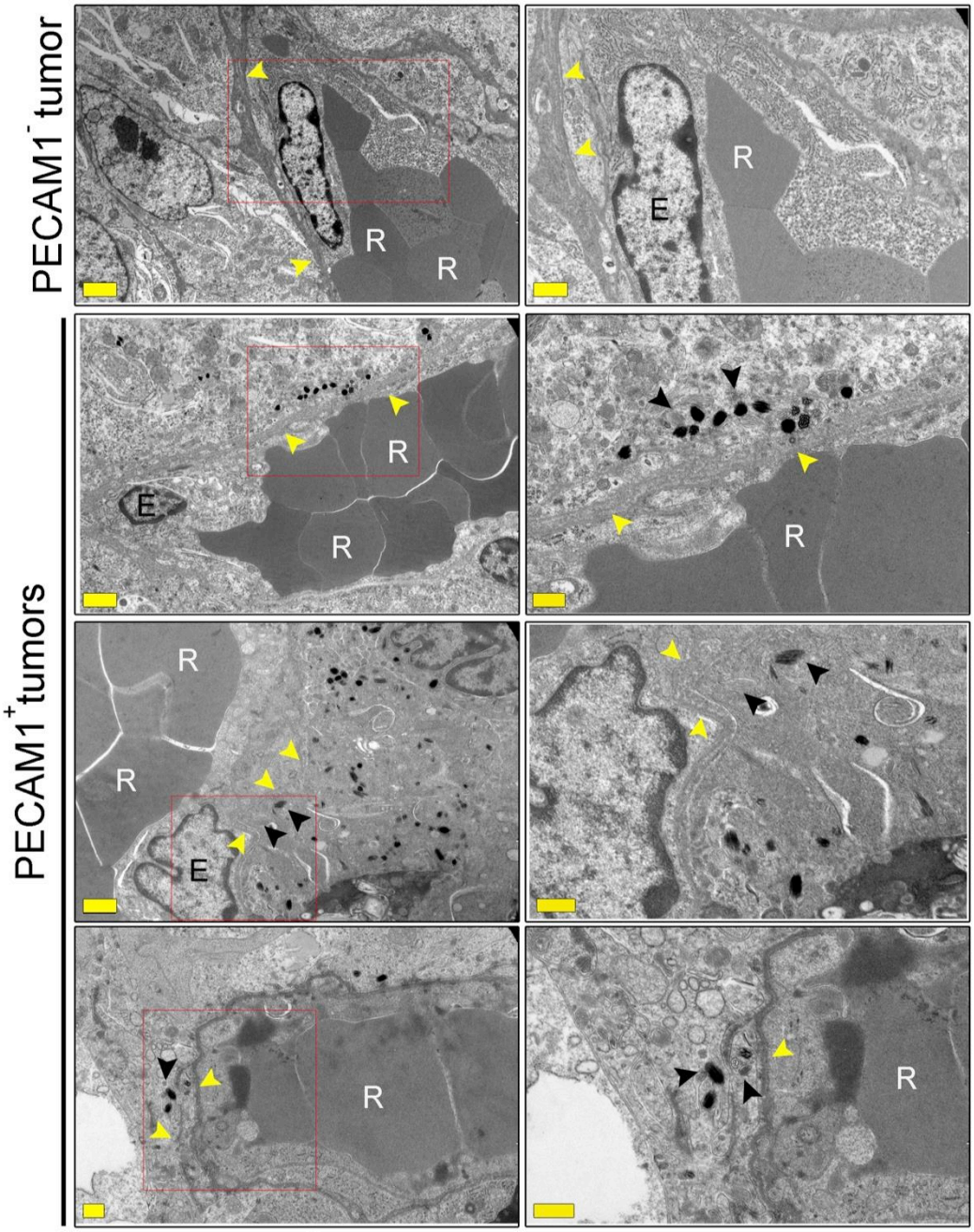
PECAM1- tumor
PECAM1+ tumors
R
E

Supplementary Figure 2.8. Transmission electron microscopy of PECAM-1$^+$ tumor cells in contact with erythrocytes.
Top row: A PECAM-1$^-$ tumor showing electron-dense basal lamina (yellow arrows) and an endothelial cell body (E) juxtaposed to erythrocytes (R), while no melanasome-containing cells are evident. Remaining rows: PECAM-1$^+$ melanoma cells were frequently found in close proximity to or directly abutting the basal lamina. Melanasome (black arrows) containing cells were frequently found in direct contact with the endothelium or basal lamina. Additionally, we found instances where a melanosomes-containing cell process appears to infiltrate into the basal lamina (bottom panel: boxed region), suggesting these cells could interdigitate with the endothelium in these vessels. (scale bar: left column (top to bottom) 2 μm, 1 μm, 1 μm, 0.5 μm. Right column (top to bottom) 1 μm, 0.5 μm, 0.5 μm, 0.5 μm)

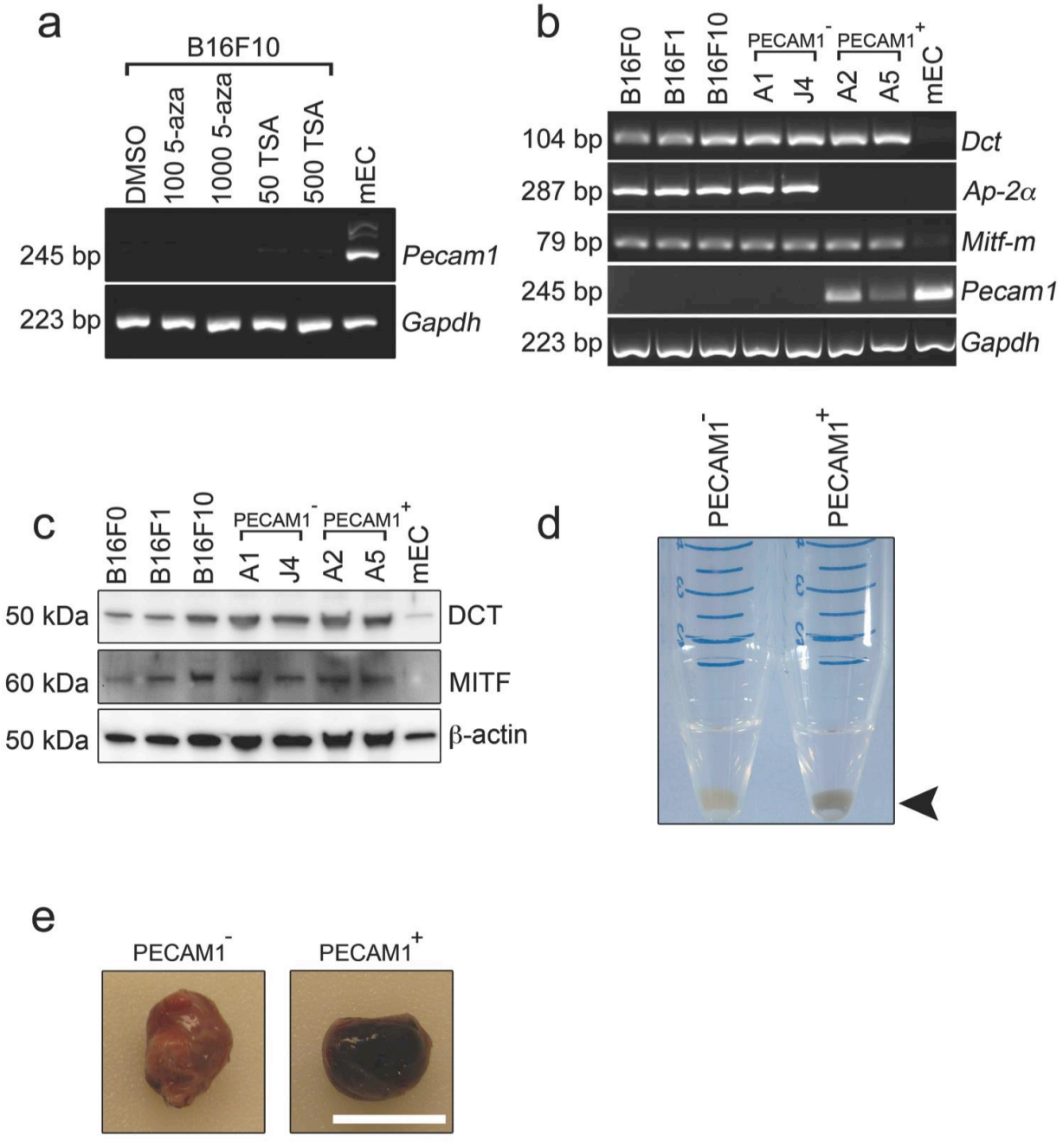
a
B16F10
DMSO
100 5-aza
1000 5-aza
50 TSA
500 TSA
mEC
245 bp
Pecam1
223 bp
Gapdh
b
B16F0
B16F1
B16F10
PECAM1-
A1
J4
PECAM1+
A2
A5
mEC
104 bp
Dct
287 bp
Ap-2α
79 bp
Mitf-m
245 bp
Pecam1
223 bp
Gapdh
c
B16F0
B16F1
B16F10
PECAM1-
A1
J4
PECAM1+
A2
A5
mEC
50 kDa
DCT
60 kDa
MITF
50 kDa
β-actin
d
PECAM1-
PECAM1+
e
PECAM1-
PECAM1+

Supplementary Figure 2.9. Additional characterization of PECAM-1$^-$ and PECAM-1$^+$ melanoma cells.
(a) PECAM-1 expression is not induced in B16F10 tumor cells upon treatment with 5-aza or TSA. Cells were treated for seven days at the indicated concentrations (nM). (b) Expression of additional melanoma markers and PECAM-1 in PECAM-1$^-$ and PECAM-1$^+$ clones. (c) Melanoma markers DCT (~ 50kDa) and MITF (~ 60kDa) migrate at their predicted sizes by western blotting. Blots were stripped and reprobed with β-actin antibodies to show equal loading. (d) PECAM-1+ tumor cells typically produced more pigment than their PECAM-1$^-$ counterparts in culture. (e) Tumors derived from PECAM-1$^+$ tumor cells were more pigmented than their counterparts. (scale bars = 1 cm)

a

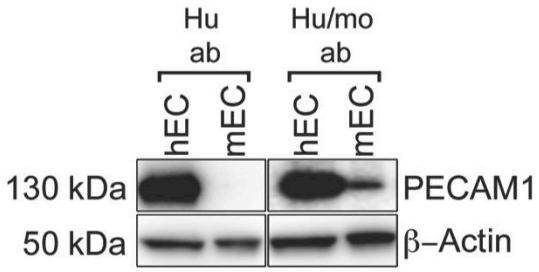
Hu
ab
Hu/mo
ab
hEC
mEC
hEC
mEC
130 kDa
PECAM1
50 kDa
β–Actin

b

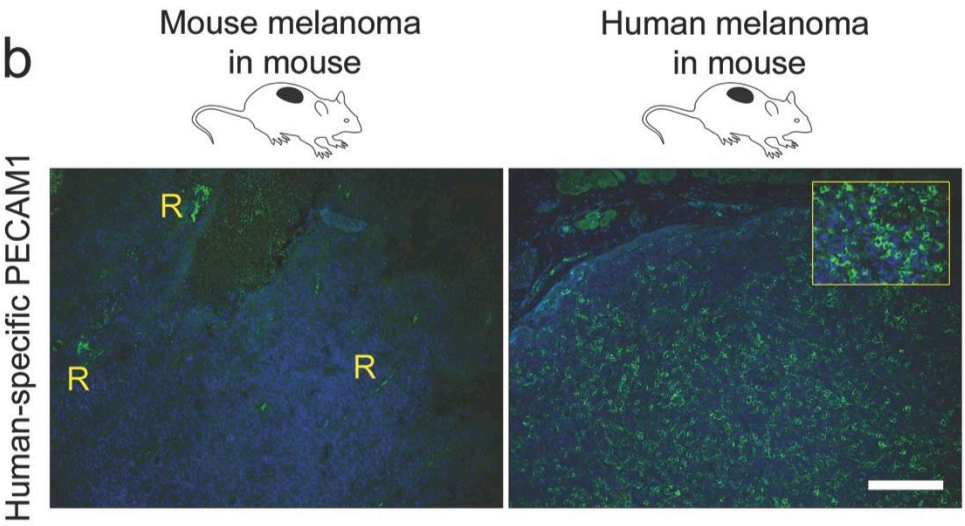
Mouse melanoma
in mouse
Human melanoma
in mouse
Human-specific PECAM1
R
R
R

Supplementary Figure 2.10. Specificity of human-specific versus pan-species PECAM-1 antibodies.

(a) Western blotting of EC lysates using human specific (Hu) and human/mouse-specific (Hu/mo) PECAM-1 antibodies. Note that there is no cross-reactivity of the human-specific antibody with mouse EC. Blots were stripped and re-probed with β-actin antibodies to show equal loading. (b) Human-specific PECAM-1 antibodies used for immunohistochemistry of mouse B16F10 or human SBCl2 tumors engrafted in mice. No specific staining was detected in B16F10 tumors and only background autofluorescence from red blood cells (R) was observed. The inset is a zoomed image showing distinctive membrane/cytoplasmic PECAM-1 staining in SBCl2 tumors. (scale bar = 100 μm)

Tables

Supplementary Table 2.1. Table of PCR primers.

Accession no.	Gene	Forward primer	Reverse primer
NM_000442.4	hPECAM1	GCAGCATCGTGGTCAACATAA	GCAGGACAGGTTCAGTCTTTCA
NM_001795.3	hVE-cadherin	AAGGACATAACACCACGAAACG	CAAACTGCCCATACTTGACTGTG
NM_011547.3	mAP-2α	TTTGCGCTAACCCAGAGAGT	TTGCGACTGGGGGTAGATAG
NM_009755.3	mBmp1	GAGTCCTGCTTCCCTCAATCA	TGTCACCATCTGCCTGTCAC
NM_007561.3	mBmpR2	TCTTGCCGTCTGGCTCATTC	GGTGGGAGATTGCGGGTT
NM_010024.3	mDCT	GGCGTGCTGAACAAGGAATG	GTGTCTGTTTGCACCTCTGC
NM_001159571.1	mEphb4 receptor	GCCTCAGGAAGCAGAGCAAT	ACCGTGCCCGATGAGATACT
NM_011808.2	mEts1	ATAGTTGTGACCGCCTCACC	TTCCTCTTTCCCCATCTCCT
M32599.1	mGAPDH	AACTTTGGCATTGTGGAAGG	ACACATTGGGGGTAGGAACA
NM_010493.2	mIcam1	CGCTGTGCTTTGAGAACTGTG	GAGGTCCTTGCCTACTTGCTG
NM_008601.3	mMitf-M	GTCACTACCAGGTGCAGACC	TGCTTTACCTGGTGCCTCTG
NM_010928.2	mNotch2	AGACTGGCGACTTCACTTTCG	CATCCACACAAACTCCTCCATT
NM_008808.3	mPdgfa	GCCAAAGTGGAGTATGTCAGGA	CGATGGTCTGGGTTCAGGTT
L06039.1	mPECAM1	TGCAGGAGTCCTTCTCCACT	ACGGTTTGATTCCACTTTGC
NM_001032378.1	mPECAM1 qRT-PCR	AAGCCAACAGCCATTACGGT	AGCCTTCCGTTCTCTTGGTG
NM_009035.4	mRbpj	CCAAGTGCCCTCCAATGAGT	TGTGGACGATGTGACACTGG
NM_011580.3	mThbs1	AATGTGGTGCGTGTCCTCCT	GATTGAAGCAAGCATCAGGCA
D00131.1	mTyrosinase	ATGGGTCAACACCCATGTTT	TCAGGTGTTCCATCGCATAA
NM_009868.4	mVECadherin	ACCGGATGACCAAGTACAGC	TTCTGGTTTTCTGGCAGCTT
NM_010612.2	mVEGFR2	GGCGGTGGTGACAGTATCTT	GTCACTGACAGAGGCGATGA
	mPECAM1 promoter1	AAGGAAGCCCCCTCATTAAA	AAAAGTCAATGGCCAACAGG
	mPECAM1 promoter2	AAGGAAGCCCCCTCATTAAA	AATGTCCCACAGACCTCCTG

Supplementary Table 2.2. Table of human cell lines.
Human melanoma cell lines (left) and normal human melanocytes (right) and raw PECAM-1 fluorescence values from microarray are listed.

Cell Line	Value	Cell Line	Value
SKMEL115	1	NHM16TERT	1.11
SKMEL131	1.07	NHM16TERT	1.12
SKMEL5	1.08	NHM21TERT	1.13
SKMEL186	1.1	NHM7TERTP	1.13
SKMEL130	1.17	NHM16PMA	1.21
UACC257	1.18	NHM7ET1	1.22
WM1232	1.18	NHM16ET1	1.26
SKMEL103	1.23	NHM24PMA	1.3
SKMEL173	1.23	NHM13PMA	1.31
PMWK	1.24	NHM20PMA	1.33
SKMEL100	1.28	NHM24ET1	1.33
SKMEL147	1.28	NHM11ET1	1.35
SKMEL28	1.28	NHM17PMA	1.35
SKMEL24	1.29	NHM7PMA	1.35
RPMI8332	1.3	NHM7TERTE	1.36
SKMEL153	1.3	NHM11PMA	1.41
SKMEL181	1.3	NHM21TERT	1.42
SKMEL190	1.3		
SKMEL178	1.33		
SKMEL224	1.33		
SKMEL27	1.35		
SKMEL23	1.42		
A2058	1.43		
MEL537	1.43		
SKMEL239	1.43		
SKMEL88	1.43		
SKMEL78	1.45		
SKMEL235	1.49		
MEL505	1.53		
A375	1.58		
SKMEL187	1.6		
WM35	1.6		
VMM39	1.67		
SKMEL119	1.94		
WM2664	1.94		
MALME3	1.95		
1205LU	2.11		
WM1158	2.76		
RPMI7951	2.88		
SBCL2	3.62		

Supplementary Table 2.3. Table of antibodies and dilutions.

Antibody	Manufacturer/Catalog #	Dilution	Application
PE-mouse anti-human PECAM1	Ancell 158-2B3	1:50	Flow Cytometry
PE-rat anti-mouse PECAM1	BD Pharmingen 553373	1:100	Flow Cytometry
rat anti-mouse PECAM1	BD Pharmingen 550274	1:200	IHC
rat anti-mouse PECAM1 clone 390	BD Pharmingen 558736	10 µg/mL	Blocking Experiments
mouse anti-human/mouse AP-2α	Santa Cruz Biotechnology sc12726	2 µg/reaction	ChIP
rabbit anti-mouse S100B	Biocare Medical CP021	1:500	IHC
rabbit anti-mouse MITF	Santa Cruz Biotechnology sc-25386	1:500	WB
rabbit anti-mouse DCT	Santa Cruz Biotechnology sc25544	1:500	WB
mouse anti-mouse PECAM1	Santa Cruz Biotechnology sc376764	1:500	WB
mouse anti-mouse β-actin	Sigma Aldrich A1978	1:1000	WB
PerCP-Cy5.5-rat anti-mouse CD45	BD Pharmingen 550994	1:100	Flow Cytometry
PerCP-Cy5.5-rat IgG	BD Pharmingen 550764	1:100	Flow Cytometry
rabbit anti-human PECAM1	Abcam ab76533	1:100	IHC
rat anti-mouse CD144	BD Pharmingen 550548	1:100	IHC
chicken anti-GFP	Abcam ab139070	1:400	IHC
APC-hamster IgG	BD Pharmingen 553974	1:100	Flow Cytometry
anti-phosphotyrosine antibody, clone 4G10	Millipore 05-321	1:1000	WB
PE-rat IgG	BD Pharmingen 553930	1:100	Flow Cytometry
APC-hamster anti-mouse CD54	BD Pharmingen 561605	1:100	Flow Cytometry
Peroxidase labeled horse anti-mouse IgG	VectorLabs PI-2000	1:10000	WB
Peroxidase labeled goat anti-rabbit IgG	VectorLabs PI-1000	1:10000	WB
Alexa Fluor 488 goat anti-rat IgG	Invitrogen A11006	1:200	IHC
Alexa Fluor 488 goat anti-rabbit IgG	Invitrogen A11034	1:200	IHC
Alexa Fluor 594 goat anti-rabbit	Invitrogen A11037	1:200	IHC
Alexa Fluor 594 goat anti-rat IgG	Invitrogen A11007	1:200	IHC

REFERENCES

Cao, G., O'Brien, C. D., Zhou, Z., Sanders, S. M., Greenbaum, J. N., Makrigiannakis, A., & DeLisser, H. M. (2002). Involvement of human PECAM-1 in angiogenesis and in vitro endothelial cell migration. American Journal of Physiology. Cell Physiology, 282 (5), C1181–C1190. http://doi.org/10.1152/ajpcell.00524.2001

Carson, C., Omolo, B., Chu, H., Zhou, Y., Sambade, M. J., Peters, E. C., et al. (2012). A prognostic signature of defective p53-dependent G1 checkpoint function in melanoma cell lines. Pigment Cell & Melanoma Research, 25 (4), 514–526. http://doi.org/10.1111/j.1755-148X.2011.01010.x/suppinfo

Dankort, D., Curley, D. P., Cartlidge, R. A., Nelson, B., Karnezis, A. N., Damsky, W. E., Jr, et al. (2009). BrafV600E cooperates with Pten loss to induce metastatic melanoma. Nature Genetics, 41 (5), 544–552. http://doi.org/10.1038/ng.356

DeLisser, H. M., Christofidou-Solomidou, M., Strieter, R. M., Burdick, M. D., Robinson, C. S., Wexler, R. S., et al. (1997). Involvement of endothelial PECAM-1/CD31 in angiogenesis. The American Journal of Pathology, 151 (3), 671–677.

DeLisser, H., Liu, Y., Desprez, P.-Y., Thor, A., Briasouli, P., Handumrongkul, C., et al. (2010). Vascular endothelial platelet endothelial cell adhesion molecule 1 (PECAM-1) regulates advanced metastatic progression. Proceedings of the National Academy of Sciences of the United States of America, 107 (43), 18616–18621. http://doi.org/10.1073/pnas.1004654107

Dudley, A. C., Khan, Z. A., Shih, S.-C., Kang, S.-Y., Zwaans, B. M. M., Bischoff, J., & Klagsbrun, M. (2008). Calcification of Multipotent Prostate Tumor Endothelium. Cancer Cell, 14 (3), 201–211. http://doi.org/10.1016/j.ccr.2008.06.017

Dudley, A. C., Udagawa, T., Melero-Martin, J. M., Shih, S. C., Curatolo, A., Moses, M. A., & Klagsbrun, M. (2010). Bone marrow is a reservoir for proangiogenic myelomonocytic cells but not endothelial cells in spontaneous tumors. Blood, 116 (17), 3367–3371. http://doi.org/10.1182/blood-2010-02-271122

Eyles, J., Puaux, A.-L., Wang, X., Toh, B., Prakash, C., Hong, M., et al. (2010). Tumor cells disseminate early, but immunosurveillance limits metastatic outgrowth, in a mouse model of melanoma. Journal of Clinical Investigation, 120 (6), 2030–2039. http://doi.org/10.1172/JCI42002DS1

Francescone, Ralph, Steve Scully, Brooke Bentley, Wei Yan, Sherry L Taylor, Dennis Oh, Luis Moral, and Rong Shao. 2012. "Glioblastoma-Derived Tumor Cells Induce Vasculogenic Mimicry Through Flk-1 Protein Activation.." Journal of Biological Chemistry 287 (29): 24821–31. doi:10.1074/jbc.M111.334540.

Gessner, R. C., Aylward, S. R., & Dayton, P. A. (2012). Mapping Microvasculature with Acoustic Angiography Yields Quantifiable Differences between Healthy and Tumor-bearing Tissue Volumes in a Rodent Model. Radiology, 264 (3), 733–740. http://doi.org/10.1148/radiol.12112000

Gumina, R. J., Kirschbaum, N. E., Piotrowski, K., & Newman, P. J. (1997). Characterization of the human platelet/endothelial cell adhesion molecule-1 promoter: identification of a GATA-2 binding element required for optimal transcriptional activity. Blood, 89 (4), 1260–1269.

Hanna, S. C., Krishnan, B., Bailey, S. T., Moschos, S. J., Kuan, P.-F., Shimamura, T., et al. (2013). HIF1α and HIF2α independently activate SRC to promote melanoma metastases. Journal of Clinical Investigation, 123 (5), 2078–2093. http://doi.org/10.1172/JCI66715DS1

Hendrix, Mary J C, Elisabeth A Seftor, Angela R Hess, and Richard E B Seftor. 2003. "Vasculogenic Mimicry and Tumour-Cell Plasticity: Lessons From Melanoma.." Nature Reviews Cancer 3 (6): 411–21. doi:10.1038/nrc1092.

Hendrix, M. J., Seftor, E. A., Meltzer, P. S., Gardner, L. M., Hess, A. R., Kirschmann, D. A., et al. (2001). Expression and functional significance of VE-cadherin in aggressive human melanoma cells: role in vasculogenic mimicry. Proceedings of the National Academy of Sciences of the United States of America, 98 (14), 8018–8023. http://doi.org/10.1073/pnas.131209798

Hu, F. N., Wang, R. Y., & Hsu, T. C. (1987). Clonal origin of metastasis in B16 murine melanoma: a cytogenetic study. Journal of the National Cancer Institute, 78 (1), 155–163.

Kendal, W. S., Wang, R. Y., Hsu, T. C., & Frost, P. (1987). Rate of generation of major karyotypic abnormalities in relationship to the metastatic potential of B16 murine melanoma. Cancer Research, 47 (14), 3835–3841.

Kogan, P., Johnson, K. A., Feingold, S., Garrett, N., Guracar, I., Arendshorst, W. J., & Dayton, P. A. (2011). Original Contribution. Ultrasound in Medicine & Biology, 37 (6), 900–908. http://doi.org/10.1016/j.ultrasmedbio.2011.03.011

Lin, E. Y., Li, J. F., Gnatovskiy, L., Deng, Y., Zhu, L., Grzesik, D. A., et al. (2006). Macrophages Regulate the Angiogenic Switch in a Mouse Model of Breast Cancer. Cancer Research, 66 (23), 11238–11246. http://doi.org/10.1158/0008-5472.CAN-06-1278

Roland, C. L., Lynn, K. D., Toombs, J. E., Dineen, S. P., Udugamasooriya, D. G., & Brekken, R. A. (2009). Cytokine Levels Correlate with Immune Cell Infiltration after Anti-VEGF Therapy in Preclinical Mouse Models of Breast Cancer. PLoS ONE, 4 (11), e7669. http://doi.org/10.1371/journal.pone.0007669.t002

Streeter, J. E., Gessner, R., Miles, I., & Dayton, P. A. (2010). Improving sensitivity in ultrasound molecular imaging by tailoring contrast agent size distribution: in vivo studies. Molecular Imaging, 9 (2), 87–95.

Sullivan, L. A., Carbon, J. G., Roland, C. L., Toombs, J. E., Nyquist-Andersen, M., Kavlie, A., et al. (2010). r84, a Novel Therapeutic Antibody against Mouse and Human VEGF with Potent Anti-Tumor Activity and Limited Toxicity Induction. PLoS ONE, 5 (8), e12031. http://doi.org/10.1371/journal.pone.0012031.g005

Wang, Rong, Kalyani Chadalavada, Jennifer Wilshire, Urszula Kowalik, Koos E Hovinga, Adam Geber, Boris Fligelman, Margaret Leversha, Cameron Brennan, and Viviane Tabar. 2010. "Glioblastoma Stem-Like Cells Give Rise to Tumour Endothelium." Nature 468 (7325). Nature Publishing Group: 829–33. doi:10.1038/nature09624.

Xiao, L., Harrell, J. C., Perou, C. M., & Dudley, A. C. (2013). Identification of a stable molecular signature in mammary tumor endothelial cells that persists in vitro. Angiogenesis, 17 (3), 511–518. http://doi.org/10.1007/s10456-013-9409-y

Xiao, L., McCann, J. V., & Dudley, A. C. (2015). Isolation and Culture Expansion of Tumor-specific Endothelial Cells. Journal of Visualized Experiments, (104). http://doi.org/10.3791/53072

CHAPTER 3: Conclusions and Future Directions[3]

Summary of results

We have identified a subpopulation of PECAM-1$^+$ melanoma cells that was "hidden" within heterogeneous and predominantly PECAM-1$^-$ melanoma tumors. Initial gene expression and western blot results revealed this subpopulation of cells expressed the endothelial selective marker PECAM-1, as well as other endothelial markers including Icam1, but lacked other canonical endothelial markers, and expressed several melanoma genes including Tyr and Dct. We were able to confirm that the PECAM-1$^+$ subfraction existed as a stable (~0.2%) yet minor population within B16F10 tumors, and ruled out the possibility of cell fusion with host endothelial cells by retrieving GFP$^+$/PECAM-1$^+$ tumor cells from wildtype mice.

Single-cell cloning revealed that PECAM-1 expression by B16F10 was stable, as clones retained ~99-100% positivity over time. Furthermore, these clones adopted an "endothelial-like" phenotype *in vitro*. When plated on Matrigel they formed a branched tube-like structure, a hallmark of endothelial cells and VM-competent tumor cells. Importantly, this phenotype was blocked with PECAM-1 blocking antibodies, confirming it was at least partially PECAM-1-dependent. This is consistent with data in mesothelioma cells where forced overexpression of PECAM-1 caused a tube-formation phenotype in similar conditions (Cao et al. 2002). These data were further supported by knockdown and overexpression studies, as PECAM-1-KD repressed

[3] Chapter 3 is adapted in part from Dunleavey, J.M. et al. Vascular channels formed by subpopulations of PECAM1$^+$ melanoma cells. *Nature Comm*. **5.** 1-16. (2014)

tube formation in PECAM-1$^+$ cells and PECAM-1-OE enhanced tube formation in PECAM-1$^-$ cells.

We found that the *in vitro* vascular-like phenotype of PECAM-1$^+$ melanoma translated into a striking *in vivo* vascular phenotype. Clonally derived PECAM-1$^+$ melanoma displayed large blood-filled channels, which were not observed in PECAM-1$^-$ counterparts. Furthermore, PECAM-1$^+$ melanoma cells, when labeled with GFP and observed under fluorescence microscopy, appeared to be present at the edge of blood vessels and in close proximity to endothelial cells. High-resolution confocal microscopy and transmission electron microscopy revealed that these cells appear to affiliate with endothelial cells and were in direct contact with the perfused vasculature, suggesting that the vascular-like phenotype of these cells allowed them to interact with the luminal surface of blood vessels. Supporting this hypothesis, when PECAM1$^+$ tumor cells were engrafted into PECAM-1-KO mice, large, blood filled channels were lost compared to tumors formed in WT mice. Taken together, these data suggest that PECAM-1$^+$ melanoma engage in PECAM-1-dependent VM.

We determined the mechanism for PECAM-1 expression in melanoma was governed by the transcription factor AP-2α. PECAM-1$^+$ melanoma exhibited a striking loss of AP-2α expression, and AP-2α was found by ChIP to bind the PECAM-1 promoter. siRNA targeting of AP-2α upregulated PECAM-1 expression in PECAM-1$^-$ clones and whereas ectopic expression of AP-2α blocked PECAM-1 expression in PECAM-1$^+$ clones.

Melanoma appears to display a spectrum of PECAM-1 expression and PECAM-1-positive tumor cells were present in a fraction of human tumors. We were also able to isolate and purify PECAM-1$^+$ melanoma cells from a genetically modified mouse model of melanoma. Twenty-five percent of human melanoma cell lines expressed higher levels of PECAM-1 than

normal human melanocytes. These human PECAM-1$^+$ melanoma displayed *in vitro* tube formation in the same manner as our mouse models. When we engrafted the human clone with the highest basal PECAM-1 expression into NSG mice, we found what appeared to be blood vessels in the resulting tumors with human tumor cells expressing human PECAM-1 incorporated.

We found that when unsorted B16F10 melanoma were engrafted into mice and challenged with an anti-VEGF therapeutic analog, PECAM-1$^+$ melanoma was enriched ~6-fold. PECAM-1$^+$/VEGFR-2$^-$ cells therefore might supplant vascular EC that are lost following treatment with anti-angiogenic therapy and form PECAM-1-dependent "bridges" between tumor cells and neighboring EC (Fig. 3.1a, b). Supporting this hypothesis, clonal populations of PECAM-1$^+$ melanoma were refractory to VEGF inhibition, while PECAM-1$^-$ melanoma displayed similar growth dynamics to unsorted B16F10 when challenged with a VEGF inhibitor.

Future Directions

Future studies on PECAM-1 expression by melanoma

The expression of PECAM-1 by melanoma cells may represent a new form of VM. Our model suggests that PECAM-1-dependent VM may differ from previously described models in which tumor cell- to -EC mosaicism was a passive process where tumor cell-endothelial contacts were transient and weak (Chang et al. 2000; di Tomaso et al. 2005). Instead, expression of PECAM-1 by tumor cells may serve to actively stabilize cell-cell interactions between PECAM-1$^+$ tumor cells and EC. PECAM-1 is typically concentrated at cell-cell borders by a process known as "diffusion trapping" which leads to aggregation of PECAM-1 protein at sites where two PECAM-1$^+$ cells meet (Sun et al. 2000; Feng et al. 2004). Homophilic binding of PECAM-1 between immunoglobulin domains 1 and 2 (IgD1/2) has been shown to strengthen endothelial

barriers, and can be increased by ligand binding at the Ig6 domain of the extracellular region (Mei et al. 2014; Paddock et al. 2016; Privratsky et al. 2011) Indeed, homophilic PECAM-1-PECAM-1 binding was suggested, many years ago, to underlie *in vitro* tumor cell adhesion to EC in co-culture studies (Tang et al. 1993). Furthermore, PECAM-1 is required for tube formation, as PECAM-1 blocking antibodies reduced the tube formation ability of PECAM-1^+ melanoma cells, similar to what has been observed in cultured EC (DeLisser et al. 1997). Notably, PECAM-1 overexpression in mesothelioma cells, which do not express PECAM-1, induces robust tube formation on Matrigel. PECAM-1 is required for tube formation in bona fide EC, whereas VE-cadherin mediates both cell-cell adhesion and vacuole fusion (Yang et al. 2010). Thus, PECAM-1 expression in melanoma may mediate cell elongation, migration, and invasion while stabilizing the junctional, homophilic complexes between neighboring cells that are necessary to create a patent lumen. Future experiments on homophilic PECAM-1 binding between tumor cells and endothelial cells *in vitro* as well as in tumors, through imaging or traditional barrier function studies (Privratsky and Newman 2014) could help explain whether PECAM-1 homophilic binding is definitively taking place in our model of VM. Additionally, a novel recent method described by the Newman group allows for interrogation of EC with individual PECAM-1 molecules attached to lipid nanodiscs (Mei et al. 2014). In a cell-free manner, we could adapt these nanodiscs to contain melanoma-derived PECAM-1 and determine binding efficiency with cultured EC, to see if melanoma-derived PECAM1 displays binding differences. These experiments could provide insight into whether current PECAM-1-blocking reagents could be adapted to inhibit tumor cell-EC affiliation.

PECAM-1 has well-known functions in shear stress signaling in the mature blood vasculature. Shear stress has been demonstrated to trigger the tyrosine phosphorylation of

PECAM-1 leading to a signaling cascade that includes Akt and eNOS (Tzima et al. 2005; Newman 2003). We found that PECAM-1 expressed in melanoma displays similar patterns of phosphorylation as cultured EC, but whether this has consequences for signaling in these melanoma is unclear. Of note, the PECAM-1 protein detected in our study appeared to be the same molecular weight as PECAM-1 derived from EC, suggesting that the species is mature, full-length PECAM-1 including the extra- and intra-cellular domains. An interesting course of study would be to determine whether the intracellular ITIM-domain-binding proteins including SHP2, PI3K and β-catenin (reviewed in depth by P.J. Newman (Newman 2003)) bind PECAM-1 in melanoma as they do in EC, and whether these signaling pathways are differentially regulated in PECAM-1^+ melanoma compared to PECAM-1^- clones. This of particular interest as PI3K and Akt are thought to contribute to a pro-survival phenotype, which if activated in a subpopulation of melanoma could contribute to long term survival of the tumor (Liu et al. 2009; Ojesina et al. 2014).

Another prominent feature of PECAM-1 signaling is suppression of apoptosis, which could offer a competitive survival advantage to a tumor comprised of a heterogeneous mixture of tumor cells that include a PECAM-1^+ fraction (Gao et al. 2003; Bergom, Gao, and Newman 2005). Specifically, when PECAM-1was overexpressed in HEK293 cells and mesothelioma cells, cells became resistant to the DNA-damaging agent etoposide (Bergom et al. 2006). Furthermore, forced expression of the pro-apoptotic TNFα receptor on cultured endothelial cells activated PECAM-1, which counteracted the pro-apoptotic signaling by activating Akt (Cheung et al. 2015). This signaling is independent of the homophilic binding capacity of PECAM-1, and appears to be dependent on the C-terminal intracellular domain of the molecule (Bergom et al. 2008). These studies suggest a potential role for PECAM-1 expression by tumor cells as an

inhibitor of apoptosis and prospective mechanism for resistance to cytotoxic chemotherapy. It would be extremely interesting to interrogate B16F10 tumors as well as PECAM-1^{+} and PECAM-1^{-} clonal populations derived from this cell line with current chemotherapeutics. If PECAM-1 serves as an apoptotic suppressor in these cells. I speculate that drug-resistant unsorted B16F10 would display an increase in PECAM-1^{+} tumor cells compared to control, and that PECAM-1^{+} clonal melanoma may display intrinsic resistance to these agents.

An important question raised by our work is whether PECAM-1 represents a potential target for therapy, either in conjunction with traditional cytotoxic chemotherapies or in combination with existing anti-angiogenesis strategies. Because of its importance in shear stress signaling and responses to atherogenic stimuli, many groups are interested in blocking PECAM-1 signaling (Dasgupta et al. 2010). Importantly, preclinical modeling found that PECAM-1-KO, as well as WT mice treated with PECAM-1 blocking antibodies displayed reduced metastatic progression and cachexia (DeLisser et al. 2010). Interestingly, this study used and found striking inhibition of metastasis with the B16F10 cell line, which we describe harboring a PECAM-1^{+} subfraction that engages in PECAM-1-dependent VM. While the authors of the blocking study did not examine VM in their model, as our findings were not yet published, it stands to reason that PECAM-1 blockade would also block the PECAM-1-dependent VM. As a corollary to this, a recent high-profile study found that VM-competent cells allow for direct dissemination of tumor cells into the vasculature and promoted metastatic seeding (Wagenblast et al. 2015). Taken together, these two studies suggest that VM can promote metastasis and B16F10 metastasis is blocked, at least partially, by PECAM-1 blockade. Combined with our data showing PECAM-1-dependent VM in B16F10, this suggests that blocking VM may in fact reduce metastasis.

An important role for PECAM-1 is in diapedesis, or the extravasation of circulating leukocytes from the blood vasculature. PECAM-1 is expressed in both immune cells and EC, and has been shown to regulate the early stages of leukocyte tethering. It is thought that PECAM-1 acts as an early tether which engages circulating leukocytes, brings them adjacent to the vessel wall, and allows the engagement of other adhesion molecules like CD99 (Torzicky et al. 2012). An interesting question is whether VM-engaging tumor cells, particularly those expressing PECAM-1, may contribute to the recruitment of tumor infiltrating leukocytes (TILs). Tumor-associated M2 macrophages are thought to be a key mediator of tumor progression, and secrete a pro-inflammatory cytokine mixture that has been shown to partially fuel tumor growth (Quail and Joyce 2013; Lança and Silva-Santos 2014). We did not observe major differences in immune cell infiltration in PECAM-1^{+} or PECAM-1^{-} tumors (data not shown), but did not exhaustively address this question. However, when PECAM-1 was blocked either genetically or with an antibody, metastasis was reduced but no difference in macrophage infiltration was observed (DeLisser et al. 2010). These data suggest that while PECAM-1 has an important, but dispensable role in canonical diapedesis, especially in inflammation-related responses (Nourshargh, Krombach, and Dejana 2006; Duncan et al. 1999; Thompson et al. 2001) the contribution of PECAM-1 to immune cell infiltration into the tumor may be limited, regardless of whether it is expressed on EC or in tumor cells. However, it would be interesting to revisit recent studies investigating metastatic mechanisms using the B16F10 model to determine if PECAM-1^{+} melanoma are involved (Peinado et al. 2012). It is possible that if PECAM1 is not altering immune cell infiltration that perhaps it allows for a tumor-cell "diapedetic mimicry" where tumor cells use PECAM1 to adhere to the vessel wall like immune cells and improve extravasation and seeding. Supporting this, VM-competent cells in a recent study were shown to

improve metastatic seeding by increasing tumor cell contact with blood flow (Wagenblast et al. 2015), which could be augmented by tumor expression of pro-extravasatory factors.

Lastly, we found that PECAM-1$^+$ melanoma displayed a slight growth delay compared to PECAM-1$^-$ counterparts. It may be possible that the acquisition of vascular-like characteristics comes at the expense of reduced tumorigenicity, or that perhaps signaling through PECAM-1 may represent a form of contact inhibition and a slower rate of growth despite the cells' ability form vascular-like channels.

Gene expression in PECAM-1$^+$ melanoma

We found a distinct gene signature in PECAM-1$^+$ melanoma which included both endothelial selective markers as well as a host of other genes. It is unclear what role, if any, these genes may play in the VM phenotype. Of note, from our microarray analysis, we found that *Slpi*, a gene recently implicated in VM in breast cancer, appeared upregulated, as well as the serine protease inhibitor *Pai-1* (*Serpine1*), a related family member of another VM-involved gene *Serpine2* (Buchholz et al. 2003), which was implicated in VM in the same study (Wagenblast et al. 2015). As the involvement of these genes in VM was unknown while we were performing our study, it would be interesting to determine whether they contribute to the PECAM-1-dependent form of VM we have described. Blocking PECAM-1 in our hands reduced tube formation by ~50%, and a redundant mechanism for VM formation could explain the lack of a binary response in these assays. Knockdown or knockout of these genes individually, or in conjunction with PECAM-1 blockade, could help determine what role, if any, they play in PECAM-1-mediated VM. As a corollary to this, another course of study could be to examine the role other genes identified in our array play in VM or tumor progression. We identified a number of genes with known endothelial function that were upregulated in PECAM-1$^+$ melanoma including

CD54/ICAM1 and thrombospondin 1 (Thbs1) . Whether these genes are involved in VM is unknown, but current tools for modulating gene expression would allow for relatively easy gene knockout of interest using CRISPR/Cas9 (Ran et al. 2013). Thbs1 is a particularly interesting gene for study in these cells, as upregulated Thbs1 has been shown to inhibit tumor growth,and can promote dormancy or quiescence in metastatic microvascular niches (Lawler 2002; Ghajar et al. 2013). We noted that PECAM-1^{+} melanoma grow more slowly than PECAM-1^{-} clones, and these data could be explained by increased levels of the Thbs1.

AP-2α loss in PECAM-1^{+} melanoma: implications for aggressiveness

AP-2α is a putative tumor suppressor which slows or blocks tumor cell growth in melanoma (Bar-Eli 1999), glioblastoma (Heimberger et al. 2005), prostate (Ruiz et al. 2001; Ruiz et al. 2004), breast (Bosher, Williams, and Hurst 1995) and colon (Li, Löhr, and Dashwood 2009). Previous studies in melanoma have shown AP-2α acts as a transcriptional repressor of melanoma cell adhesion molecule (MCAM), activator of KIT, PAR-1, and VEGF (Jean et al. 1998; Huang et al. 1998; Ruiz et al. 2004). Importantly, loss of AP-2α has been shown to be a key regulator of the shift from the radial growth phase (RGP) of melanoma to the vertical growth phase (VGP) (Mobley et al. 2012) and is correlated with melanoma aggressiveness (Gershenwald et al. 2001; Huang et al. 1998). AP-2α also controls melanoma cell motility and its expression is diminished in aggressive forms of melanoma and breast cancer (Karjalainen et al. 1998; Pellikainen et al. 2002). While PECAM-1 was not previously described as a target gene for AP-2α, the loss of this factor in PECAM-1^{+} melanoma is extremely interesting. First, we have described a novel negative regulator of PECAM-1 expression, whose transcriptional control remains relatively unclear (Gumina et al. 1997). Several transcription factors have binding sites

in the PECAM-1 promoter, but to our knowledge AP-2α is the first transcription factor shown to repress PECAM-1 signaling directly.

Although the focus of our study was on PECAM-1 expression by melanoma, other transcriptional targets of AP-2α were identified by our microarray analysis. Specifically, Id1, which is regulated by the AP-2α target MCAM (Zigler et al. 2011), and plasminogen activator inhibitor-1 (Pai-1) (Bar-Eli 1999) were both upregulated in PECAM-1^+ melanoma as determined by microarray. Characterizing whether the loss of AP-2α in fact drives these altered gene expression changes would allow us to determine whether adoption of PECAM-1 expression is part of the spectrum of increased melanoma aggressiveness, and is worthy of further analysis.

While we identified a mechanism for AP-2α-mediated repression of PECAM-1, how AP-2α is lost in a subpopulation of B16F10 remains unclear. It is possible that signaling upstream of AP-2α is controlling its loss. It is known that CREB/cAMP is capable of downregulating AP-2α in melanoma (Melnikova et al. 2010). While we did not assay cAMP activity in our study, determining the status of cAMP signaling or whether differentially regulated G-protein coupled receptors are activating CREB through PKA would allow us to understand if CREB is modulating the phenotype we observed in PECAM-1^+ melanoma. Furthermore, a recent interest across cell biology is post-transcriptional regulation of gene expression by microRNA (miRNA) species. A recent study found that mir-214 indirectly represses AP-2α expression, and was dubbed a potential "melano-miR" (Bar-Eli 2011; Penna et al. 2011). Whether similar repression of AP-2α in PECAM-1^+ melanoma occurs is not known, but our lab and others have recently adopted the NanoString microarray which allows for screening of miRNA species. This could allow us to ask which miRNAs are differentially regulated in PECAM-1^+ clones compared to negative counterparts.

Tumor cell-derived PECAM-1: mechanisms for resistance to anti-angiogenic therapies?

In **CHAPTER ONE** I addressed the current state of anti-angiogenesis strategies either in the clinic or in development. Briefly, strategies targeting the VEGF axis, and to a lesser extent, Ang/Tie2 signaling have been largely disappointing. While new drugs including pazaponib and nintendanib which exhibit multikinase inhibition, including FGFRs and PDGFRs, have promise, it remains to be seen whether targeting the endothelium through growth factor receptor inhibitors will be successful. Of note, practically no success has been seen in melanoma patients with regard to anti-angiogenic strategies (Kim et al. 2011). Why melanoma resists these therapies remains an open question, but one hypothesis is that as a relatively well-vascularized organ and the long period of development of skin lesions, melanoma may not rely on VEGF-mediated angiogenesis for sustained growth (Helfrich et al. 2010). Vessel co-option and expansion via non-angiogenic means could provide these tumors an innate resistance to anti-angiogenic agents.

We found a population of melanoma cells which was able to actively affiliate with the endothelial cells of blood vessels. Whether VM aids the co-optive phenotype seen in many non-angiogenic tumors is unknown, but the prevalence of VM in melanoma could provide a mechanism for tumors to affiliate more closely with pre-existing endothelium. Advances in *in vivo* imaging could allow us to model nascent tumors and visualize tumor cells and perfused blood with molecular dyes. Perhaps using intravital imaging we could identify VM in living tumors, and determine whether PECAM-1$^+$ tumor cells allow for increased vessel cooption. Furthermore, we could treat mice with inhibitors of angiogenesis and observe the dynamics of vessel response. The ability to image tumors *in vivo* to monitor responses to anti-angiogenic strategies would allow us to determine how PECAM-1$^+$ tumor cells contributed to resistance, and

test our hypothesis that these cells supplant vulnerable endothelial cells in the face of VEGF inhibition.

Perhaps the most pressing question raised by our findings is whether PECAM-1 represents a new druggable target for treatment of solid tumors (Debs, patent.), particularly melanoma. As I noted previously, relatively little has been done in the field of tumor biology to target PECAM-1. Currently, just two studies in mice have extensively looked at PECAM-1 blockade and found that in mouse models blocking PECAM-1 reduced late-stage metastatic growth as well as primary tumor burden, and noted decreased tumor angiogenesis (Zhou et al. 1999; DeLisser et al. 2010). These studies each used the B16F10 model, and it is possible that part of the response to treatment came from inhibition of PECAM-1-dependent VM. PECAM-1 represents an attractive target, as it is dispensable in development and adult animals, with defects in inflammation and atherosclerosis being the major adult phenotypes (Duncan et al. 1999). Furthermore, as a cell-surface molecule, PECAM-1 can be and has been targeted by antibodies, which have become a major targeting tool in cancer therapy. Our findings suggest that perhaps targeting PECAM-1 alongside traditional anti-angiogenic agents will result in better response to therapy, particularly in tumors which possess PECAM-1^{+} subfractions. However, before PECAM-1 could be considered as a target, larger-scale screens for PECAM-1 positivity need to be completed. While we found ~25% of the human melanoma cell lines we screened possessed higher-than-basal levels of PECAM-1, large-scale genomics datasets of primary patient samples should be examined as well. If PECAM-1 is broadly expressed in a large percentage of human patients, then development of human-tolerated anti-PECAM-1 blocking antibodies could improve the efficacy of anti-angiogenesis therapy, and provide more tools for the new era of individualized medicine.

Figures

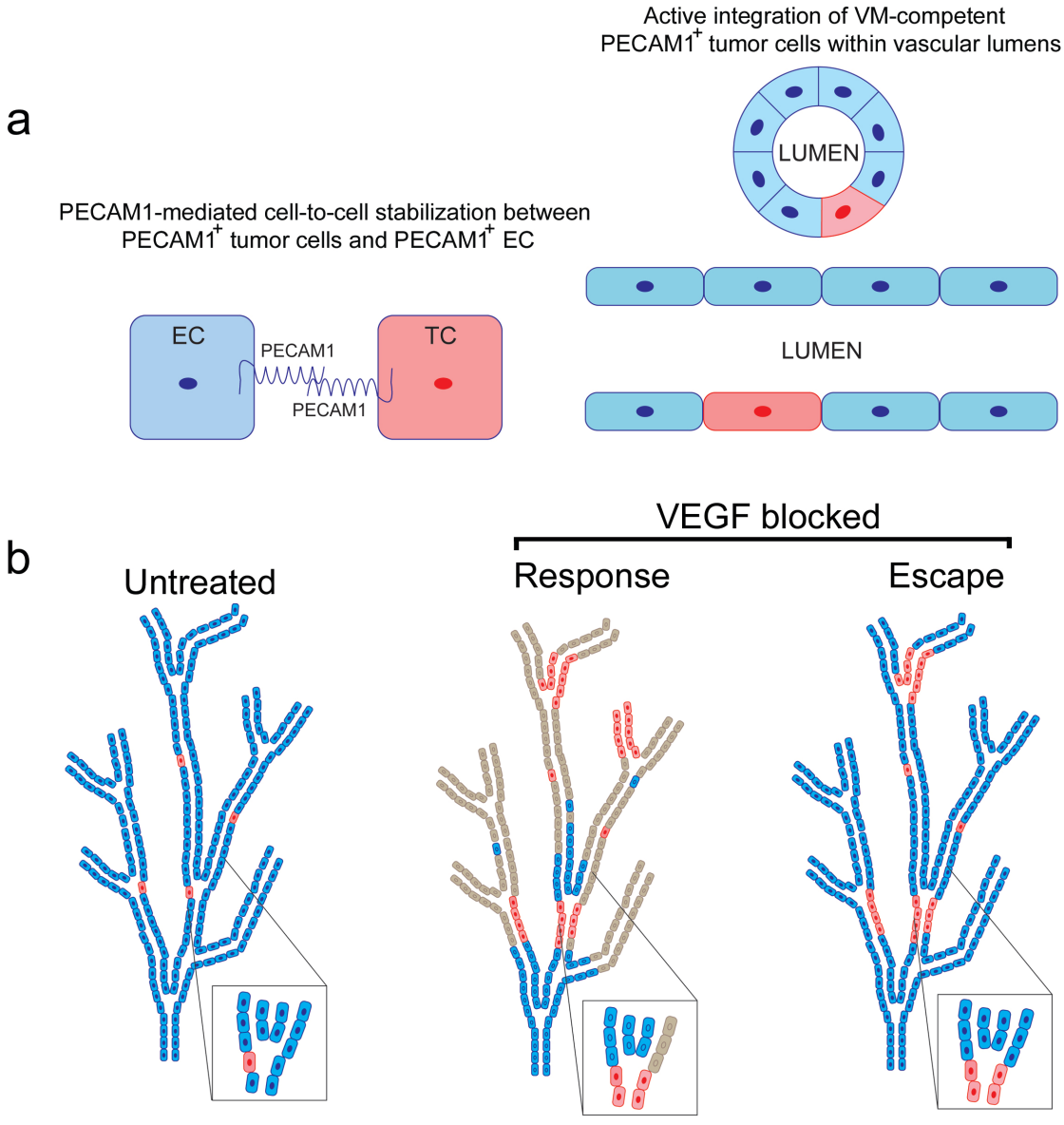

Vascular-like “bridges” formed by interactions between PECAM1+ tumor cells and EC may protect tumors following VEGF inhibition

Figure 3.1. A model for a PECAM-1-dependent form of vasculogenic mimicry.
(a) PECAM-1 plays a well-characterized role in stabilizing junctions between EC and leukocytes and between two EC. Tumor cell expression of PECAM-1 may also stabilize interactions between tumor cells (TC) and EC or between two PECAM-1^+ TC to form stable junctions. (b) In tumors where PECAM-1^+ tumor cells are present, VEGF-independent "bridges" would not be affected by anti-VEGF therapies and could supplant host endothelium following VEGF inhibition. "Channels" formed exclusively by PECAM-1^+ TC could also be insensitive to VEGF blockade.

REFERENCES

Bar-Eli, M. 1999. "Role of AP-2 in Tumor Growth and Metastasis of Human Melanoma.." *Cancer Metastasis Reviews* 18 (3): 377–85.

Bar-Eli, Menashe. 2011. "Searching for the 'Melano-miRs': miR-214 Drives Melanoma Metastasis.." *The EMBO Journal* 30 (10): 1880–81. doi:10.1038/emboj.2011.132.

Bergom, Carmen, Cathy Paddock, Cunji Gao, Trudy Holyst, Debra K Newman, and Peter J Newman. 2008. "An Alternatively Spliced Isoform of PECAM-1 Is Expressed at High Levels in Human and Murine Tissues, and Suggests a Novel Role for the C-Terminus of PECAM-1 in Cytoprotective Signaling.." *Journal of Cell Science* 121 (Pt 8): 1235–42. doi:10.1242/jcs.025163.

Bergom, Carmen, Cunji Gao, and Peter J Newman. 2005. "Mechanisms of PECAM-1-Mediated Cytoprotection and Implications for Cancer Cell Survival.." *Leukemia & Lymphoma* 46 (10): 1409–21. doi:10.1080/10428190500126091.

Bergom, Carmen, Reema Goel, Cathy Paddock, Cunji Gao, Debra K Newman, Shigemi Matsuyama, and Peter J Newman. 2006. "The Cell-Adhesion and Signaling Molecule PECAM-1 Is a Molecular Mediator of Resistance to Genotoxic Chemotherapy.." *Cancer Biology & Therapy* 5 (12): 1699–1707. doi:10.4161/cbt.5.12.3467.

Bosher, J M, T Williams, and H C Hurst. 1995. "The Developmentally Regulated Transcription Factor AP-2 Is Involved in C-erbB-2 Overexpression in Human Mammary Carcinoma.." *Proceedings of the National Academy of Sciences* 92 (3): 744–47.

Buchholz, Malte, Anja Biebl, Albrecht Neesse, Martin Wagner, Takeshi Iwamura, Gerhard Leder, Guido Adler, and Thomas M Gress. 2003. "SERPINE2 (Protease Nexin I) Promotes Extracellular Matrix Production and Local Invasion of Pancreatic Tumors in Vivo.." *Cancer Research* 63 (16): 4945–51.

Cao, Gaoyuan, Christopher D O'Brien, Zhao Zhou, Samuel M Sanders, Jordan N Greenbaum, Antonis Makrigiannakis, and Horace M DeLisser. 2002. "Involvement of Human PECAM-1 in Angiogenesis and in Vitro Endothelial Cell Migration.." *American Journal of Physiology. Cell Physiology* 282 (5): C1181–90. doi:10.1152/ajpcell.00524.2001.

Chang, Y S, E di Tomaso, D M McDonald, R Jones, R K Jain, and L L Munn. 2000. "Mosaic Blood Vessels in Tumors: Frequency of Cancer Cells in Contact with Flowing Blood.." *Proceedings of the National Academy of Sciences* 97 (26): 14608–13. doi:10.1073/pnas.97.26.14608.

Cheung, Kenneth, Liang Ma, Guosu Wang, David Coe, Riccardo Ferro, Marco Falasca, Christopher D Buckley, Claudio Mauro, and Federica M Marelli-Berg. 2015. "CD31 Signals Confer Immune Privilege to the Vascular Endothelium." *Proceedings of the National Academy of Sciences of the United States of America* 112 (43): E5815–24.

doi:10.1073/pnas.1509627112.

Dasgupta, Bidisha, Tina Chew, Alana deRoche, and William A Muller. 2010. "Blocking Platelet/Endothelial Cell Adhesion Molecule 1 (PECAM) Inhibits Disease Progression and Prevents Joint Erosion in Established Collagen Antibody-Induced Arthritis.." *Experimental and Molecular Pathology* 88 (1): 210–15. doi:10.1016/j.yexmp.2009.09.013.

Debs, Robert. n.d. Anti-PECAM Therapy, Compositions, Methods, and Uses. Edited by Sutter West Bay Hospitals D/B/A, California Pacific Medical Center.

DeLisser, H M, M Christofidou-Solomidou, R M Strieter, M D Burdick, C S Robinson, R S Wexler, J S Kerr, et al. 1997. "Involvement of Endothelial PECAM-1/CD31 in Angiogenesis.." *The American Journal of Pathology* 151 (3): 671–77.

DeLisser, Horace, Yong Liu, Pierre-Yves Desprez, Ann Thor, Paraskevei Briasouli, Chakrapong Handumrongkul, Jonathon Wilfong, et al. 2010. "Vascular Endothelial Platelet Endothelial Cell Adhesion Molecule 1 (PECAM-1) Regulates Advanced Metastatic Progression.." *Proceedings of the National Academy of Sciences of the United States of America* 107 (43): 18616–21. doi:10.1073/pnas.1004654107.

di Tomaso, Emmanuelle, Diane Capen, Amy Haskell, Janet Hart, James J Logie, Rakesh K Jain, Donald M McDonald, Rosemary Jones, and Lance L Munn. 2005. "Mosaic Tumor Vessels: Cellular Basis and Ultrastructure of Focal Regions Lacking Endothelial Cell Markers.." *Cancer Research* 65 (13): 5740–49. doi:10.1158/0008-5472.CAN-04-4552.

Duncan, G S, D P Andrew, H Takimoto, S A Kaufman, H Yoshida, J Spellberg, J L de la Pompa, et al. 1999. "Genetic Evidence for Functional Redundancy of Platelet/Endothelial Cell Adhesion Molecule-1 (PECAM-1): CD31-Deficient Mice Reveal PECAM-1-Dependent and PECAM-1-Independent Functions.." *Journal of Immunology (Baltimore, Md. : 1950)* 162 (5): 3022–30.

Feng, Dian, Janice A Nagy, Kathryn Pyne, Harold F Dvorak, and Ann M Dvorak. 2004. "Ultrastructural Localization of Platelet Endothelial Cell Adhesion Molecule (PECAM-1, CD31) in Vascular Endothelium.." *The Journal of Histochemistry and Cytochemistry : Official Journal of the Histochemistry Society* 52 (1): 87–101.

Gao, Cunji, Weiyong Sun, Melpo Christofidou-Solomidou, Motoshi Sawada, Debra K Newman, Carmen Bergom, Steven M Albelda, Shigemi Matsuyama, and Peter J Newman. 2003. "PECAM-1 Functions as a Specific and Potent Inhibitor of Mitochondrial-Dependent Apoptosis.." *Blood* 102 (1): 169–79. doi:10.1182/blood-2003-01-0003.

Gershenwald, J E, W Sumner, T Calderone, Z Wang, S Huang, and M Bar-Eli. 2001. "Dominant-Negative Transcription Factor AP-2 Augments SB-2 Melanoma Tumor Growth in Vivo.." *Oncogene* 20 (26): 3363–75. doi:10.1038/sj.onc.1204450.

Ghajar, Cyrus M, Héctor Peinado, Hidetoshi Mori, Irina R Matei, Kimberley J Evason, Hélène

Brazier, Dena Almeida, et al. 2013. “The perivascular niche regulates breast tumour dormancy.” *Nature Cell Biology* 15 (6). Nature Publishing Group: 1–14. doi:10.1038/ncb2767.

Gumina, R J, N E Kirschbaum, K Piotrowski, and P J Newman. 1997. “Characterization of the Human Platelet/Endothelial Cell Adhesion Molecule-1 Promoter: Identification of a GATA-2 Binding Element Required for Optimal Transcriptional Activity..” *Blood* 89 (4): 1260–69.

Heimberger, Amy B, Eric C McGary, Dima Suki, Maribelis Ruiz, Huamin Wang, Gregory N Fuller, and Menashe Bar-Eli. 2005. “Loss of the AP-2alpha Transcription Factor Is Associated with the Grade of Human Gliomas..” *Clinical Cancer Research : an Official Journal of the American Association for Cancer Research* 11 (1): 267–72.

Helfrich, Iris, Inka Scheffrahn, Sönke Bartling, Joachim Weis, Verena von Felbert, Mark Middleton, Masahi Kato, Süleyman Ergün, Hellmut G Augustin, and Dirk Schadendorf. 2010. “Resistance to Antiangiogenic Therapy Is Directed by Vascular Phenotype, Vessel Stabilization, and Maturation in Malignant Melanoma.” *The Journal of Experimental Medicine* 207 (3): 491–503. doi:10.1161/01.RES.81.4.567.

Huang, S, D Jean, M Luca, M A Tainsky, and M Bar-Eli. 1998. “Loss of AP-2 Results in Downregulation of C-KIT and Enhancement of Melanoma Tumorigenicity and Metastasis..” *The EMBO Journal* 17 (15): 4358–69. doi:10.1093/emboj/17.15.4358.

Jean, D, J E Gershenwald, S Huang, M Luca, M J Hudson, M A Tainsky, and M Bar-Eli. 1998. “Loss of AP-2 Results in Up-Regulation of MCAM/MUC18 and an Increase in Tumor Growth and Metastasis of Human Melanoma Cells..” *The Journal of Biological Chemistry* 273 (26): 16501–8.

Karjalainen, J M, J K Kellokoski, M J Eskelinen, E M Alhava, and V M Kosma. 1998. “Downregulation of Transcription Factor AP-2 Predicts Poor Survival in Stage I Cutaneous Malignant Melanoma..” *Journal of Clinical Oncology : Official Journal of the American Society of Clinical Oncology* 16 (11): 3584–91.

Kim, K B, J A Sosman, J P Fruehauf, G P Linette, S N Markovic, D F McDermott, J S Weber, et al. 2011. “BEAM: a Randomized Phase II Study Evaluating the Activity of Bevacizumab in Combination with Carboplatin Plus Paclitaxel in Patients with Previously Untreated Advanced Melanoma.” *Journal of Clinical Oncology* 30 (1): 34–41. doi:10.1200/JCO.2011.34.6270.

Lança, Telma, and Bruno Silva-Santos. 2014. “The Split Nature of Tumor-Infiltrating Leukocytes.” *OncoImmunology* 1 (5): 717–25. doi:10.4161/onci.20068.

Lawler, Jack. 2002. “Thrombospondin-1 as an Endogenous Inhibitor of Angiogenesis and Tumor Growth..” *Journal of Cellular and Molecular Medicine* 6 (1): 1–12.

Li, Qingjie, Christiane V Löhr, and Roderick H Dashwood. 2009. “Activator Protein 2alpha

Suppresses Intestinal Tumorigenesis in the Apc(Min) Mouse.." *Cancer Letters* 283 (1): 36–42. doi:10.1016/j.canlet.2009.03.026.

Liu, Pixu, Hailing Cheng, Thomas M Roberts, and Jean J Zhao. 2009. "Targeting the Phosphoinositide 3-Kinase Pathway in Cancer." *Nature Publishing Group* 8 (8): 627–44. doi:10.1038/nrd2926.

Mei, Heng, Jay M Campbell, Cathy M Paddock, Panida Lertkiatmongkol, Michael W Mosesson, Ralph Albrecht, and Peter J Newman. 2014. "Regulation of Endothelial Cell Barrier Function by Antibody-Driven Affinity Modulation of Platelet Endothelial Cell Adhesion Molecule-1 (PECAM-1)." *Journal of Biological Chemistry* 289 (30): 20836–44. doi:10.1074/jbc.M114.557454.

Melnikova, Vladislava O, Andrey S Dobroff, Maya Zigler, Gabriel J Villares, Russell R Braeuer, Hua Wang, Li Huang, and Menashe Bar-Eli. 2010. "CREB Inhibits AP-2α Expression to Regulate the Malignant Phenotype of Melanoma." Edited by Roger Chammas. *PLoS ONE* 5 (8): e12452. doi:10.1371/journal.pone.0012452.g005.

Mobley, Aaron K, Russell R Braeuer, Takafumi Kamiya, Einav Shoshan, and Menashe Bar-Eli. 2012. "Driving Transcriptional Regulators in Melanoma Metastasis." *Cancer Metastasis Reviews* 31 (3-4): 621–32. doi:10.1007/s10555-012-9358-8.

Newman, P J. 2003. "Signal Transduction Pathways Mediated by PECAM-1: New Roles for an Old Molecule in Platelet and Vascular Cell Biology." *Arteriosclerosis, Thrombosis, and Vascular Biology* 23 (6): 953–64. doi:10.1161/01.ATV.0000071347.69358.D9.

Nourshargh, Sussan, Fritz Krombach, and Elisabetta Dejana. 2006. "The Role of JAM-a and PECAM-1 in Modulating Leukocyte Infiltration in Inflamed and Ischemic Tissues.." *Journal of Leukocyte Biology* 80 (4): 714–18. doi:10.1189/jlb.1105645.

Ojesina, Akinyemi I, Lee Lichtenstein, Samuel S Freeman, Chandra Sekhar Pedamallu, Ivan Imaz-Rosshandler, Trevor J Pugh, Andrew D Cherniack, et al. 2014. "Landscape of Genomic Alterations in Cervical Carcinomas." *Nature* 506 (7488). Nature Publishing Group: 371–75. doi:10.1038/nature12881.

Paddock, Cathy, Dongwen Zhou, Panida Lertkiatmongkol, Peter J Newman, and Jieqing Zhu. 2016. "Structural Basis for PECAM-1 Homophilic Binding.." *Blood* 127 (8): 1052–61. doi:10.1182/blood-2015-07-660092.

Peinado, Héctor, Maša Alečković, Simon Lavotshkin, Irina Matei, Bruno Costa-Silva, Gema Moreno-Bueno, Marta Hergueta-Redondo, et al. 2012. "Melanoma Exosomes Educate Bone Marrow Progenitor Cells Toward a Pro-Metastatic Phenotype Through MET.." *Nature Medicine* 18 (6): 883–91. doi:10.1038/nm.2753.

Pellikainen, Johanna, Vesa Kataja, Kirsi Ropponen, Jari Kellokoski, Timo Pietiläinen, Jan Böhm, Matti Eskelinen, and Veli-Matti Kosma. 2002. "Reduced Nuclear Expression of

Transcription Factor AP-2 Associates with Aggressive Breast Cancer.." *Clinical Cancer Research : an Official Journal of the American Association for Cancer Research* 8 (11): 3487–95.

Penna, Elisa, Francesca Orso, Daniela Cimino, Enrico Tenaglia, Antonio Lembo, Elena Quaglino, Laura Poliseno, et al. 2011. "microRNA-214 Contributes to Melanoma Tumour Progression Through Suppression of TFAP2C." *The EMBO Journal* 30 (10). Nature Publishing Group: 1990–2007. doi:10.1038/emboj.2011.102.

Privratsky, J R, C M Paddock, O Florey, D K Newman, W A Muller, and P J Newman. 2011. "Relative Contribution of PECAM-1 Adhesion and Signaling to the Maintenance of Vascular Integrity." *Journal of Cell Science* 124 (9): 1477–85. doi:10.1242/jcs.082271.

Privratsky, Jamie R, and Peter J Newman. 2014. "PECAM-1: Regulator of Endothelial Junctional Integrity." *Cell and Tissue Research* 355 (3): 607–19. doi:10.1007/s00441-013-1779-3.

Quail, Daniela F, and Johanna A Joyce. 2013. "Microenvironmental Regulation of Tumor Progression and Metastasis." *Nature Medicine* 19 (11): 1423–37. doi:10.1038/nm.3394.

Ran, F Ann, Patrick D Hsu, Jason Wright, Vineeta Agarwala, David A Scott, and Feng Zhang. 2013. "Genome Engineering Using the CRISPR-Cas9 System." *Nature Protocols* 8 (11): 2281–2308. doi:10.1038/nprot.2013.143.

Ruiz, M, P Troncoso, C Bruns, and M Bar-Eli. 2001. "Activator Protein 2alpha Transcription Factor Expression Is Associated with Luminal Differentiation and Is Lost in Prostate Cancer.." *Clinical Cancer Research : an Official Journal of the American Association for Cancer Research* 7 (12): 4086–95.

Ruiz, Maribelis, Curtis Pettaway, Renduo Song, Oliver Stoeltzing, Lee Ellis, and Menashe Bar-Eli. 2004. "Activator Protein 2alpha Inhibits Tumorigenicity and Represses Vascular Endothelial Growth Factor Transcription in Prostate Cancer Cells.." *Cancer Research* 64 (2): 631–38.

Sun, J, C Paddock, J Shubert, H B Zhang, K Amin, P J Newman, and S M Albelda. 2000. "Contributions of the Extracellular and Cytoplasmic Domains of Platelet-Endothelial Cell Adhesion Molecule-1 (PECAM-1/CD31) in Regulating Cell-Cell Localization.." *Journal of Cell Science* 113 (Pt 8) (April): 1459–69.

Tang, D G, Y Q Chen, P J Newman, L Shi, X Gao, C A Diglio, and K V Honn. 1993. "Identification of PECAM-1 in Solid Tumor Cells and Its Potential Involvement in Tumor Cell Adhesion to Endothelium.." *Journal of Biological Chemistry* 268 (30): 22883–94.

Thompson, R D, K E Noble, K Y Larbi, A Dewar, G S Duncan, T W Mak, and S Nourshargh. 2001. "Platelet-Endothelial Cell Adhesion Molecule-1 (PECAM-1)-Deficient Mice Demonstrate a Transient and Cytokine-Specific Role for PECAM-1 in Leukocyte Migration

Through the Perivascular Basement Membrane.." *Blood* 97 (6): 1854–60.

Torzicky, Martin, Petra Viznerova, Susanne Richter, Herbert Strobl, Clemens Scheinecker, Dagmar Foedinger, and Elisabeth Riedl. 2012. "Platelet Endothelial Cell Adhesion Molecule-1 (PECAM-1/CD31) and CD99 Are Criticalin Lymphatic Transmigration of Human Dendritic Cells." *Journal of Investigative Dermatology* 132 (4). Elsevier Masson SAS: 1149–57. doi:10.1038/jid.2011.420.

Tzima, Eleni, Mohamed Irani-Tehrani, William B Kiosses, Elizabetta Dejana, David A Schultz, Britta Engelhardt, Gaoyuan Cao, Horace DeLisser, and Martin Alexander Schwartz. 2005. "A Mechanosensory Complex That Mediates the Endothelial Cell Response to Fluid Shear Stress." *Nature Cell Biology* 437 (7057): 426–31. doi:10.1038/nature03952.

Wagenblast, Elvin, Mar Soto, Sara Gutiérrez-Ángel, Christina A Hartl, Annika L Gable, Ashley R Maceli, Nicolas Erard, et al. 2015. "A Model of Breast Cancer Heterogeneity Reveals Vascular Mimicry as a Driver of Metastasis." *Nature*, April. doi:10.1038/nature14403.

Yang, Suya, Jennifer Graham, Jeanne W Kahn, Eric A Schwartz, and Mary E Gerritsen. 2010. "Functional Roles for PECAM-1 (CD31) and VE-Cadherin (CD144) in Tube Assembly and Lumen Formation in Three-Dimensional Collagen Gels." *Ajpa* 155 (3). American Society for Investigative Pathology: 887–95. doi:10.1016/S0002-9440(10)65188-7.

Zhou, Z, M Christofidou-Solomidou, C Garlanda, and H M DeLisser. 1999. "Antibody Against Murine PECAM-1 Inhibits Tumor Angiogenesis in Mice.." *Angiogenesis* 3 (2): 181–88.

Zigler, M, G J Villares, A S Dobroff, H Wang, L Huang, R R Braeuer, T Kamiya, et al. 2011. "Expression of Id-1 Is Regulated by MCAM/MUC18: a Missing Link in Melanoma Progression." *Cancer Research* 71 (10): 3494–3504. doi:10.1158/0008-5472.CAN-10-3555.